

12-2020

## The Persistence of Acid Mine Drainage at an East Texas Coal Mine

Sarah Zagurski  
Stephen F Austin State University, sarah@zagurski2.net

Follow this and additional works at: <https://scholarworks.sfasu.edu/etds>



Part of the [Environmental Monitoring Commons](#), [Geochemistry Commons](#), and the [Geology Commons](#)

[Tell us](#) how this article helped you.

---

### Repository Citation

Zagurski, Sarah, "The Persistence of Acid Mine Drainage at an East Texas Coal Mine" (2020). *Electronic Theses and Dissertations*. 358.

<https://scholarworks.sfasu.edu/etds/358>

This Thesis is brought to you for free and open access by SFA ScholarWorks. It has been accepted for inclusion in Electronic Theses and Dissertations by an authorized administrator of SFA ScholarWorks. For more information, please contact [cdsscholarworks@sfasu.edu](mailto:cdsscholarworks@sfasu.edu).

---

# The Persistence of Acid Mine Drainage at an East Texas Coal Mine

## Creative Commons License



This work is licensed under a [Creative Commons Attribution-Noncommercial-No Derivative Works 4.0 License](https://creativecommons.org/licenses/by-nc-nd/4.0/).

THE PERSISTENCE OF ACID MINE DRAINAGE AT AN  
EAST TEXAS COAL MINE

By

Sarah Zagurski, Bachelor of Science in Geology and Environmental Science

Presented to the Faculty of the Graduate School of

Stephen F. Austin State University

In Partial Fulfillment

Of the Requirements

For the Degree of

Master of Science in Environmental Science

STEPHEN F. AUSTIN STATE UNIVERSITY

December, 2020

THE PERSISTENCE OF ACID MINE DRAINAGE AT AN  
EAST TEXAS COAL MINE

By

Sarah Zagurski, Bachelor of Science in Geology and Environmental Science

APPROVED:

---

Dr. Kenneth Farrish, Thesis Director

---

Mr. Jason Paul, Committee Member

---

Dr. Yuhui Weng, Committee Member

---

Dr. Mindy Faulkner, Committee Member

---

Pauline Sampson, Ph.D.  
Dean of Research and Graduate Studies

## ABSTRACT

The objective of this study was to estimate the time it will take for acid forming materials (pyrite) to be weathered to a state of equilibrium and thus cease to produce acid in ground and surface waters within Oak Hill Mine. This was accomplished using an ex-situ kinetic leaching study incorporating a humidity cell in a controlled laboratory setting. Leaching was conducted on soil cores obtained from the vadose zone at Oak Hill Mine and the humidity cell was used to accelerate oxidation of the pyrite within the cores.

An in-situ field study was also conducted that monitored groundwater conditions monthly to determine current redox conditions of the reclaimed mine site. Groundwater data was compared to the leachate humidity cell data to determine scaling factors that could be applied to the laboratory-based humidity cell experiment. These scaling factors coupled with regression analysis were then used to extrapolate the length of time it would take pyrite to fully oxidize at the mine site back to a state of equilibrium.

The data suggests that acid mine drainage will persist at the site within a range of 9 to 48 years. The results determined from this study are expected to

help Luminant find the most cost-efficient remediation strategy to acid mine drainage in the study area.

## ACKNOWLEDGEMENTS

I would first like to express my sincere gratitude to Luminant Mining Company for funding my research and providing me the opportunity to grow in my knowledge and experience by using their mine site as real world research experience. I am appreciative of all those at Luminant that who kept me accountable and safe while doing my field work and research including Sid Stroud, Justin Ewing, Jeff Noble, and Milton Smith, as well as the entire Environmental Research Steering Committee. I am very appreciative of the department of Environmental Science for providing my base fellowship and for supporting me from my undergraduate studies all the way through the completion of my master's degree.

I would also like to give many thanks to my advisor, Jason Paul, who guided me through my project at all stages and made sure my research was as thorough as possible. My committee members, Dr. Kenneth Farrish, Dr. Yuhui Weng, and Dr. Mindy Faulkner provided me with a world of insight in which my project would be incomplete without. A special thanks also goes out to all of those who gave up their time to assist me with long days of field work including Brianna Clark, Hannah Bays, Sarah Hall, Karlen Cantu, and Colby Reece.

## TABLE OF CONTENTS

ABSTRACT .....	ii
ACKNOWLEDGEMENTS.....	iii
TABLE OF CONTENTS .....	iv
LIST OF FIGURES .....	vi
LIST OF TABLES .....	viii
LIST OF EQUATIONS.....	x
INTRODUCTION .....	1
Objectives .....	2
LITERATURE REVIEW .....	4
Pyrite Oxidation Rate Factors .....	4
Overview of Leaching Studies.....	6
Scaling Factors .....	7
AMD Indicators.....	12
Equilibrium and Kinetic Conditions .....	14
Site Geology.....	16
Site Specific Studies.....	17
METHODS.....	21
Humidity Cell .....	21
Leachate Testing.....	24
<i>Ion Chromatography (IC)</i> .....	25
Most Probable Numbers .....	25
Groundwater Sampling.....	26
Groundwater Data and Modeling .....	28
Statistical Modeling .....	29
RESULTS AND DISCUSSION .....	33
Soil Core Analysis.....	33



Humidity Cell Leachate Analysis.....	35
Groundwater Data.....	41
Vadose Zone Calculations .....	45
Scaling Factor Calculations.....	46
AMD Prediction Calculations.....	52
Limitations to AMD predictions.....	60
CONCLUSION.....	63
LITERATURE CITED .....	65
APPENDIX A – FIGURES .....	69
APPENDIX A – TABLES .....	97
APPENDIX B – ACRONYMS .....	112
VITA .....	114

## LIST OF FIGURES

Figure 1. The Conceptual Model for Scaling Minesite-Drainage Chemistry, with General Ranges of Scale for Various Types of Geochemical Testwork and Models (from Morin and Hutt, 2007a). .....	15
Figure 2. Eh-pH diagram for sulfur-iron-water systems at 25° C (from Descostes et al., 2004).....	16
Figure 3. Humidity cell leachate pH from week 0 to week 48. ....	36
Figure 4. Humidity cell leachate Eh values from week 19 to week 48. ....	37
Figure 5. Eh vs. pH cross comparison in the humidity cells.....	39
Figure 6. pH values of the wells of interest from September 2019 through August 2020. ....	41
Figure 7. Eh values of the wells of interest from March 2020 through August 2020. ....	42
Figure 8. Eh vs pH cross comparison for the monitoring wells from March through August. ....	43
Figure 9. Groundwater elevation map within the mined pit at Oak Hill Mine, Henderson Texas. ....	44

Figure 11. Slope of logarithmic predictor equations versus the initial percent of sulfur in the soil.....	54
Figure 12. Intercept of logarithmic predictor equations versus the initial percent of sulfur in the soil.....	54
Figure 13. The release rate of sulfate (y) and the pH of the humidity cells to determine the sulfate release rate at equilibrium (with a maximum sulfate release value of 100 mg/kg). ....	56
Figure 14. The release rate of acidity (y) and the pH of the humidity cells to determine the acidity release rate at equilibrium (with a maximum acidity release value of 100 mg/kg). ....	60

## LIST OF TABLES

Table 1. Stabilizations ranges used for water quality for low-flow micropurge groundwater sampling. ....	27
Table 2. Total Sulfur, sulfate, and acidity for the chosen, combined, and homogenized samples from each selected well prior to leaching. ....	34
Table 3. Total Sulfur, sulfate, and acidity for the chosen, combined, and homogenized samples from each selected well after the completion of leaching. ....	34
Table 4. Linear pH trends for Humidity Cell leachate with a starting pH below site background levels. ....	38
Table 5. The most probable number of iron and sulfur oxidizing bacteria per gram of soil for each humidity cell. ....	40
Table 6. Soil volume and soil mass data for the zones of influence for each lake of interest. ....	45
Table 7. Water volume data for the zones of influence for each lake of interest. ....	46
Table 8. Soil to water ratios for the humidity cells. ....	48
Table 9. Soil to water ratios for the zone of influence for the lakes of interest. ....	49

Table 10. Soil to water scaling factors for each humidity cell and zone of influence combination.....	50
Table 11. Scaling factor for each variable considered in the study.....	51
Table 12. Line of best fit equation and R2 values for sulfate release for each humidity cell with an initial pH less than 4.7 (Figures 2a-10a). ....	52
Table 13. Lab release rate equations based upon a uniform model (Eq. 6) for each humidity cell where x=time.....	53
Table 14. Field sulfate release equations and equilibrium time predictions for the lab and the field. ....	58
Table 15. Line of best find equation and R2 values acidity release for each humidity cell with an initial pH less than 4.7. ....	59

## LIST OF EQUATIONS

Eqaution 1.	$CSF = SF_1 * SF_2 * SF_3 * SF_4$ .....	8
Eqaution 2.	$R_{field} = R_{lab} \times CSF$ .....	12
Eqaution 3.	$pH = -\log [H^+]$ ,.....	12
Eqaution 4.	$L_e = C_e \times M_e$ .....	30
Eqaution 5.	$L_n = i - 0n(C_i \times M_i)$ .....	30
Eqaution 6.	$1.000 \times 1.000 \times 1.000 \times 0.0026 \times 29.33 = 0.0769$ .....	52
Eqaution 7.	$Sulfate = a \ln(\text{time}) + b$ .....	53

## INTRODUCTION

Acid Mine Drainage (AMD) is the result of sulfide minerals, such as pyrite, converting from solid phase to solution phase. This increases acidity and solubility of metals in groundwater, surface water, and soils (Skousen et al., 2016). The effects of AMD can adversely impact vegetation and aquatic life, cause habitat alteration, and inhibit the use of water for agriculture, industry, or other purposes. AMD is a global problem for both surface mining and underground mining. It is also affiliated with both hard rock and soft rock mining. This is due to the mining process where sulfide minerals are redistributed and reduced metal sulfides are placed in more oxygenated environments.

AMD drainage has been a concern at the Luminant Oak Hill mine near Henderson, Texas. It has been reported that surface water lakes have become acidic due to acidic groundwater seeps (such as in lakes DII-35R, DII-55R, and DII-58R within Luminant Oak Hill Mine) (Pastor et al., 2014, Paul, 2020). Mining has been permitted at this site since 1993 and the remediation process began in 2011. Lakes DII-35R and DII-55R were established prior to 2005 and are approximately 22 and 16 acres, respectively. Both lakes have had pH values between 2 to 3.4 since 2014 (PBW, 2014). Lake DII-58R was established in

2011, is about 4 acres, and was first reported to have a low pH (2.5) in December, 2016.

The National Pollution Discharge Elimination System (NPDES) requires final surface water pH values between 6 and 9. NPDES is regulated by the US EPA and enforced by Railroad Commission of Texas (RRC). Without achieving the required pH level, the mine cannot release the land from bond. Treatment of the lakes currently consists of adding caustic soda (NaOH) to surface waters to neutralize pH, which is costly and must be regularly maintained. The addition of caustic soda to neutralize surface water has not been successful in sustaining long-term neutral pH at some reclamation sites and, therefore, has not allowed Luminant to release these lands from bond. Acid drainage from groundwater is seeping into the lakes causing the pH to continue to decrease even after treatment methods. Current neutralizing methods for treatment are costing from \$600,000 to \$850,000 annually based on discussions with Luminant

## Objectives

The objective of this study was to determine the longevity of AMD due to pyrite oxidation. The results will help Luminant determine the best management approach for treatment of the acid seeps. Comparing bench top reaction rates from the humidity cell coupled with regression modeling and field scaling



determinations will help determine an estimated time frame in which acidity production will persist.

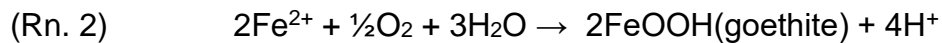
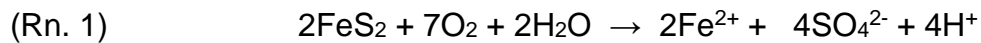
The objective of this study were carried out through the following stages:

1. Determine the current state of the groundwater quality (pH, ORP, DO, elevation) in the field.
2. Evaluate pyrite oxidation rates by evaluating sulfate release in a benchtop humidity cell leaching study.
3. Apply laboratory sulfate release rates to field release rates through the use of scaling factors
4. Use regression analysis to predict the time in which acid mine drainage will persist at Oak Hill Mine.

# LITERATURE REVIEW

## Pyrite Oxidation Rate Factors

AMD occurs as groundwater percolates through the vadose zone and comes in contact with pyritic material in the soil. The water then reacts with the pyrite, forming acid as seen in the following reactions:

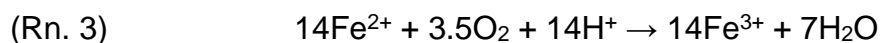


Acidic water can then flow from the vadose zone into the saturated zone and eventually interface with surface waters (Holmes, 1999, Paul, 2020).

The rate of the reactions above is affected by many variables. These variables include weather conditions such as temperature, rainfall, humidity, groundwater elevation, microbes within the soil (i.e. acidophiles), and local geology. These factors influence the amount of oxygen present in the system, the amount of sulfide available for conversion, other competing ions in the system, and the rate at which oxidation can occur (British Columbia AMD Task Force, 1989).

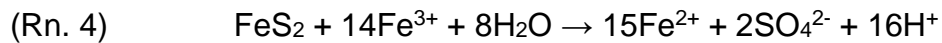
Acidification of surface and groundwater water will continue until there are no longer acid forming materials readily available for oxidation within the soil. This occurs when the pyrite in the soil has been weathered to a point where oxidation is occurring at a negligible rate or no longer has access to oxygen or water (Pozo-Antonio, 2013). Water pH can also increase once alkaline producing materials are greater than acidic producing materials. Alkalinity is the resistance of a site to generate acidic conditions. This can occur naturally when the mineralogy of the area contains base forming cations such as  $\text{Na}^+$ ,  $\text{Mg}^{2+}$ ,  $\text{Ca}^{2+}$ , and  $\text{K}^+$  that dissolve due to precipitation or groundwater fluctuation (McCauley et al., 2017). The time range in which pH will increase is based upon the reaction rate variables listed above. However, this wide variety of factors makes the time prediction of the acid mine drainage and the resulting pH challenging (Morin, 2013).

Microbes in the soil (e.g. *Acidithiobacillus thiooxidans* and *Acidithiobacillus ferrooxidans*) contribute significantly to the development of AMD due to their ability to convert ferrous iron ( $\text{Fe}^{2+}$ ) to ferric iron ( $\text{Fe}^{3+}$ ) (Reaction 3) which creates the necessary product for Reaction 4 to take place (Baker and Banfield, 2003).



Reaction 3 can occur spontaneously, but often occurs with microbes as a catalyst. This reaction is important because ferric iron acts as an oxidizer, which

can then lead to the production of acidity without the presence of free oxygen as shown in Reaction 4 below (Baker and Banfield, 2003). This allows pyrite to oxidize at deeper depths or within the phreatic zone where little to no oxygen is present.



Ferric iron leads to a greater production of net acidity because 16 moles of hydrogen ions are released for every 14 moles of ferric iron consumed.

Groundwater elevation becomes significantly more important once ferric iron is solubilized. The acidity generated in groundwater may then be transmitted to surface water contingent on site-specific topography, precipitation, and geologic factors such as hydraulic conductivity, the presence and location of aquitards, and secondary porosity (Holmes, 1999).

## Overview of Leaching Studies

Leaching tests can be used to determine the geochemical effects of soil and quantify the mobilization of constituents of concern (Hagemen, 2003). Leaching is accomplished by moving water through the soil at a predetermined rate and volume and testing the leachate to determine soluble constituents. There are two main types of leaching tests: static and kinetic. Static leaching tests are short duration with the goal of leaching the maximum amount of acid from soil. Kinetic leaching tests last for a longer duration of time such as weeks to years in order to

aid in determination of geochemical process occurring within the soil (Hagemen, 2003). Kinetic leaching studies are preferred to static leaching studies when trying to predict future conditions because they allow for the calculation of release rates of constituents of concern. A humidity cell is a type of kinetic leaching system that is used to increase oxidation reactions within a confined area.

The use of humidity cells to predict acid mine drainage is a technique that has been used for many years. ASTM Standard D5744-18 Standard Test Method for Laboratory Weathering of Solid Material Using a Humidity Cell (ASTM D5744-18) provides a detailed description of how to operate a humidity cell. The cells increase oxidation of pyritic material such as that found in cores from Oak Hill Mine. This aids in determining the release rates of ions of concern and making future water quality predictions. Humidity cells are typically used in hard rock mining and have been underutilized for surface mine overburden, but are considered a useful predictive method that could be applied more often for this type of environment.

## Scaling Factors

Scaling factors are values that are used to apply benchtop leachate data to field data. Variations in oxygen content, temperature, particle size, and other factors that may influence the geochemical parameters in the field must be

considered when scaling humidity cell oxidation rates to field rates. Each of these variables are considered scaling factors (SF) that when multiplied together allow for the calculation of the cumulative scaling factor (CSF) as seen in equation 1 (Morin, 2013):

$$\text{(Eq. 1)} \quad \text{CSF} = \text{SF}_1 * \text{SF}_2 * \text{SF}_3 * \text{SF}_4 \dots$$

While there may be many variables that differ between the kinetic test and the field, the use of too many scaling factors could lead to the under estimation of constituent release rates in the field. Based on previous studies, cumulative scaling factors typically fall in the range of 0.05 to 0.60 (Hanna and Lapakko, 2012). Each scaling factor is typically less than 1 because kinetic leaching tests usually overestimate the chemical release of AMD. The cumulative scaling factor continues to decrease as each scaling factor is multiplied, which may eventually lead to the model underestimating the AMD release in the field. Thus, the investigator must carefully determine which scaling factors are most appropriate for inclusion in the CSF calculation in order to minimize error.

One example of a scaling factor to consider is temperature variation from the lab to the field. Field release rates for AMD may be heavily dependent on temperature, and therefore temperature is considered one of the most important scaling factors to consider contingent upon site conditions (Kempton, 2012). In warmer climates where soil does not regularly freeze, the use of temperature as

a scaling factor may lead to an underestimation of the cumulative scaling factor and case studies have chosen to leave that factor out (Morin, 2013). Studies have concluded that temperature differences of less than 20 °C did not impact of oxidation rates of pyrite (Shawn and Samuels, 2012, Hannah and Lapakko, 2012).

Particle size of pyrite is also considered a major scaling factor. Larger particle sizes of acid forming material are less reactive due to less oxidative surface area when compared to smaller particle sizes. Based off the ASTM Standard D5744-18 Standard Test Method for Laboratory Weathering of Solid Material Using a Humidity Cell (ASTM D5744-18), it is suggested to grind or crush samples to reduce the particle size of the material. Kempton (2012) concluded that particles greater than 20 cm in diameter would not contribute to AMD. Some studies suggest that a particle size of 6 mm is representative of the reactive particle sizes of pyrite. Morin (2013) suggested that this is an oversimplification and particle size distribution, including larger particle sizes, should be taken into consideration when formulating scaling factors on a site-specific basis.

Humidity cells contain a limited volume of soil and have higher soil to water ratios than what is encountered under natural field conditions. The variable can be accounted for through the use of a scaling factor. This scaling factor helps to address the removal and transport of acidity (Morin, 2013). In small scale

studies, there is typically a much higher water to soil contact. This leads to significantly increased mineral flushing than would happen under natural conditions. Humidity cell studies that flood the humidity cell each week will likely have 100 percent of reactant products being flushed each week while field flushing can be around 5 percent in typical rain events and up to 40 percent in high flow rain events (Morin and Hutt, 1994).

Pore gas content is another consideration when determining scaling factors. Oxidation reactions require the presence of oxygen unless another catalyst is present (such as ferric iron for the oxidation of pyrite) (Holmes, 1999, Baker and Banfield, 2003). Humidity cells tests that inject air through the bottom of the cell have significantly increased pore oxygen content than what would be found in the field. Pore gas oxygen content is not necessarily a reliable indicator though since oxygen is consumed in an oxidation reaction. Pore gas containing low oxygen may not indicate that less reaction is occurring but rather that oxygen is being consumed faster than it is being replenished in the system (Morin, 2013). This may indicate an area where oxidation is occurring fastest. Alternatively, other oxidizers such as ferric iron can drive the rate of oxidation (Baker and Banfield, 2003).

As mentioned before, microbes largely impact the rate of pyrite oxidation by catalyzing the production of ferric iron. An overabundance of microbes in a



humidity cell will lead to a vast overestimation of oxidation rates. Conversely, the lack of microbes in a humidity cell may lead to the scaling factor underestimating oxidation rates if not considered. If is not completely understood the extent in which microbes will affect acid mine drainage, but there have been a variety of studies that look at abiotic versus biotic oxidation rates in lab to help quantify the affect of microbes (McKibben and Barnes, 1986; Olson 1991; Alpers and Nordstrom, 1999). Abiotic oxidation rates of pyrite fall in the range of 0.3 to  $3 \times 10^{-9} \text{ mol L}^{-1} \text{ s}^{-1}$  according to McKibbens and Barnes (1986). Olson (1991) estimated biotic oxidation rates of pyrite to be  $8.8 \times 10^{-8} \text{ mol L}^{-1} \text{ s}^{-1}$  in a separate study. These rates vary by several orders of magnitude, further emphasizing the variable effects of microbes on AMD. The use of bacteria as a scaling factor should be used cautiously since studies on the effect of acidophiles on acid mine drainage is not fully understood.

It can be concluded that scaling factors are highly subjective and vary significantly in magnitude. There could potentially be hundreds to thousands of scaling factors at a single site. Considerations such as these make cumulative scaling factors highly site specific (Morin, 2013).

Scaling factors can also be interconnected, leading to further underestimations in field predictions (Kempton, 2012). In other words, two or more scaling factors can account for overlapping variables that would lead to

these variable being mathematically accounted for multiple times. Due to these inherent geochemical links, it is suggested that only one to three scaling factors should be utilized for the most accurate AMD predictions (Morin, 2013).

The cumulative scaling factor is then applied to the sulfate release rate derived from the humidity cell (Eq. 2).

$$(Eq. 2) \quad R_{\text{field}} = R_{\text{lab}} \times \text{CSF}$$

Equation 2 was modified from Kempton's (2012) equation where each individual scaling factor was substituted for the cumulative scaling factor.

### AMD Indicators

While the RRC regulates mines for surface water pH, the use of pH as a direct indicator for AMD can be difficult to evaluate if testing is done for a short period of time. A stable or nearly stable pH does not necessarily indicate that a change in the rate of AMD is occurring. Large changes in acidity are required to make small changes in pH values. Acidity measures the quantity of a base required to neutralize the H<sup>+</sup> ions. pH is the -log of hydrogen ion concentration (Eq. 3).

$$(Eq. 3) \quad \text{pH} = -\log [\text{H}^+],$$

Based on Equation 3, H<sup>+</sup> concentrations must decrease by a factor of 10 in order for pH to increase by a value of 1 (Soult, 2019). This means that lower pH

values, such as those seen on the study site, require a larger quantity of base to change pH. Thus, acidity drastically decreases as pH increases and vice versa. Soil alkalinity, however, may cause misleading data when using acidity as a predictor. Alkaline substrates may diminish over time and no longer provide a buffer to the AMD. If data is collected for a short period of time, acidity values may not accurately represent future conditions due to the rate of spent alkalinity (Sexsmith and MacGregor, 2014).

Sulfate release is another indicator of AMD. Since sulfate is a direct product of the oxidation of pyrite, oxidation rates can be predicted by calculating weekly sulfate loadings from the leachate produced from a humidity cell (British Columbia AMD Task Force, 1989). When using sulfate as an AMD indicator, it is important to ensure that there are no other minerals present that could leach sulfate and cause an error within oxidation rate calculations (British Columbia AMD Task Force, 1989).

Many humidity cell studies discuss lag time before the cells begin to generate acidity. Lag time is the time in which it takes for acidic conditions to develop (Sexsmith and MacGregor, 2014). This lag time is typically seen in studies that are conducted prior to mining in efforts to determine whether the site has acid producing potential and is dependent on the neutralization potential of the site. The site in this study has been closed for over a decade and is already producing

AMD. Lag times are unlikely to be observed at locations such as the study site where oxidation has been ongoing for a number of years.

## Equilibrium and Kinetic Conditions

Humidity cells typically target kinetic reaction rates rather than those at equilibrium. Kinetic rates occur when the environment is unstable, such as when reduced sulfide minerals are brought to the surface during mining. Kinetic rates in the lab can be scaled to kinetic rates in the field. Equilibrium is not scale dependent. Therefore, if equilibrium constituent release rates are observed in a humidity cell, then no scaling factor is needed to relate lab data to field data (Morin, 2013). Kinetic rates in the humidity cell are not applicable to equilibrium rates. The relationship of scaling factors for kinetics and equilibrium is demonstrated in Figure 1.

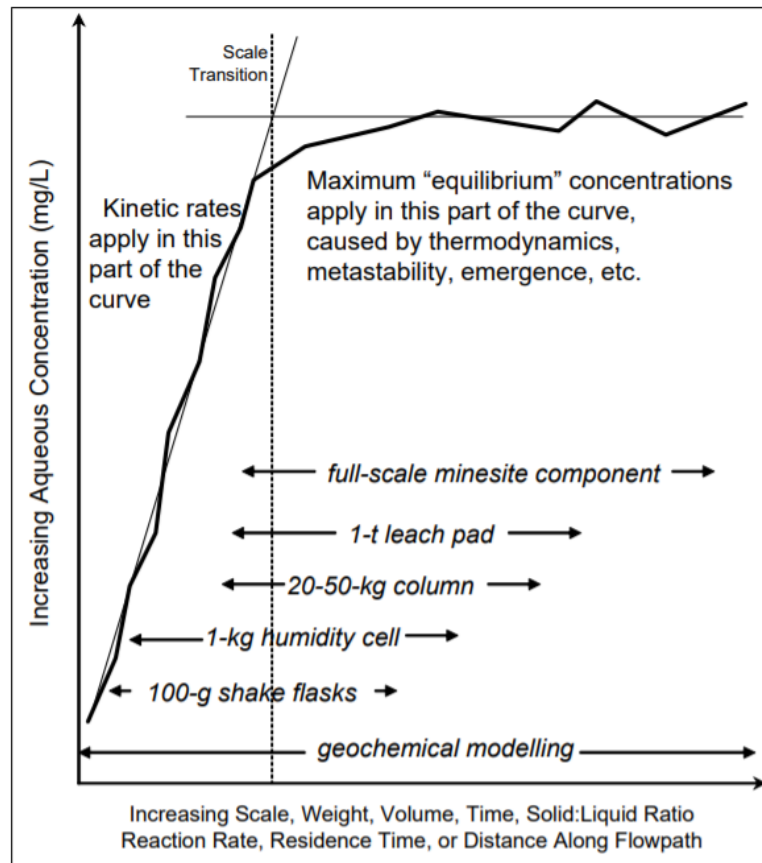


Figure 1. The Conceptual Model for Scaling Minesite-Drainage Chemistry, with General Ranges of Scale for Various Types of Geochemical Testwork and Models (from Morin and Hutt, 2007a).

Minerals also have stability parameters based on their oxidation/reduction potential and pH. The Eh-pH diagram in Figure 2 shows the stable minerals of an iron and sulfur dominated system. This helps determine if a mineral is at equilibrium or if it will undergo a chemical transformation such as oxidation or reduction. It can be seen that pyrite is stable when pH is between 3 and 6 and the redox potential (Eh) is low. At lower pH values and higher redox potentials, pyrite oxidation products, such as goethite, become the stable mineral.

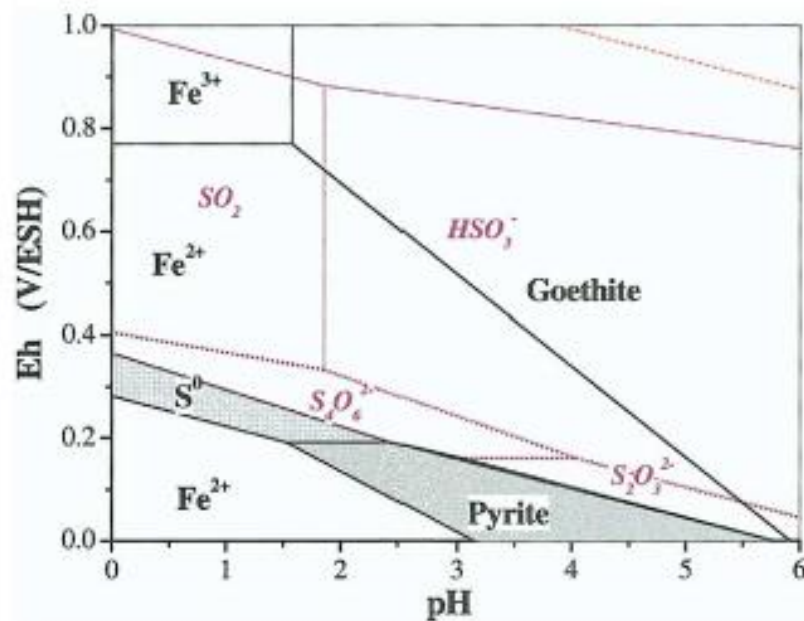


Figure 2. Eh-pH diagram for sulfur-iron-water systems at 25° C (from Descostes et al., 2004)

## Site Geology

The local geology is influenced by several factors. The stratigraphic units that make up the area within Oak Hill Mine include alluvial deposits, the lower Reklaw Formation, the Carrizo Formation, and the Wilcox Group (US EPA, USGS, 2018). The Reklaw formation is an Eocene deposit made of fine to very fine grained quartz sand near the top of the deposit fining downwards to a silty clay with localized beds of lignite and finally clay at the lowest portion of the formation. Only the lower portions of the Reklaw are present on the site due to erosion (US EPA, 1983). The Carrizo formation is also an Eocene deposit and is primarily

composed of sand in the upper lithologic section fine grained quartz sand with small amount of gravel in the lower section (US EPA, 1983). The Wilcox Group was deposited during the late Paleocene and is composed of alternating layers of silty and sandy clay with interbedded seams of lignite (Klein, 2000), as this was an estuarine depositional environment that allowed for high deposits of organic matter along with the sediment. The Wilcox group is up to 500 feet thick and makes up the majority of study site. Lignite occurs between 10 to 150 feet below the surface with the minable lignite falling within a shallow groundwater system (US EPA, 1983), resulting in the reclaimed sites having some restored groundwater flow. The overburden that fills the old mine pits includes parts of the Reklaw, Carrizo, and Wilcox formations. These units contain sulfide-rich minerals such as pyrite that oxidize as they are exposed to the near surface environment (Mercier, 2011). Rainfall and groundwater flowing through these reclaimed, oxidized areas, leads to acid production and transportation.

### Site Specific Studies

The study conducted by Pastor et al., (2014) concluded that any lake receiving more than 10 percent of its water from low pH groundwater recharge will not maintain a pH greater than 6. Lakes DII-35R, DII-55R, and DII-58R (Figure 1a) at Oak Hill Mine have all previously exhibited a pH range of 2-3.45 and receive over 50 percent of their water volume from groundwater seeps

(Pastor et al., 2014). A study conducted by Paul (2020) titled, *Tracing Persistent Sources of Low pH to Surface Waters at a Former East Texas Lignite Mine* (in edit), showed framboidal pyrite in the soil around lakes DII-35R, DII-55R, and DII-58R. Framboidal pyrite has high surface area to volume ratio causing high amounts of acidity to be released into the lake (Devasayaham, 2007).

Overburden from mining at Oak Hill Mine is highly heterogeneous and semi-inverted. This brings poorly weathered pyrite sediments to the near surface causing an increase in acidity and oxidation in the soil (Mercier, 2014). Mercier also stated that the background pH levels prior to mining were only 4.7 to 4.8, indicating that AMD has created a decrease in pH of up to -2.7 pH units and due to the local geology, the water may never reach a pH of 6. Over time, the pH may gradually increase back to background levels once most of the pyrite has oxidized and the soil returns to a state of equilibrium. Alkaline amendments or implementation of natural systems (i.e. *Typha sp.* in bioremediation wetlands) that generate alkalinity will likely still be required to raise pH to the regulatory limit of pH 6 (Chen et al., 2014).

The land around lakes DII-35R, DII-55R, and DII-58R within the Oak Hill Mine has recently been studied in depth with cores taken in the summer of 2016 (Paul, 2020). This study conducted X-ray diffraction (XRD), scanning electron microscopy (SEM), and transmissive electron microscopy to determine the



mineralogy of the soil. The 4 inch diameter cores in this study were collected every 2 feet between 4 and 60 feet below the ground surface. Select half foot intervals were taken from each 2 feet in depth that were most representative of the interval with the exception of poor recovery cores. After collection and analysis, the cores were stored at -20°C (Paul, 2020). The mineral analysis from the cores further shows that the site is highly heterogeneous in both the horizontal and vertical directions. It also shows that the only source of sulfate present on site is from pyrite oxidation. Based on groundwater sulfate concentrations, the site has hot spot areas that are contributing more acidity to lakes than other areas. This could mean that some areas are either non-acid producing areas or have already oxidized the acid forming material within that localized area. Other locations may still have time before reaching their maximum acid production peak. Based upon hydrograph data from Paul (2020), groundwater elevation is stable throughout the year, varying only by an annual maximum of 2 inches at all measured monitoring well locations. Depth to groundwater is shallow on site (less than 15 meters btoc) and has significant interaction with the surface lakes of interest. This shallow aquifer is unconfined with water table elevations reflecting regional changes in surface topography. Local groundwater flow moves towards the lakes of interest from the southeast to the northeast. A baseline for the proposed humidity cell study has been established with the core data from the area around DII-35R, DII-55R, and DII-

58R and it is proposed that these cores can be used as a substrate for a humidity cell study.

A leaching study was conducted at the Martin Lakes Mine in the form of a lysimeter study. This study resulted in the determination that the mine spoil would not produce AMD (Doolittle, 1987). In a separate study, in-situ field-based tests including lysimeters, were compared to lab-based humidity cells. It was determined that properly conducted laboratory tests were similar in accuracy to those done in the field (Bennett et al., 2000). Doolittle's study showed the effect site specific geology is very important, as AMD formed at the study site within the same geologic units which was within 15 miles of the site of the lysimeter testing that predicted AMD would not form.

## METHODS

### Humidity Cell

The cores used in this study were chosen by varying sulfur content based on XRF analysis and identification of acid forming material (pyrite) from SEM data previously analyzed by Paul (2020) as well as geographic location to the lakes of interest. This is to assure that there was sufficient pyrite content and variation of soil in order to conduct the experiment and provide an accurate range of data. Two consecutive half-foot interval cores were combined to reach the desired 1 kg of soil needed for the leaching test. A third or fourth interval was combined if more soil was needed. Each sample of soil was tested for total sulfur, sulfate, and acidity. Total sulfur was determined using EPA method 6010C Inductively Coupled Plasma-Atomic Emission Spectrometry conducted at Ana-Lab Corporation in Kilgore, Texas. Sulfate was analyzed using EPA method 9056A Determination of Inorganic Anions Using Ion Chromatography and acidity was determined using Standard Method 2310B Titration Method. The initial weight of each cell was recorded before and after the soil sample had been placed inside the humidity cell.

Prior to use in humidity cells, an aliquot of 5 cm<sup>3</sup> was taken from each core sample and oven-dried at 105°C until the sample reached a constant weight. The sample aliquots were used to determine the total density (Blake and Hartge, 1986) and the moisture correction (Gardener, 1986) for the samples. A total of 10 composite samples were made, each consisting of four grab samples from a single core in order to make up sufficient volume (1 kg) for the humidity cell experiment. The composite samples were each wet sieved through a 2 mm sieve and then hand mixed. Then, 1 kg of soil (moisture corrected) from each sample was placed into the humidity cell. The samples were packed by adding 100 g of soil and then placing a 1 kg weight on top of the soil to create even compaction throughout the cell. This was done until 1 kg of soil was reached in each cell.

A humidity cell leaching study was conducted based on the ASTM Standard D5744-18 Standard Test Method for Laboratory Weathering of Solid Material Using a Humidity Cell (ASTM D5744-18). The purpose of the humidity cell leaching experiment was to simulate the oxidation of pyrite in the vadose zone. The vadose zone is the unsaturated area above the water table where pore space contains both air and water. Humidity cells mimic this condition since they do not experience full saturation and go through periods of wetting and drying. The humidity cell set-up in this experiment consisted of ten cells that have a 10.2

cm (4 in) inside diameter and are 20.3 cm (8in) tall. The bottom of the cells were perforated to allow leachate to drain into a collection flask. Polyester fiber was placed at the bottom of each cell to act as a filter to prevent sample loss during the leaching process. The top of the cells were left open to allow for ambient air exchange. The humidity cells were placed in an incubator set at a constant temperature (25°C) and humidity (60%) throughout the experiment. Each cell was flooded with 500 mL of deionized water on the same day once every week for up to 52 weeks or until the sulfate from the leachate was stable. Prior to cell flooding, an initial leach (week 0) was conducted in order to remove any salt (primarily sulfates) that may be present within the sample. Any cells that remain flooded with water after 24 hours (due to primarily clay texture) were disturbed to create secondary porosity to aid in drainage time. This was done by using a 2 mm stainless steel rod to puncture 20 holes through the clay-rich soil within the cell.

The cells were removed from the climate-controlled incubator and weighed prior to weekly flooding. Distilled and deionized (DI) water was discharged from a separatory funnel down the side of the cell to reduce sample agitation. Leachate was then drained from the base of the cell into a jar and drainage continued until the following morning to allow for full drainage. Once the weekly leach was completed, the weight of the cell was recorded. The difference in weight after the

cell was leached and the weight before the cell was leached were used to determine pore-water mass retention after the leaching period was completed. The cells were then placed back in the incubator for the next 6 days until leaching began again. The leachate was then tested to determine its changes in pH, ORP, sulfate, and acidity.

Once the full humidity cell test had been completed, the soil from the cells was dried at 40°C until a constant weight was achieved. These weights were recorded and the soil from each cell was tested for total sulfur, sulfate, and alkalinity, which was analyzed in the same manner as the initial soil samples.

### Leachate Testing

Each week, the leachate was tested for pH and ORP as the leachate was being collected using a pH and ORP probe. The final leachate was filtered through a 0.45 µm filter. Any solids collected on the filter were then returned to the respective humidity cell. The leachate was then tested for sulfate and acidity. The chemical analysis testing was done each week for the first five weeks and then every other week until weekly sulfate release and weekly acidity data stabilized. The tests were continued until sulfate stabilized or a rate shift occurred for four consecutive weeks or until 52 weeks of testing were completed.

### Ion Chromatography (IC)

Ion chromatography was conducted in the Plant, Soils, and Water Analysis laboratory at Stephen F. Austin State University and was used to determine the presence of sulfate within the leachate according to EPA Method 300.1 (US EPA, 1999). A lab blank and an equipment blank were tested for each batch and one duplicate sample was tested by picking one of the leachate collections at random.

### Most Probable Numbers

The presence of *Acidithiobacillus thiooxidans* and *Acidithiobacillus ferrooxidans* was tested for during the beginning, middle, and end of the leaching period (Mendez et al., 2007). Presence of oxidizing bacteria is an essential measurement in humidity cells, as it can lead to greatly increased rates of oxidation where pyrite can oxidize without the presence of oxygen.

The most probable numbers (MPN) procedure was used to determine the amount of acidophiles present in the leachate each week. The procedure was done by first making three solutions: 9K minimum salts medium, Starkey's medium, and Zwittergent extract (Mendez et al., 2007). Then 10 mL of the leachate solution was added to a 100 mL jar and then filled to the top with the Zwittergent extract. Serial dilutions for  $10^{-2}$  to  $10^{-7}$  dilutions were made with both

the 9K minimum salts medium and Starkey's medium. A positive and negative control was made for comparison. The samples were then incubated at 30°C and monitored every other day. Iron oxidizer colonies appear orange and sulfur oxidizer colonies decrease in pH when present in a sample. The amount of bacteria present in leachate was calculated using EPA's most probable number calculator (US EPA, 2013).

### Groundwater Sampling

Groundwater samples were taken once a month and tested for pH, ORP, dissolved oxygen, temperature, and specific conductance (SC). Fifteen wells were selected from the study site that best corresponded with the location of the selected core samples and the lakes of interest. Groundwater samples were collected from the monitoring wells using a low-flow (micropurge) procedure (US EPA, 2017). Water was pumped at a rate between 200 and 500 ml per minute from the well until the water quality reached stabilized readings that were taken every three to five minutes. The water quality parameters and stability ranges used for data collection are listed in Table 1.



Table 1. Stabilizations ranges used for water quality for low-flow micropurge groundwater sampling.

Water Quality Indicator Parameter	Stabilization ranges (Three successive readings)
pH	$\pm 0.1$ standard units
Specific Conductance	$\pm 3\%$
Dissolved Oxygen	$\pm 10\%$
Turbidity	$\pm 10\%$
Oxidation Reduction Potential	$\pm 10$ millivolts
Temperature	Not used for stabilization

Water quality was considered stabilized when three of the five parameters remained constant for three consecutive readings (US EPA, 2017).

A Geotech Geopump Series II peristaltic pump was used for water collection on all wells with a depth to water less than 25 ft. Wells that had a depth to water greater than 25 feet required the use of a Mega Monsoon pump in order to have enough power to pump water from at greater depth.

## Groundwater Data and Modeling

Collected groundwater data was compared to previous groundwater data results collected from the same well sites from Paul's (2020) previous studies. Collected well depths, well depths from Paul's (2020) study and well depths from USGS and surface lake data from groundwater fed lakes were used to create a groundwater contour map within ArcMap using nearest neighbor interpolation methods. Groundwater elevations were then compared with digital elevation model surface land elevations to calculate the volume of the vadose zone within the zone of influence for each lake.

The zone of influence for each lake was defined as any area within the mined pit that was up gradient in the water table from the lake where groundwater is subject to flow into the lake. The surface area of the mined pit was calculated from historical aerial images acquired from USGS for the years 1989 to 2001 (Figure 2a). Flow maps within the pit area were generated using the flow direction tool under the hydrology toolbox of the spatial analyst toolset in ArcMap. The flow direction map was used to define where the groundwater influx in the lakes was coming from. The groundwater contour elevation map, which was generated into a raster format, was subtracted from the land surface digital elevation model (DEM) for each zone of influence to determine the volume of

soil. The mass of soil was then calculated based on the average density of the soil.

The soil mass and volume of rainfall was then used to determine soil to water ratios for the field that will then be compared to soil to water ratios from the lab. These calculations were used as one of the scaling factors for converting lab oxidation rate to field oxidation rates. The vadose soil volume calculation was converted to soil mass based on the average density of the tested soil cores. Daily rainfall data was compiled from the National Oceanic and Atmospheric Administration (NOAA) from January 2010 to present to calculate average weekly rainfall. Rainfall volume was then converted from inches of rain per week to ml of rain within each zone of influence.

Daily high and daily low temperature data collected from NOAA, as well as collected groundwater temperature were used to determine if temperature was a necessary scaling factor for the humidity cells.

## Statistical Modeling

Statistical modeling allows for the prediction of future impact of water quality due to the input of AMD. Statistical regression modeling was used for laboratory data correlations in order to provide site specific geochemical predictions (Neter et al., 1996). Weekly sulfate release rates, acidity, and pH values were used to

make a line of best fit through the use of regression to find long term predictions. The type of regression utilized was varied based on the data trend. Regression was conducted for each humidity cell individually instead of combining all the humidity cell's data together. Since the site is highly heterogenous, this allowed for more accurate equations and provided a predicted time range from slowest to fastest oxidation rate of AFM. The regression model provided data trends and a coefficient of determination that helped determine the accuracy and reliability of the collected data (Neter et al., 1996).

Weekly loading of sulfate as well as total loading of sulfate was calculated using equations 4 and 5 respectively.

(Eq. 4) 
$$L_e = C_e \times M_e$$

Where:

$L_e$  = loading of constituents in the residue,  $\mu\text{g}$ ,

$C_e$  = concentration of the constituent in the residue,  $\mu\text{g/g}$ , and

$M_e$  = mass of the dried weathered residue in the filter media.

(Eq. 5) 
$$L_n = \sum_{i=0}^n (C_i \times M_i)$$

where:

$L_n$  = cumulative loading of the constituent for the  $n$  weeks,  $\mu\text{g}$ ,

$n$  = total number of weeks,

$i$  =  $i^{\text{th}}$  week,

$C_i$  = effluent concentration for the  $i^{\text{th}}$  week,  $\mu\text{g/g}$ , and

$M_i$  = effluent mass for the  $i^{\text{th}}$  week. g.

Missing data values for cumulative loading from weeks where sulfate release was not measured were interpreted based on the predicted values from the trendline for each cell (British Columbia AMD Task Force, 1989).

Predictive equations using regression modeling were then used on the sulfate loading and cumulative sulfate loading values. Modeling is necessary to provide predictions on water quality but has inherent limitations. Predicting future concentration has many variables that cannot always be accounted for but allow for the highest degree of accuracy when paired with kinetic test modeling and field data. In order to relate the field and lab data, scaling factors must be applied to the regression models.

Scaling factors were calculated by looking at field characteristics compared to lab characteristics to create field to lab ratios that were then multiplied together using Equation 1 to create a cumulative scaling factor. This scaling factor was then applied to each line of best fit equation to get the final equations used to predict field water quality using equation 2.

The equations predict the time range that AMD will persist which corresponds with the point in time equilibrium is reached at the site. Equilibrium was determined by graphing the release rate of sulfate or acidity (along the y axis)

and the pH (along the x axis). The rate of sulfate and acidity release when the pH equals background condition (4.7) was considered the release rate at equilibrium.

## RESULTS AND DISCUSSION

### Soil Core Analysis

The soil cores used in the humidity cell study were selected based on the levels of sulfur in the cores and whether or not pyrite was identified in the cores as determined from the Paul (2020) study. Geographic location of the core samples to the lakes of interest was also taken into consideration. The sulfur concentrations at each core depth are provided in Table 1a, Appendix A. Prior to leaching, soil was also tested for bulk density and determined to have an average density of 1.391 g/cm<sup>3</sup> (Table 2a, Appendix A). The soil samples were also weighed before and after drying and were determined to have an average water content of 15.68 percent.

In instances where the volume of a specific core grab sample had insufficient volume, adjacent depth samples were composited and analyzed for total sulfur, sulfate, and acidity as seen in Table 2. The soil within the humidity cells was re-analyzed for total sulfur, sulfate, and acidity at the end of the 52 week leaching study (Table 3). Paul (2020) concluded that there was no natural alkalinity in the soil to buffer acid mine drainage.

Table 2. Total Sulfur, sulfate, and acidity for the selected, combined, and homogenized samples from each selected well prior to leaching.

	Sulfur (mg/kg)	Sulfate (mg/kg)	Acidity ( $\mu$ Eq/kg)	Acidity (as CaCO <sub>3</sub> , mg/L)
Well 16	234	299	13800	555
Well 17	<150	153	6770	248
Well 18	1980	224	25400	1020
Well 19	4470	1160	47500	2040
Well 22	5690	313	40100	1580
Well 24	<120	43.1	6530	278
Well 25	1090	1190	21800	925
Well 26	354	144	8870	370
Well 28	<140	26.7	6520	278
Well 30	145	40	13200	555

Table 3. Total Sulfur, sulfate, and acidity for the selected, combined, and homogenized samples from each selected well after the completion of leaching.

	Sulfur (mg/kg)	Sulfate (mg/kg)	Acidity ( $\mu$ Eq/kg)	Acidity (as CaCO <sub>3</sub> , mg/L)
Well 16	<89	7.88	6500	287
Well 17	<117	<3.45	6610	287
Well 18	1210	137	8400	383
Well 19	314	74.5	6780	287
Well 22	752	140	6600	287
Well 24	<109	4.08	2110	95.5
Well 25	566	26.7	8970	383
Well 26	251	<3.56	2270	95.5
Well 28	<123	<3.63	4640	192
Well 30	169	7.57	10900	478



## Humidity Cell Leachate Analysis

The leachate from the humidity cell was tested for sulfate and acidity every week for the first five weeks and then biweekly until week 48. Leachate was tested every week for weeks 48 to 52. The leachate sulfate values for each week are shown in Table 3a, Appendix A, and graphs for each humidity cell are shown in Figures 2a-11a, Appendix A. Cumulative sulfate concentration throughout the duration of the study are shown in Figures 12a-21a, Appendix A. Cumulative concentrations are the summation of the sulfate release each week to display the total amount of sulfate that had been released since the beginning of the experiment (British Columbia AMD Task Force, 1989). The rate of sulfate release began to plateau near the end of the study period but was still consistently decreasing in all of the cells with an initial pH below 4.7 (background conditions) by the completion of the study at 52 weeks. Early sulfate release values that did not affect pH are likely due to an accumulation of sulfate in the soil that had not completely flushed from the core samples. Acidity consistently decreased for each humidity cell with a pH below 4.7 (Table 4a; Figures 22a-30a, Appendix A). Since both sulfate and acidity release from the humidity cells show significant trends, they are both considered for prediction of acid mine drainage and are further discussed in a later section.

Eh and pH Analysis

Humidity cell leachate was tested every week for pH and Eh (Figure 3 and 4, respectively). A graph and trend line for the pH values for each humidity cell are shown in Figures 31a-40a, Appendix A. Eh values prior to week 19 are likely inaccurate due to a faulty probe that did not properly hold calibration. Therefore, only values from week 19 and onward are displayed since only this time period thereafter is considered representative of the actual data at the site. It should also be noted that Eh values are more representative of true value when pH is less than 4.

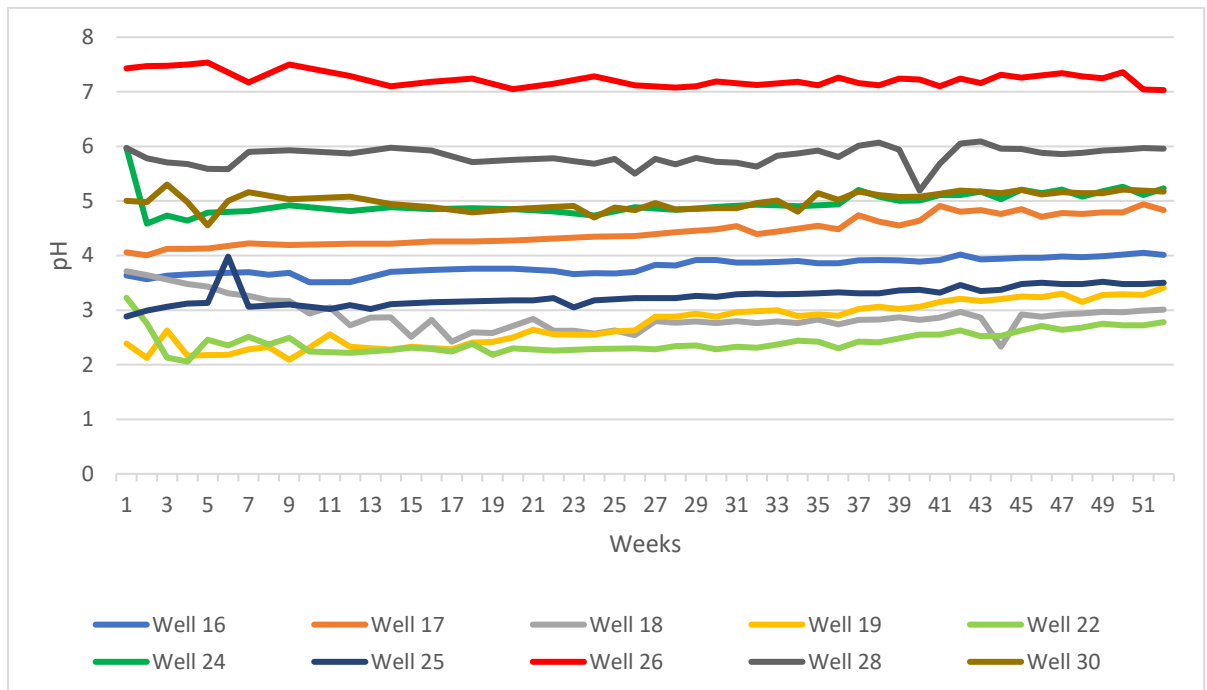


Figure 3. Humidity cell leachate pH from week 0 to week 52.

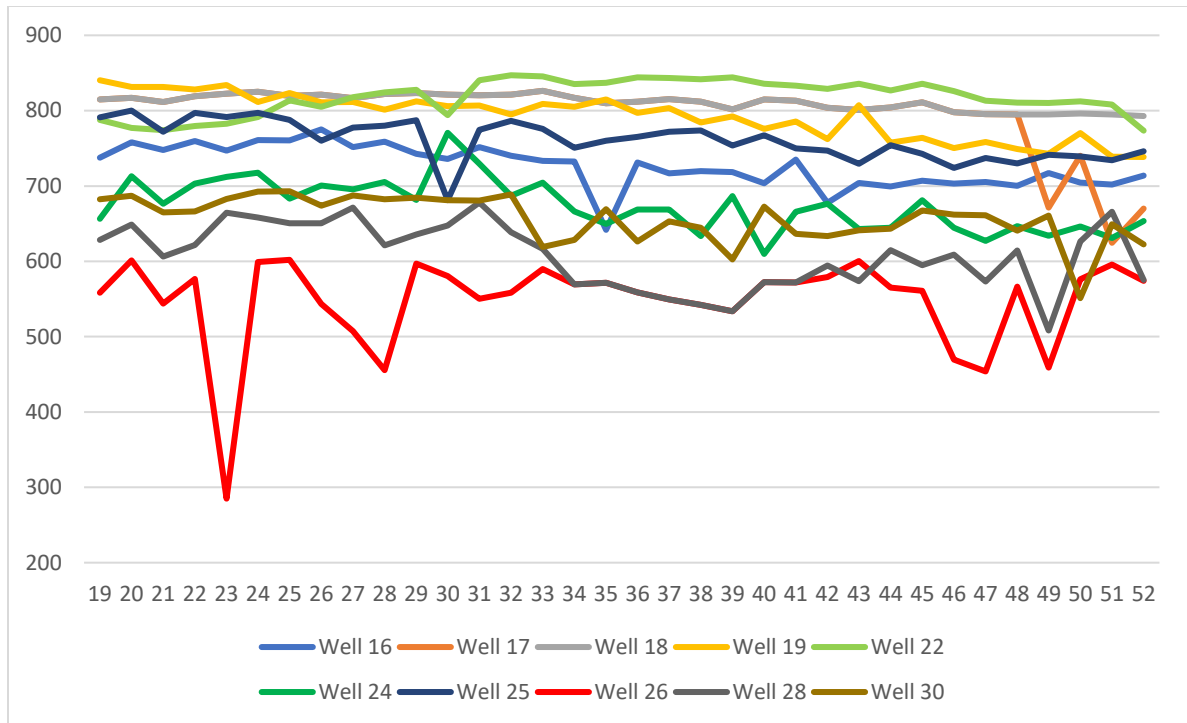


Figure 4. Humidity cell leachate Eh values from week 19 to week 48.

The background pH level at the site was 4.7 to 4.8 (Mercier, 2011). Humidity cells with cores from Wells 16, 17, 18, 19, 22, and 25 were the only cells (out of a total of 10) to exhibit a pH below background pH. Therefore, the other tested well cores (24, 26, 28, and 30) were not considered as representative sites that would contribute AMD to the lakes of interest and are thus excluded from predicting the longevity of AMD contribution.

Based on the data, pH values within each well showed little variance for the full 52 week testing period (Figure 3). Humidity cells with an initial pH less than 4.7 gradually increased in pH with the following exceptions: Well 18 decreased in

pH until week 17 and Well 22 decreased until week 12. All humidity cells starting below a pH of 4.7 had linearly positive slope showing a pH increase from 0.009 to 0.02 pH units per week (Table 4). The humidity cell pH equations for Well 18 and Well 22 are represented by the rate shift change after the slope became positive. The initial decrease in leachate pH from Well 18 and 22 (Figures Figure 34a and Figure 36a) is consistent with the increase in sulfate release (Figures Figure 5a and Figure 7a) and acidity (Figures Figure 25a and Figure 27a). Sulfate release increased until week 12 in Well 18 and week 9 in Well 22. pH lagged sulfate release by three to five weeks. While pH does show a linear trend in data, the change in pH occurs at such a small scale that it is not an accurate predictor for AMD.

Table 4. Linear pH trends for Humidity Cell leachate with a starting pH below site background levels.

Humidity Cell pH Trends	
Well 16	$y = 0.0087x + 3.596$
Well 17	$y = 0.0144x + 4.083$
Well 18	$y = 0.0112x + 2.409$
Well 19	$y = 0.0246x + 2.086$
Well 22	$y = 0.0136x + 1.983$
Well 25	$y = 0.0101x + 2.969$

Where  $y = \text{pH}$  and  $x = \text{week}$

All wells except Well 26 had stable Eh throughout the experiment, with no significant trends over the period of 52 weeks (Figure 4). Variation in Eh at Well

26 may be in part due to the neutral pH of the humidity cell. Comparison of Eh vs. pH for the humidity cells (Figure 5) to the Eh-pH mineral stability diagram in Figure 2 indicate that conditions were consistently favorable for the oxidation of pyrite to form goethite and/or jarosite precipitates in all 10 humidity cells during the leachate study period. It is under these conditions that AMD would be generated with sulfate being produced as a quantifiable by-product of pyrite oxidation. .

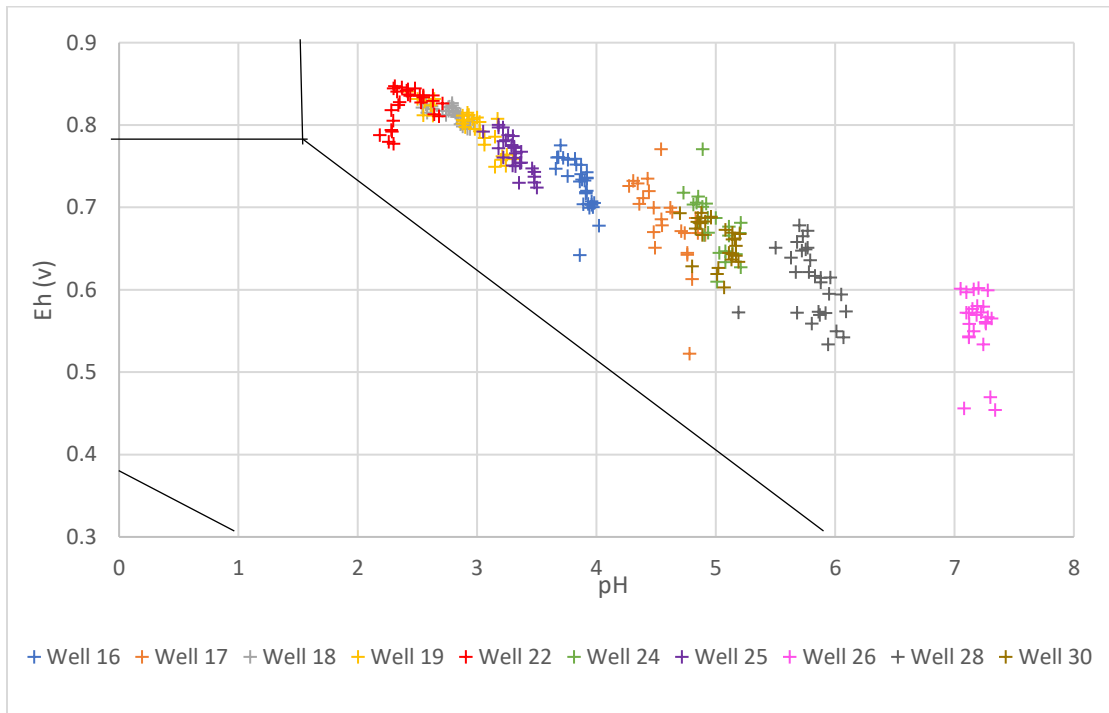


Figure 5. Eh vs. pH cross comparison in the humidity cells.

### Microbial Testing Results

Leachate was tested at the beginning, middle, and end of the study for the presence of iron oxidizing and sulfur oxidizing bacteria using the MPN method (Table 5) (Mendez et al., 2007). Sulfur oxidizing bacteria were not present in any of the humidity cells and only a few cells (Wells 19, 22, and 25) showed the presence of iron oxidizing bacteria. This data could suggest that there is a low presence of oxidizing bacteria in the field and was therefore reflected in the humidity cells. However, it is more likely that it is either the result of regular flushing of acidic material that prohibited the development of micro-acidic environments within the pore space (Morin, 2013) or due to frozen storage conditions of the soil prior to use in the humidity cells.

Table 5. The most probable number of iron and sulfur oxidizing bacteria per gram of soil for each humidity cell.

	Iron Oxidizing Bacteria		
	10 Weeks	26 Weeks MPN/ml	50 Weeks
Well 16	0	0	0
Well 17	0	0	0
Well 18	0	0	0
Well 19	0.199	0.199	0
Well 22	0.274	0.061	0
Well 24	0	0	0
Well 25	0.435	0	0
Well 26	0	0	0

Well 28	0	0	0
Well 30	0	0	0

**Groundwater Data**

Fifteen wells surrounding the lakes of interest were tested monthly from September 2019 to August 2020 for pH, Eh, dissolved oxygen, temperature, specific conductance, and turbidity (Table 5a, Appendix A). Figure 6 and Figure 7 show changes in pH and Eh respectively throughout the study period. Eh values prior to March, 2020 are likely inaccurate due to a faulty probe that did not properly hold calibration. Therefore, only values from week 19 through 52 are displayed, since only this time period is considered representative of the actual data at the site.

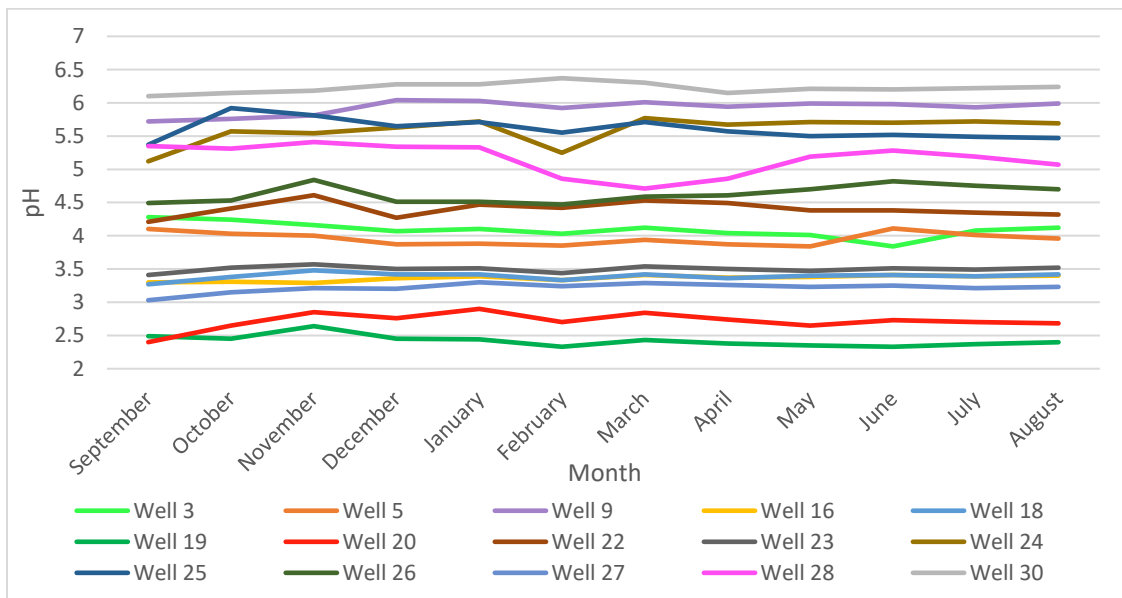


Figure 6. pH values of the wells of interest from September 2019 through August 2020.

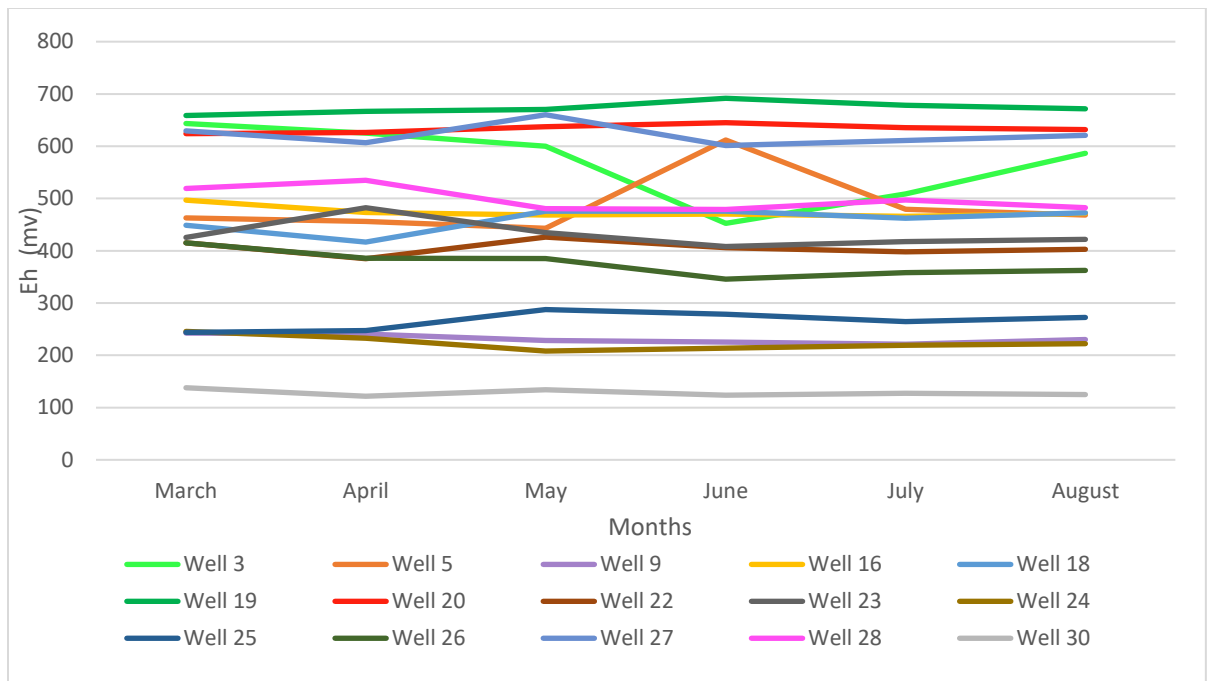


Figure 7. Eh values of the wells of interest from March 2020 through August 2020.

Eh was graphed with pH to determine which mineral phase was stable in the field. According to the data in Figure 8 and the reference diagram in Figure 2, pyrite is unstable and  $Fe^{2+}$  and goethite are stable in the field. Both  $Fe^{2+}$  and goethite are products of pyrite oxidation as seen in Reaction 1 and 2.



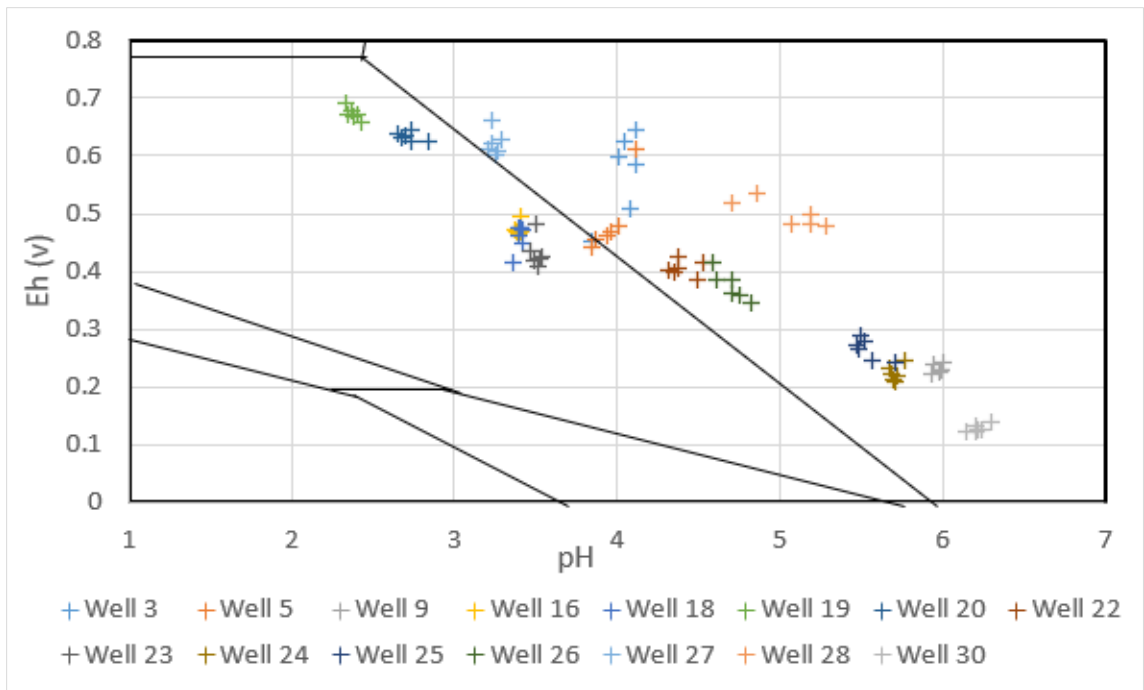


Figure 8. Eh vs pH cross comparison for the monitoring wells from March through August.

Transducer data from a previous on-site study (Paul, 2020) was used to determine average water table depths. The average depths collected in this study and data from the USGS were used to create a groundwater contour map (Figure 9). Water elevations in Figure 9 are more representative of actual water elevation near the lakes of interest because there was a greater concentration of measured data points. Water elevation further from the lakes of interest shows regional flow since there were less data points. Each point used to determine water table elevation can be seen in Figure 42a, Appendix A.

## Groundwater Elevation Within The Mined Pit Area, Oak Hill Mine, Henderson, Texas

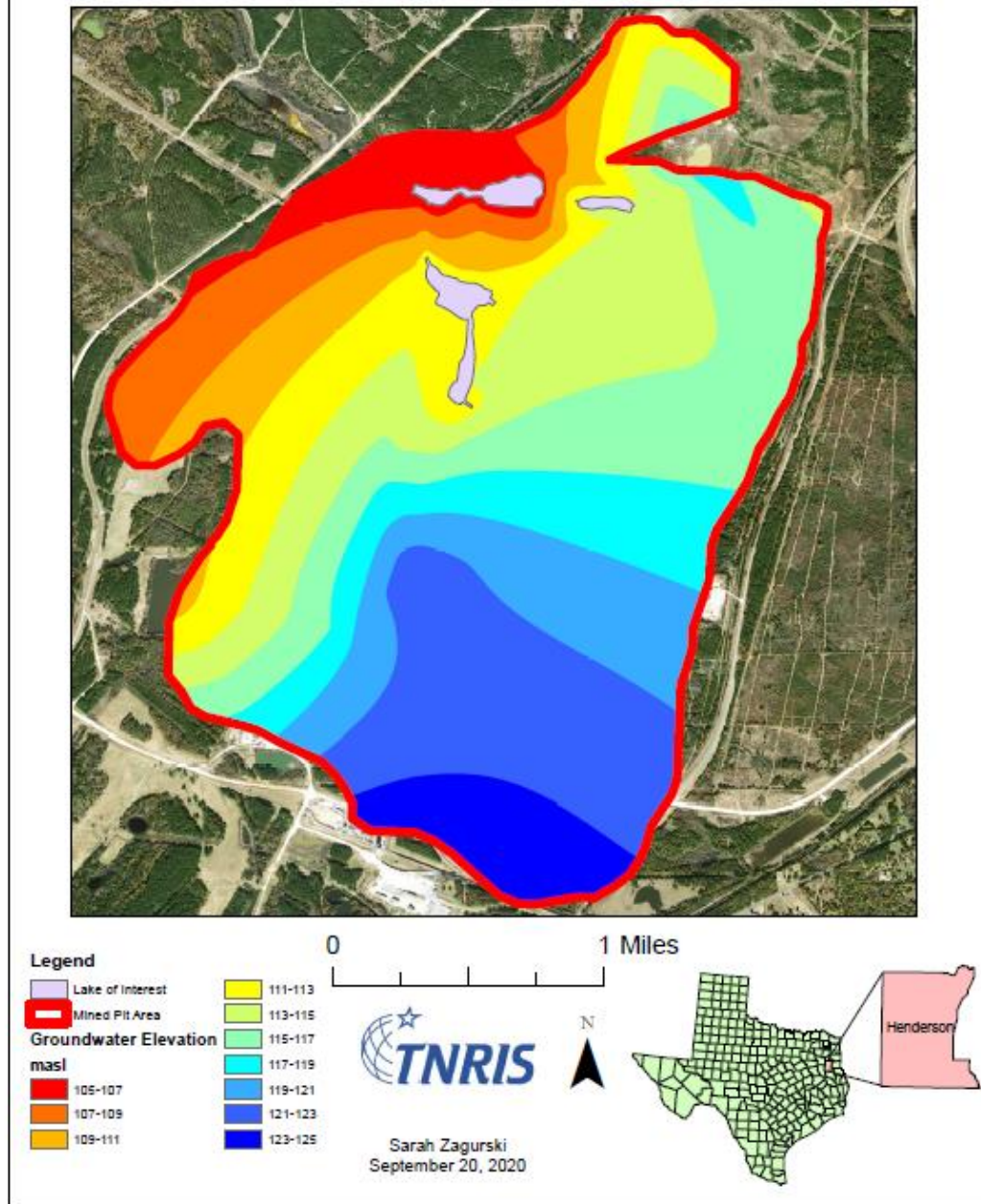


Figure 9. Groundwater elevation map within the mined pit at Oak Hill Mine, Henderson Texas.

## Vadose Zone Calculations

Historical aerial imagery was used to determine the mined pit surface area (Figure Figure 2a) within the same pit that the lakes of interest are located. The groundwater contour map (Figure 9) and a flow direction map generated in ArcGIS (Figure 43a) were used to determine the zone of influence. The zones of influence for each lake are shown in Figure 44a-Figure a - 46a, Appendix A. The result of the data gives the volume of soil for each zone of influence that was used in conjunction with the water volume data (Table 6) to create a scaling factor for water to soil ratios in the lab and field.

Table 6. Soil volume and soil mass data for the zones of influence for each lake of interest.

Lake	Volume Soil (m <sup>2</sup> )	Volume Soil (cm <sup>3</sup> )	Soil Density (g/cm <sup>3</sup> )	Soil mass (g)	Soil mass (kg)
DII55R	8.370 E+7	8.370 E+13	1.391	1.165 E+14	1.165 E+11
DII58R	1.307 E+7	1.307 E+13	1.391	1.819 E+13	1.819 E+10
DII35R	5.801 E+7	5.801 E+13	1.391	8.072 E+13	8.072 E+10

The average volume of water per week in the field was calculated based on rainfall data from the NOAA database from weather station GHCND:USC00414081 in Henderson, Texas (Table 7).

Table 7. Water volume data for the zones of influence for each lake of interest.

Lake	Surface Area (m <sup>2</sup> )	Average Rain Per Week (in)	Average Rain Per Week (m)	Volume Rain (m <sup>2</sup> )	Volume Rain Per Week (ml)
DII55R	6.411 E+6	0.9912	2.518 E+2	1.614 E+5	1.614 E+11
DII58R	9.004 E+5	0.9912	2.518 E+2	2.267 E+4	2.267 E+10
DII35R	4.375 E+6	0.9912	2.518 E+2	1.101 E+5	1.101 E+11

### Scaling Factor Calculations

Scaling factors that were considered in this study include particle size, pore gas content, temperature, soil to water ratios, and microbes. Scaling factors were determined based upon lab and field ratios in order to extrapolate field oxidation rate from lab oxidation rates.

Pyrite particle size in the field is framboidal which means that the particle size of pyrite is between silt and clay fraction size (around 0.5  $\mu\text{m}$ ) based on SEM imagery in Paul (2020). No grinding or crushing of the overburden occurred due

to the small size and the use of overburden material. The only size reduction method that was used in the study was a 2 mm sieve which would not have impeded any of the pyrite present in the soil. Since pyrite particle size was unaltered from the field to the benchtop study, the scaling factor was 1.

Pore gas content is a factor used in humidity cells to account for the time in which air is being injected into the system. This study utilized Method 2 of the ASTM Standard D5744-18 Standard Test Method for Laboratory Weathering of Solid Material Using a Humidity Cell (ASTM D5744-18) that does not inject air and relies on diffusion gas exchange from the ambient air. While depth of soil in the field may affect the pore gas content, it was determined to not be a significant factor to influence the scaling factor. This is because low oxygen concentration does not significantly retard oxidation and oxygen is not always required to oxidize pyrite (Morin, 2013). The scaling factor is, therefore, 1.

Temperature plays an important role in the rate of oxidation and was therefore considered when calculating scaling factors. The humidity cells were kept at a constant temperature of 25 °C (+/- 10 percent). Average daily high and daily low temperatures were calculated from data from NOAA and groundwater temperature was monitored for a full year in the study. The average of daily high ambient air temperature for the last 10 years falls within 10 °C of the humidity cell temperature. The average daily low temperature is 14 °C lower than the humidity

cell temperature. Monthly groundwater average temperatures ranged from 15.24 to 26.64 °C. The groundwater temperature data falls within 10 °C of the humidity temperature for every month. Soil temperature in the field likely falls between the air and water temperature values for most months. Soil temperature in the field and humidity cell temperature do not vary enough to significantly impact oxidation rates and therefore has a scaling factor of 1 (Kempton, 2012).

Soil to water ratios were evaluated for both field and lab conditions. Soil mass for the humidity cells were weighed and moisture corrected prior to leaching. Soil to water ratios were then determined based on the amount of water added to the humidity cell each week. Table 8 shows the data for lab soil to water ratios.

Table 8. Soil to water ratios for the humidity cells.

Humidity Cell	Soil Mass (kg, moisture corrected)	Water Volume (mL/Week)	Soil:Water (kg/mL/week)
Well 16	1.012	500	2.024 E+-3
Well 17	1.012	500	2.024 E+-3
Well 18	0.9276	500	1.855 E+-3
Well 19	0.8218	500	1.644 E+-3
Well 22	1.012	500	2.024 E +-3
Well 24	1.012	500	2.025 E+-3
Well 25	1.012	500	2.025 E+-3
Well 26	1.012	500	2.024 E+-3
Well 28	1.012	500	2.024 E+-3
Well 30	1.012	500	2.024 E+-3

Soil to water ratios for the field were determined by using the soil volumes from Table 6 and rainfall volumes from Table 7. Ratios were calculated from for each zone of influence for the three lakes of interest (Table 9).

Table 9. Soil to water ratios for the zone of influence for the lakes of interest.

Lake	Soil Mass (kg)	Volume Rain Per Week (mL/week)	Field Soil to Water Ratio (kg/mL/week)
DII55R	1.164 E+11	1.614 E+11	0.7215
DII58R	1.819 E+10	2.267 E+10	0.8024
DII35R	8.072 E+10	1.101E+11	0.7329

Lab to field scaling factors were then calculated using the lab soil to water ratio and the field soil to water ratio. A scaling factor was determined for each combination of humidity cell ratios and zone of influence ratios (Table 10). The average ratio was then calculated

Table 10. Soil to water scaling factors for each humidity cell and zone of influence combination.

Humidity Cell	Lake	Scaling Factor
Well 16	DII-35R	2.761 E+-3
	DII-55R	2.805 E+-3
	DII-58R	2.522 E+-3
Well 17	DII-35R	2.761 E+-3
	DII-55R	2.805 E+-3
	DII-58R	2.522 E+-3
Well 18	DII-35R	2.531 E+-3
	DII-55R	2.571 E+-3
	DII-58R	2.312 E+-3
Well 19	DII-35R	2.243 E+-3
	DII-55R	2.278 E+-3
	DII-58R	2.048 E+-3
Well 22	DII-35R	2.761 E+-3
	DII-55R	2.805 E+-3
	DII-58R	2.522 E+-3
Well 24	DII-35R	2.762 E+-3
	DII-55R	2.806 E+-3
	DII-58R	2.523 E+-3
Well 25	DII-35R	2.763 E+-3
	DII-55R	2.806 E+-3
	DII-58R	2.523 E+-3
Well 26	DII-35R	2.761 E+-3
	DII-55R	2.805 E+-3
	DII-58R	2.522 E+-3
Well 28	DII-35R	2.762 E+-3
	DII-55R	2.805 E+-3
	DII-58R	2.523 E+-3
Well 30	DII-35R	2.761 E+-3
	DII-55R	2.805 E+-3
	DII-58R	2.522 E+-3
<b>Average</b>		<b>2.623 E+-3</b>



Lastly, microbial effects were scaled from field to lab conditions. There was little microbial activity in the lab (Table 5) versus what is expected in the field. This means that the scaling factor utilized for microbial activity should be greater than one to express higher biotic oxidation rates in the field than in the benchtop study. Biotic oxidation rates within the study site were not established; therefore, study specific oxidation rates could not be utilized in the determination of the microbial scaling factor. Instead, published datum incorporating the highest abiotic oxidation rate of  $3.0 \times 10^{-9} \text{ mol L}^{-1} \text{ s}^{-1}$  (McKibben and Barnes, 1989) and the biotic rate of  $8.8 \times 10^{-8} \text{ mol L}^{-1} \text{ s}^{-1}$  (Olson, 1991) were utilized to determine the microbial scaling factor. These published abiotic and biotic rate studies were determined under similar laboratory conditions (particle size, temperature, moisture, etc.), and therefore considered comparable. The highest abiotic rate was used to avoid overestimating the effect of microbial activity (McKibben and Barnes, 1989). This makes the field to lab ratio 29.33.

The cumulative scaling factor can then be calculated according to Equation 1 based on each scaling factor variables provided in

Table 11.

Table 11. Scaling factor for each variable considered in the study.

Variable	Scaling Factor
Particle Size	1.000
Pore Gas Content	1.000

Temperature	1.000
Soil:Water	0.0026
Microbes	29.33

The cumulative scaling factor was calculated as follows:

(Eq. 6)  $1.000 \times 1.000 \times 1.000 \times 0.0026 \times 29.33 = 0.0769$

### AMD Prediction Calculations

Line of best fit equations were fitted for each humidity cell with an initial pH of less than 4.7 based on sulfate concentrations in mg/Kg. Cells that exhibited an increase in sulfate release and a decrease in pH at the beginning of the study (Well 18 and 22) were fit for the portion of the curve that exhibited a decrease in sulfate per unit of time since it is more representative of future conditions. Table 12 shows the line of best fit equation and the R<sup>2</sup> values for each of these cells.

Table 12. Line of best fit equation and R<sup>2</sup> values for sulfate release for each humidity cell with an initial pH less than 4.7 (Figures Figure 3a-Figure 11a).

Humidity Cell	Lab Sulfate Release Rate Equation (mg/Kg)	R <sup>2</sup>
Well 16	$y = 3.924e^{-0.02x}$	0.8389
Well 17	$y = -0.5440\ln(x) + 2.9537$	0.9546
Well 18	$y = -41.26\ln(x) + 184.3$	0.9480
Well 19	$y = 265.18e^{-0.066x}$	0.9462
Well 22	$y = -152.1\ln(x) + 613.7$	0.9777
Well 25	$y = 165.9x^{-0.971}$	0.8834

Where y= sulfate concentration (mg/kg) and x= time (weeks)

The equations in Table 12 are based on the best possible R<sup>2</sup> value, and therefore each cell does not have the same model. The uniform model that fits all six humidity cells that are below background concentrations is logarithmic and is as follows:

(Eq. 7) 
$$\text{Sulfate} = a \ln(\text{time}) + b$$

The equations and R<sup>2</sup> values based on this model are displayed in Table 13. The R<sup>2</sup> values are not as high for each humidity cell but allow for the comparison of reaction rates among each cell. The relationship between slope (a) and intercept (b) in Equation 6 is based on the initial sulfur content in the soil, which is shown in Figure 10 and 12 respectively. These graphs show that the slope of the equation is negatively correlated with sulfur content in the soil while the intercept is positively related to sulfur content.

Table 13. Lab release rate equations based upon a uniform model (Eq. 6) for each humidity cell where x=time.

Humidity Cell	Lab Sulfate Release Rate Equation (mg/Kg)	R <sup>2</sup>
Well 16	$y = -0.771\ln(x) + 4.762$	0.7334
Well 17	$y = -0.544\ln(x) + 2.954$	0.9546
Well 18	$y = -41.26\ln(x) + 184.3$	0.9480
Well 19	$y = -99.97\ln(x) + 378.6$	0.8902
Well 22	$y = -152.1\ln(x) + 613.7$	0.9777
Well 25	$y = -19.66\ln(x) + 73.57$	0.8624

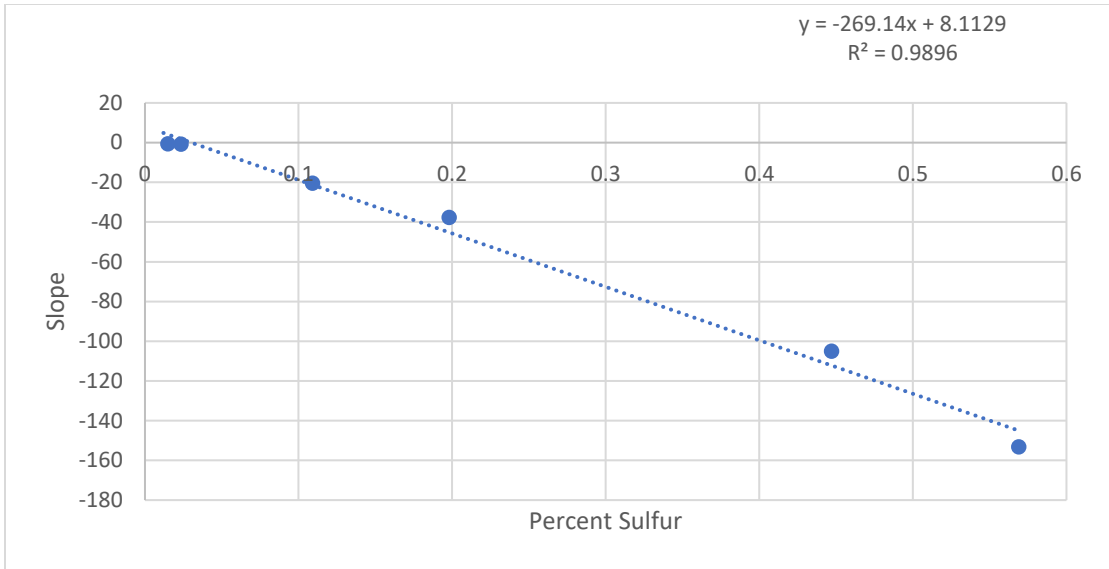


Figure 10. Slope of logarithmic predictor equations versus the initial percent of sulfur in the soil.

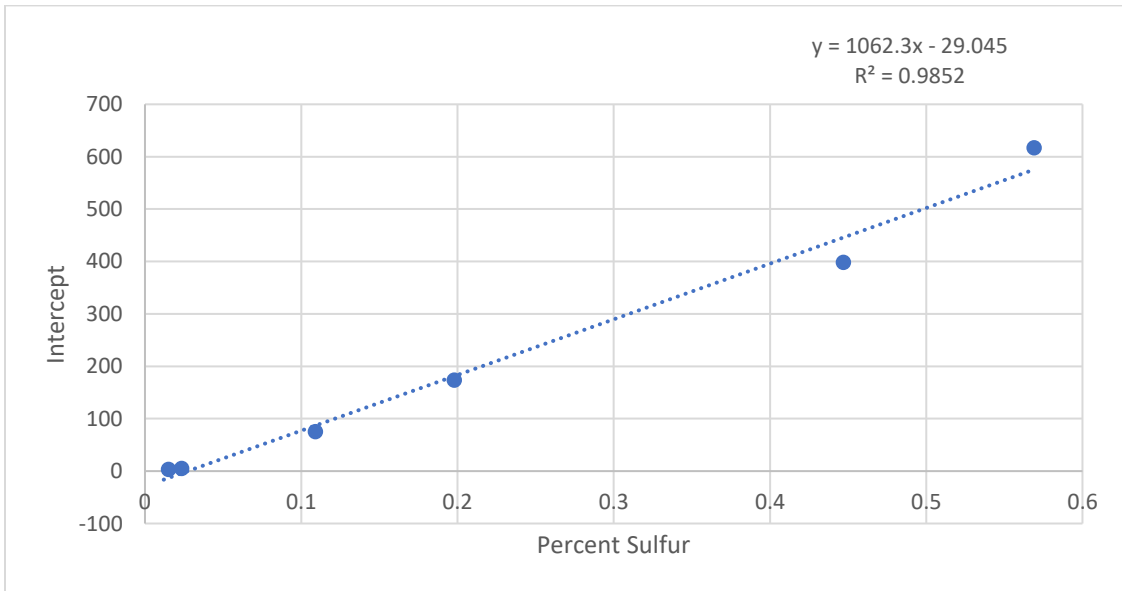


Figure 11. Intercept of logarithmic predictor equations versus the initial percent of sulfur in the soil.

While sulfate release equations based on a uniform model (Table 13) are useful in comparing the reason for different release rates, the best fit sulfate release equations (Table 12) are preferable for predictions because they better capture the trends of each individual humidity cell. This can be seen particularly in Well 16. The uniform model equation for Well 16 (Table 13) predicts initial release rates with a high degree of accuracy but then underpredicts release rates near the end of the study leading to drastically different time predictions.

The cumulative scaling factor was applied to each equation in Table 12 to determine future field conditions. This was done by multiplying the release rate in the lab by the cumulative scaling factor (0.0769) as seen in Equation 2. In order to determine the time frame in which AMD will cease and the site will return to background conditions, the release rate at equilibrium was determined by graphing the release of sulfate by the pH as seen in Figure 12. Based on this data, the sulfate release rate at equilibrium (4.7 pH) is approximately  $1 \text{ mg kg}^{-1} \text{ week}^{-1}$ .

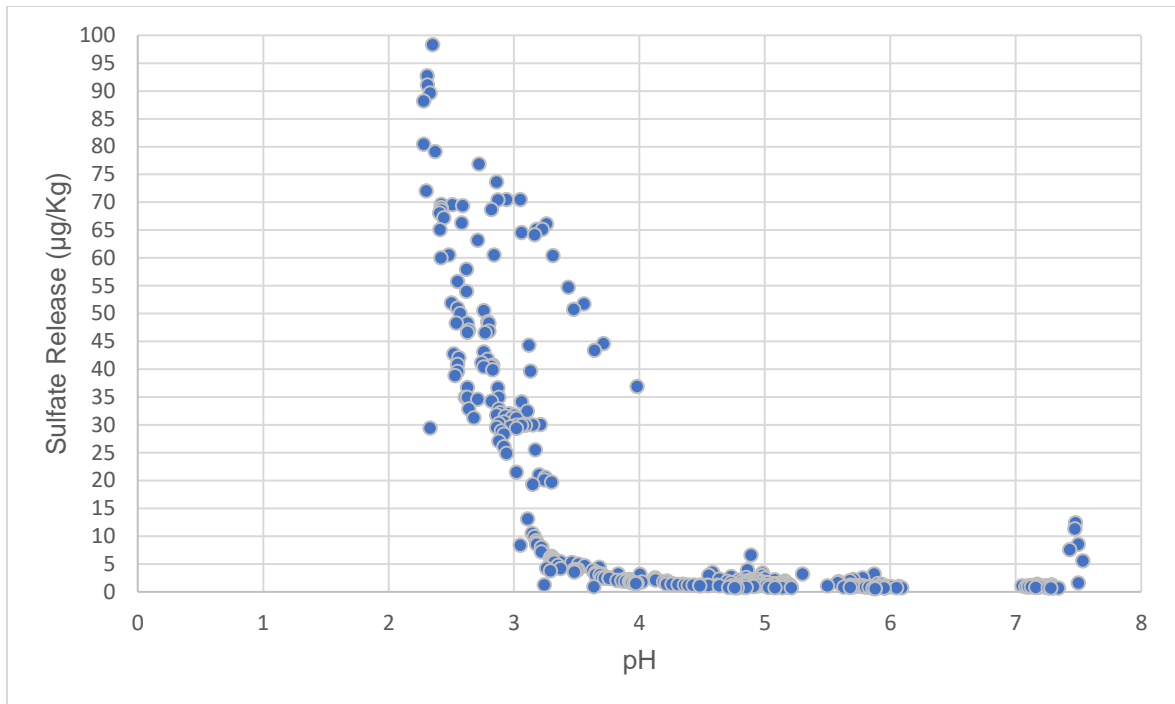


Figure 12. The release rate of sulfate (y) and the pH of the humidity cells used to determine the sulfate release rate at equilibrium (with a maximum sulfate release value of 100 mg/kg).

The scaled sulfate release equations were used to determine the time at which sulfate release equals 1 mg/kg. The scaled equations and the time predictions for the lab release rates and field release rates to reach equilibrium can be seen in Table 14.

The data shows a large variation in time in which AMD will persist. This is likely due to the mineralogy of each cell, the soil texture, and the amount of pyrite present in each overburden sample. The soil texture and mineralogy of each humidity cell is shown in Table 1a, Appendix A. There were varying amounts of

sulfur content in the post-mined soil at the study site. Well 22 contained the highest sulfur content (3060.7 mg/kg) at the study site as confirmed through x-ray fluorescence (Paul, 2020). For purposes of this study, Well 22 is considered representative of release rates of overburden with similar sulfur content and texture. Wells 26 and 28 reported no of sulfur below the detection limit of 200 mg/kg (Paul, 2020) and is considered representative of overburden with lower sulfur content and similar texture.

Table 14. Field sulfate release equations and equilibrium time predictions for the lab and the field.

Humidity Cell	Weeks in Lab	Field equation	Weeks in Field	Years in Field
Well 16	71.00	$y = 3.924e^{-0.0015x}$	911.41	17.52
Well 17	38.88	$y = -0.5440\ln(x \cdot 0.0769) + 2.954$	472.09	9.09
Well 18	157.33	$y = -41.26\ln(x \cdot 0.0769) + 184.3$	1105.23	21.25
Well 19	1326.95	$y = 265.18e^{-0.0051x}$	1094.19	21.04
Well 22	113.65	$y = -152.1\ln(x \cdot 0.0769) + 613.7$	730.35	14.05
Well 25	195.25	$y = 165.9(x \cdot 0.0769)^{-0.971}$	2513.15	48.33



Best fit curves were also determined based upon the acidity data using the equations provided in Table 15. While the trends for acidity are similar to that of pH, the acidity concentrations at equilibrium were not as well defined as seen in Figure 13. It is possible that different soil cores reached equilibrium at different acidity levels, but it is more likely due to experimental error. A weaker base ( $\text{CaCO}_3$ ) could have been used in titration rather than NaOH to give a more accurate determination for acidity, as many of the values reached a pH greater than 7 during the titration process from small amounts (.04 ml) of the titrant. The variance from the best fit lines for acidity is greater than the variance in sulfate release. It is probable that this is also due to over titration of samples. For this reason, sulfate release is the best predictor for future conditions from the collected data.

Table 15. Line of best fit equation and  $R^2$  values acidity release for each humidity cell with an initial pH less than 4.7.

Humidity Cell	Lab Acidity (mg/L)	$R^2$
Well 16	$y = -12.52\ln(x) + 56.70$	0.8466
Well 17	$y = -7.348\ln(x) + 32.70$	0.7886
Well 18	$y = 439.1e^{-0.048x}$	0.9862
Well 19	$y = 2086.1e^{-0.088x}$	0.9313
Well 22	$y = 1236e^{-0.039x}$	0.6218
Well 25	$y = 625.3x^{-0.828}$	0.8607

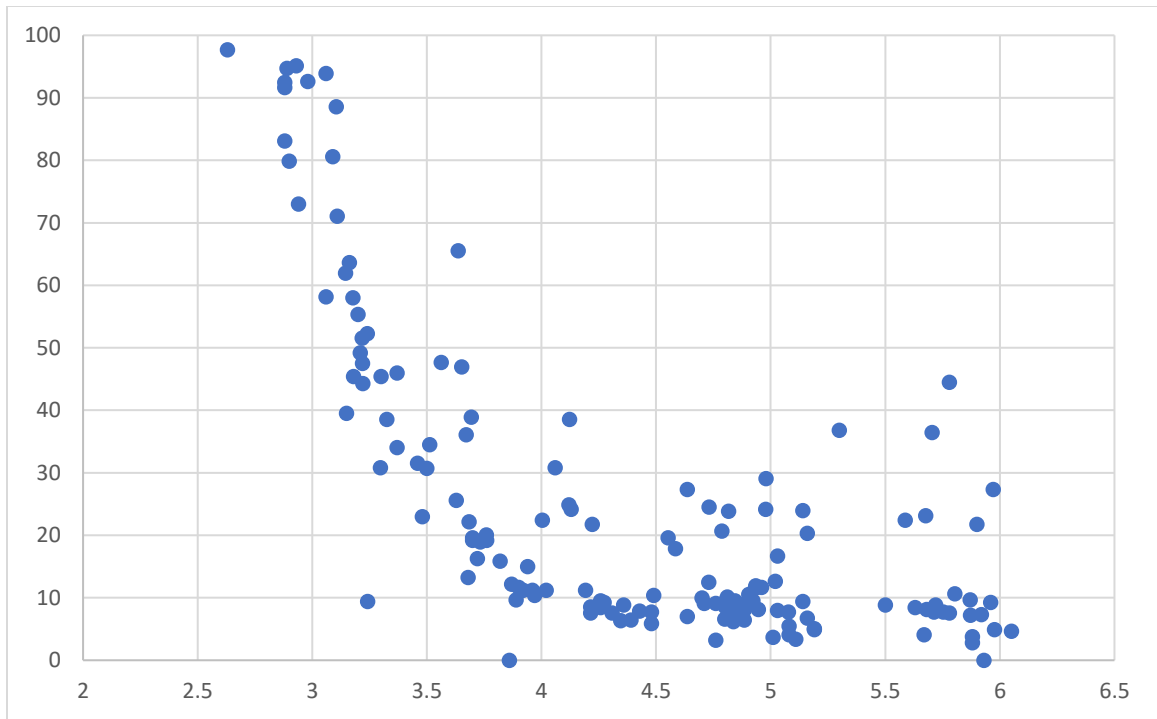


Figure 13. The release rate of acidity (y) and the pH of the humidity cells to determine the acidity release rate at equilibrium (with a maximum acidity release value of 100 mg/kg).

### Limitations to AMD predictions

Limitations of the prediction of AMD drainage are significant and should be considered when using models for future conditions. The model in this study is constrained by the following assumptions:

- 1) Reactions in the field are occurring predominately within the vadose zone of the mined pit area.
- 2) The data from the lab is representative of conditions in the field or can be adjusted through the use of scaling factors.

- 3) All rainfall that falls within the zone of influence for each lake of interest enters the vadose zone.
- 4) Microbes affect the rate of oxidation within the field.

These assumptions can affect data interpretation and prediction values of future conditions. Of special note is assumption 3, where surface runoff coefficients and evapotranspiration rates were not evaluated. This may lead to an over-estimation of water volumes entering the vadose zone leading a higher soil to water ratio in the field. This leads to a bias towards a shorter time frame for the persistence of AMD.

The coefficient of determination ( $R^2$ ) for the prediction of lab values indicate error in the models' ability to predict future conditions. Furthermore, humidity cells that still had high sulfate release values at the completion of the study (Wells 18,19, and 22) could potentially exhibit a curve more similar to Well 25 (Figure 9a, Appendix A) when sulfate values near equilibrium. This information would not be known unless humidity cell testing were to continue until sulfate release values neared equilibrium for all humidity cells. The possibility that the samples used in the study were not fully representative of the heterogenous overburden would also affect the time in which acid mine drainage would exist.

Differences in measured parameters in the lab versus parameters measured in the field must be taken into account when interpreting the data. The pH values

measured directly from the monitoring wells differed from the leachate pH values of the humidity cells. The degree of mixing in the groundwater between monitoring well locations and other surrounding areas affects the measured values and is not expected to be represented by the pH values measured in the benchtop humidity cell study. Sulfate and acidity concentration in the field is also affected by mixing of groundwater. These limitations should be considered when using the lab data for remediation purposes.

## CONCLUSION

The goal of this study was to determine the number of years it will take for the AMD around lakes DII-35R, DII-55R, and DII-58R within Oak Hill Mine to cease. This study was intended to aid Luminant in future management of the AMD seeps on the site and help in determining the most cost-efficient management approach. Modeled data from this study site may also help Luminant estimate the pyrite oxidation of other areas with similar local geology to a lesser degree of accuracy.

The data from this study suggests that portions of the heterogenous overburden do not currently contribute to AMD. For areas of the site where overburden is contributing to AMD, the time in which it will persist varies. It is estimated that overburden with lower sulfur content could cease to generate AMD within 10 years (Table 14). However, overburden with higher sulfur content may continue to produce acidic drainage below background pH levels for over 48 years (Table 14). It is likely that the persistence of AMD will fall somewhere between these time frames due to intermixing of groundwater in the heterogeneous overburden, which has variable concentrations of AFM. The data

suggests that much of the overburden will stop producing acid above background levels within the next 50 years (Table 14).

Continuing the leaching experiment for humidity cells that were still leaching sulfate at a significantly higher rate than equilibrium for a longer period of time would have improved the accuracy of acid mine drainage persistence modeling. Groundwater monitoring over a longer period of time would also aid in better interpretation of the data and scaling of the benchtop study. Future studies to follow this research would be to determine a cost-effective remediation technique to increase the pH of groundwater coming from the acid seeps that feed into lakes DII 35R, DII 55R, and DII 58R. This may include techniques such as a permeable reactive barrier upgradient of the acid seeps.

## LITERATURE CITED

- Alpers C. N., Nordstrom, D. K., 1999. Geochemistry of acid mine waters. IN: The Environmental Geochemistry of Mineral Deposits, G.S. Plumlee and M. J. Logsdon, eds., Rev. Econ. Geol. v. 6A, Soc. Econ. Geol. Inc., Littleton, CO.
- American Society for Testing and Materials. 2018. Standard Test Method for Laboratory Weathering of Solid Materials Using a Humidity Cell. ASTM D5774-18. ASTM International, West Conshohocken, PA, 2018
- Bennett J.W, Comarmond M. J., Jeffery J. J. 2000. Comparison of Oxidation Rates in Sulfidic Mine Wastes Measured in the Laboratory and Field. Australian Centre for Mining Environmental Research, Australia.
- Baker B. J., Banfield J. F. 2003. Microbial Communities in Acid Mine Drainage. Department of Earth and Planetary Sciences and Environmental Sciences Policy and Management, University of California Berkley, Berkley, California.
- Blake, G.R. and Hartge, K.H., 1986. Bulk density 1. Methods of soil analysis: part 1—physical and mineralogical methods, (methodsofsoilan1), pp.363-375.
- British Columbia Acid Mine Drainage Task Force. 1989. Draft Acid Rock Drainage Technical Guide, vol. 1. Stephen Roberston and Kristen Inc., Vancouver, B.C.
- Chen, Y., Wen, Y., Zhou, Q., Vymazal J., 2014. Effects of plant biomass on nitrogen transformation in subsurface-batch constructed wetlands: a stable isotope and mass balance assessment. *Water Research* 63:158–167.
- Descotes, M., Vitorge, P., Beaucaire, C., 2004. Pyrite Dissolution in Acidic Media. *Geochimica et Cosmochimica Acta*, v. 68, pg. 4559-4569.
- Doolittle, J. J. 1986. Pyrite Oxidation in a Minespoil Environment: a Lysimeter Study. M.S. thesis. Texas A&M University, College Station, Texas
- Gardner, W.H., 1986. Water content. *Methods of Soil Analysis: Part 1—Physical and Mineralogical Methods*, (methodsofsoilan1), pp.493-544.

- Gee, G.W. and Bauder, J.W., 1986. Particle-size analysis 1. Methods of soil analysis: Part 1—Physical and mineralogical methods, (methodsofsoilan1), pp.383-411.
- Hageman, P. L. 2003. Leaching Studies: Assessing the Toxicity Potential of Mine Waste Spoil Workshop. Billings Symposium/ASMR Annual Meeting. U.S. Department of the Interior, U.S. Geological Survey.
- Hanna, B., and K. Lapakko. 2012. Waste rock sulfate release rates at a former taconite mine, laboratory and field-scale studies. IN: Proceedings of the 2012 International Conference on Acid Rock Drainage, Ottawa, Canada, May 22-24.
- Holmes, P.R., Crundwell, F. K. 1999. The Kinetics of the Oxidation of Pyrite by Ferric Ions and Dissolved Oxygen: An Electrochemical Study. Billiton Centre for Bioprocess Modelling, University of the Witwatersrand, Johannesburg, South Africa.
- Kempton, H. 2012. A Review of Scale Factors for Estimating Waste Rock Weathering from Laboratory Tests. IN: IN: Proceedings of the 2012 International Conference on Acid Rock Drainage, Ottawa, Canada, May 22-24.
- Klein, J. M. 2000. Late Paleocene paleoenvironmental gradients in Wilcox Group strata, Big Brown Mine, TX, M.S. thesis, Texas A&M University, College Station, TX.
- McCauley, A., Jones, C., Olson-Rutz, K., 2017. Soil pH and Organic Matter. Montana State University, Bozeman, MO.
- McKibben, M. A., Barnes, h. L., 1989. Oxidation of pyrite in low temperature acidic solutions-Rate laws and surface textures: *Geochemical Cosmochimica Acta*, v. 50, pg. 1509-1520.
- Mendez, M. O., E. P. Glenn, and Rm. M. Maier. 2007. Phytostabilization potential of quailbush for mine tailings: growth, metal accumulation, and microbial community changes. *J. Environ Qual.*, 36:245-253.
- Mercier, L. J. 2014. Low pH waters in the vicinity of Oak Hill Mine: a statistical evaluation of water quality. M.S. thesis. University of Texas, Austin, TX.



- Morin, K.A., 2013. Scaling factor for humidity-cell kinetic rates for larger-scale predictions. MDAG Internet Case Study #38.  
[http://www.mdag.com/case\\_studies/cs38.html](http://www.mdag.com/case_studies/cs38.html)
- Morin, K.A., and N.M. Hutt. 1994. An empirical technique for predicting the chemistry of water seeping from mine-rock piles. IN: Proceedings of the Third International Conference on the Abatement of Acidic Drainage, Pittsburgh, Pennsylvania, USA, April 24-29, Volume 1, p. 12- 19.
- Neter, J., Kutner, M. H., Nachtsheim, C. J., Wasserman, W. 1996. Applied Linear Statistical Modeling. Fourth Edition. The McGraw-Hill Companies, Inc.
- Olson, G. J., 1991. Rate of pyrite bioleaching by *Thiobacillus ferrooxidans*-Results of an interlaboratory comparison: Applied and Environmental Microbiology, v. 57, pg. 642-644.
- Pastor, Behling & Wheeler, LLC. 2014. Acid-seep investigation report Oak Hill Mine Rusk County, Texas.
- Paul, J. C. 2020. Investigating sources of consistent low pH in surface waters at Oak Hill Mine. Ph.D. Thesis, Texas A&M University, College Station, TX (in edit).
- Pozo-Antonia, S., Puente-Luna, I., Lagueta-Lopez, S. 2013. Techniques to Correct and Prevent Acid Mine Drainage: A Review. DYNA, vol. 81, no. 186, 2014.
- Sexsmith, K., MacGregor, D., 2014. What determines lag times in humidity cell tests? IN: SME Annual Meeting and Exhibit 2014, Salt Lake City, Utah, February 23-26.
- Shaw, S., and A. Samuels. 2012. An empirical comparison of humidity cell and field barrel data to inform scale-up factors for water quality predictions. IN: Proceedings of the 2012 International Conference on Acid Rock Drainage, Ottawa, Canada, May 22-24.
- Skousen, J., Zipper, C.E., Rose, A., Ziemkiewicz, P. F., Nairn, R., McDONald, L. ., Kleinmann, R. L. 2016. Review of passive systems for acid mine drainage treatment. Mine water and the environment, vol. 36, no. 1, 2016, pp. 133–153.
- Soult, A., 2019. The pH Concept. Chemistry LibreTexts, Chapter 8, Section 6.  
[https://chem.libretexts.org/Bookshelves/Introductory\\_Chemistry/Book%3A\\_](https://chem.libretexts.org/Bookshelves/Introductory_Chemistry/Book%3A_)

Chemistry\_for\_Allied\_Health\_(Soul)/08%3A\_Properties\_of\_Solutions/8.06  
%3A\_The\_pH\_Concept.

U.S. Environmental Protection Agency. 1994. Technical Document: Acid Mine Drainage Prediction. EPA 530-R-94-036 Office of Solid Waste, Washington DC.

U.S. Environmental Protection Agency. 2017. *Suggested operating procedures for aquifer pumping tests*. USEPA Rep. EPA/540/S-93/503. Technology Innovation Office, Office of Solid Waste and Emergency Response, Washington, DC.

U.S. Environmental Protection Agency. 1999. Method 300.1, Revision 2.2: *Determination of inorganic anions by ion chromatography*. EPA-821-R-99-015. National Exposure Research Laboratory, Office of Research and Development, Cincinnati, OH.

US Environmental Protection Agency (USEPA). 1983. Environmental Impact Statement: Martin Lake D Area Lignite Surface Mine Henderson, Rusk County Texas, USEPA, EPA 906/9-83-003

U.S. Environmental Protection Agency (USEPA) 2013. MOST PROBABLE NUMBER (MPN) CALCULATOR Version 2.0 User and System Installation and Administration Manual, Washington, DC.

## APPENDIX A – FIGURES

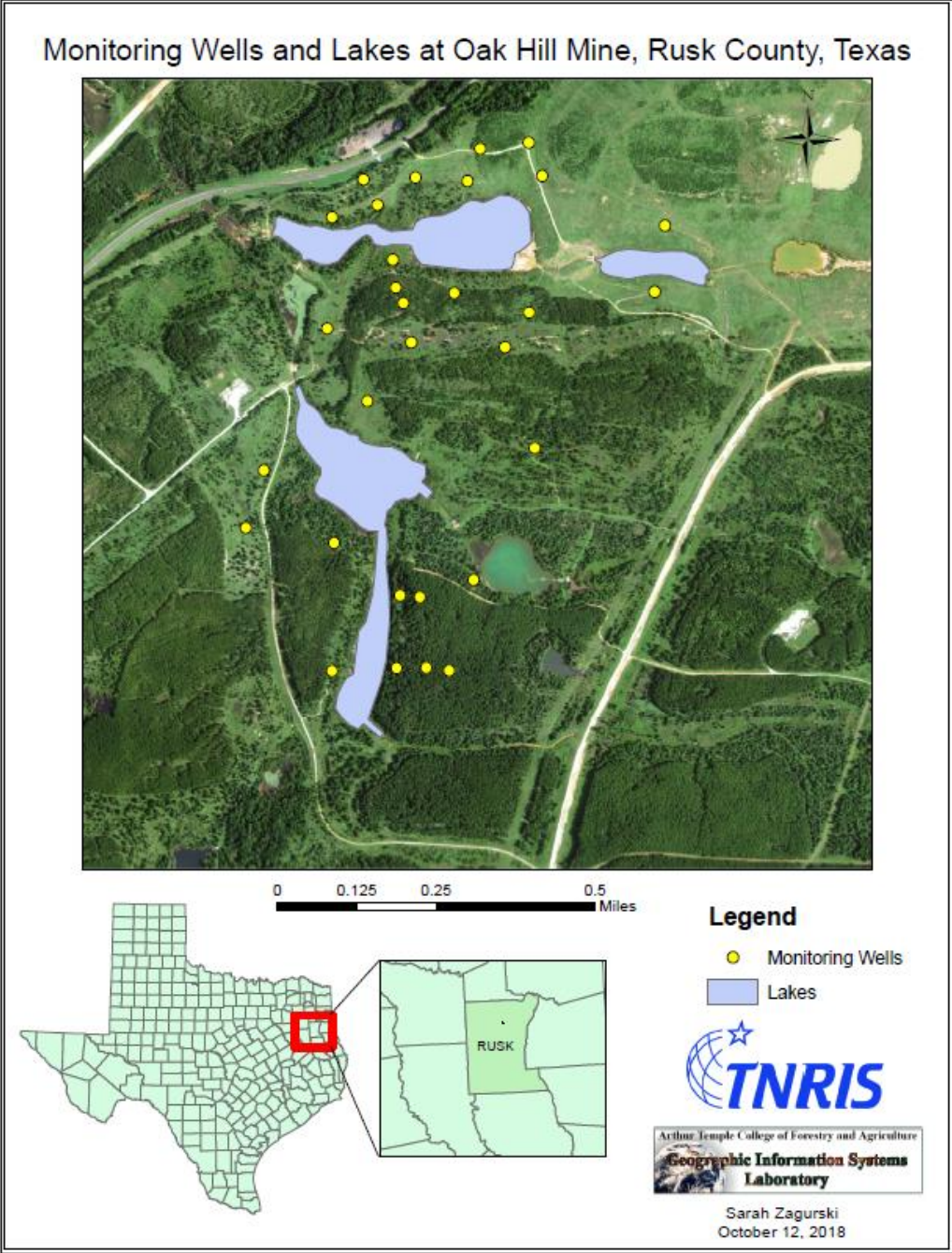


Figure 1a. Location of the three lakes of interest and the monitoring well locations where the AMD samples will be taken. (16-30)

## Mined Pit Area at Oak Hill Mine, Henderson Texas

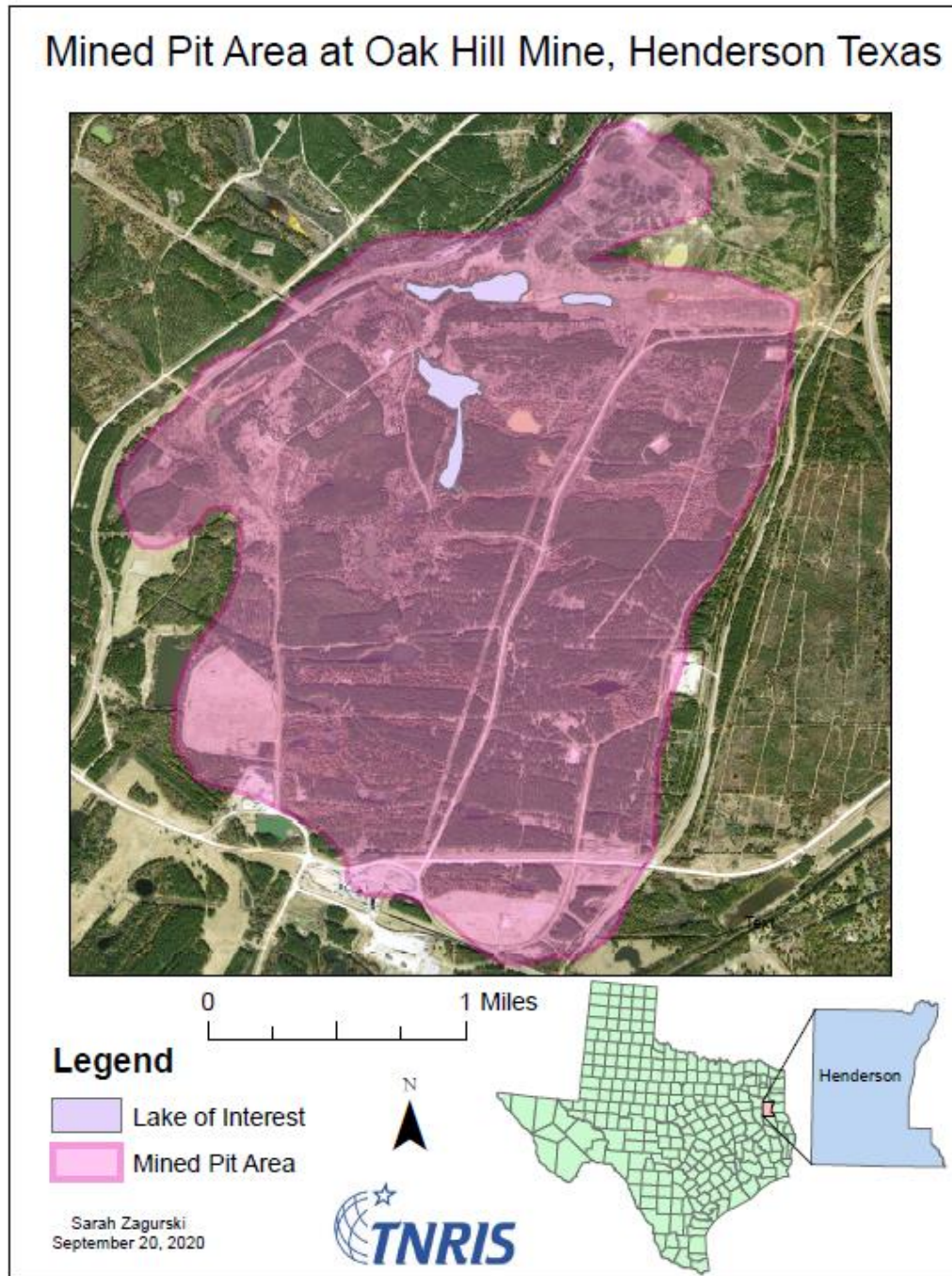


Figure 2a. Mined surface area that contained the lakes of interest at Oak Hill Mine, Henderson, Texas.

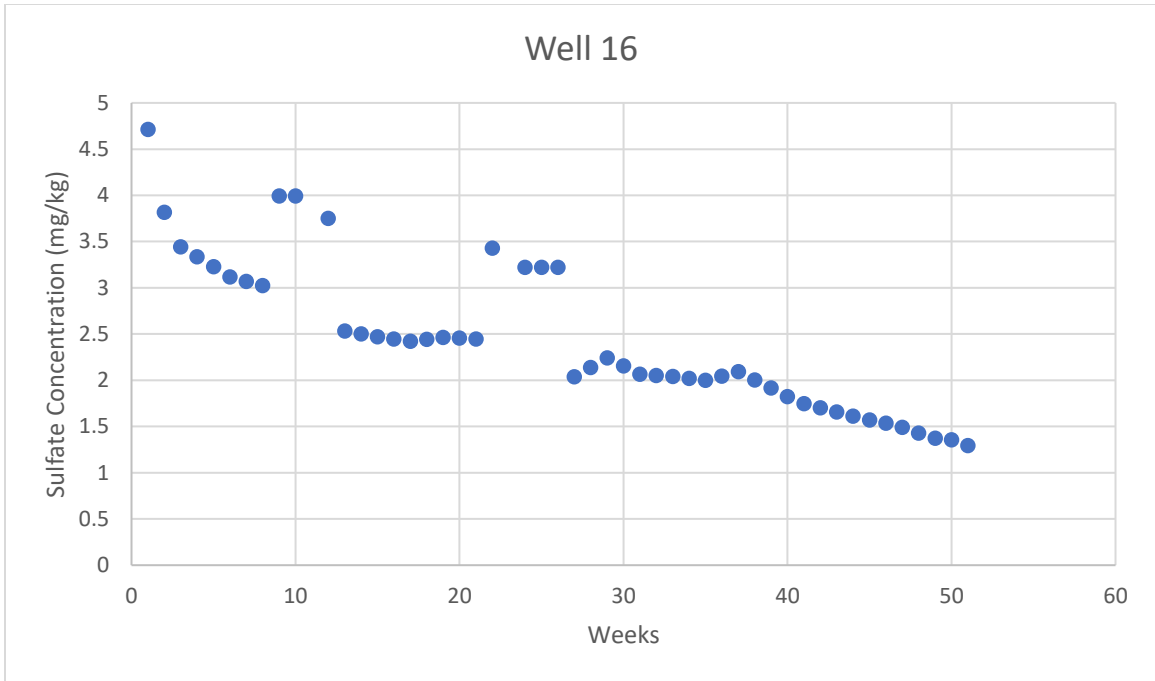


Figure 3a. Sulfate release rate for the humidity cell for Well 16.

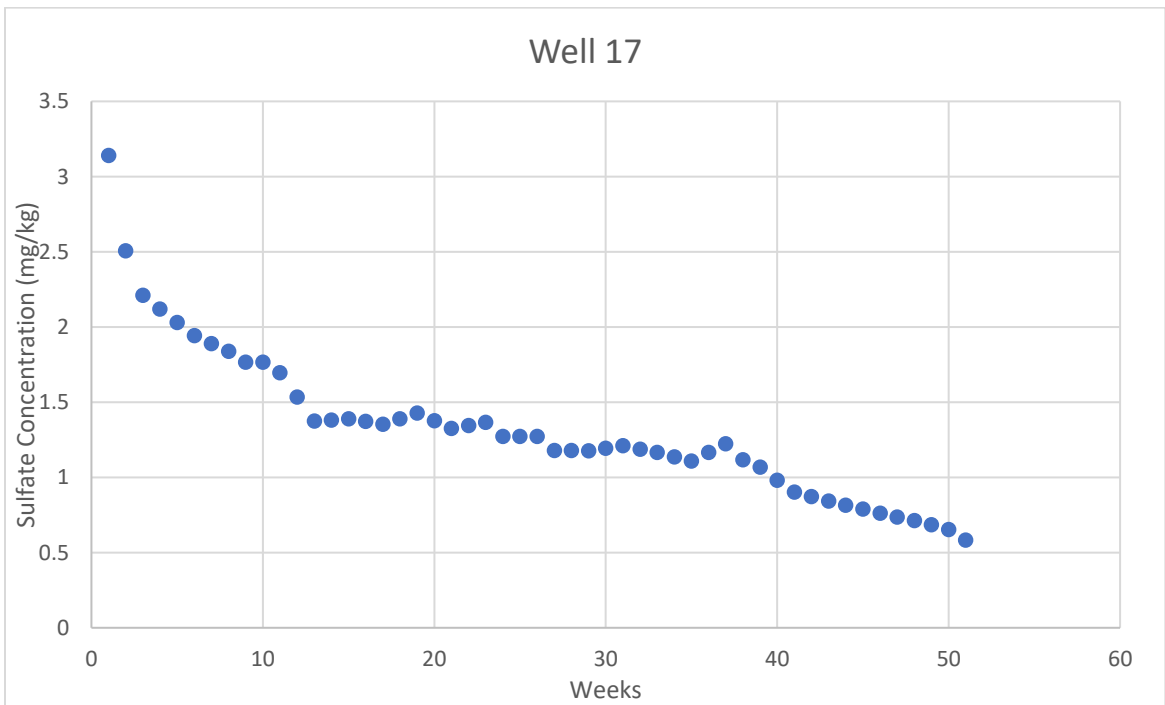


Figure 4a. Sulfate release rate per week for the humidity cell for Well 17.

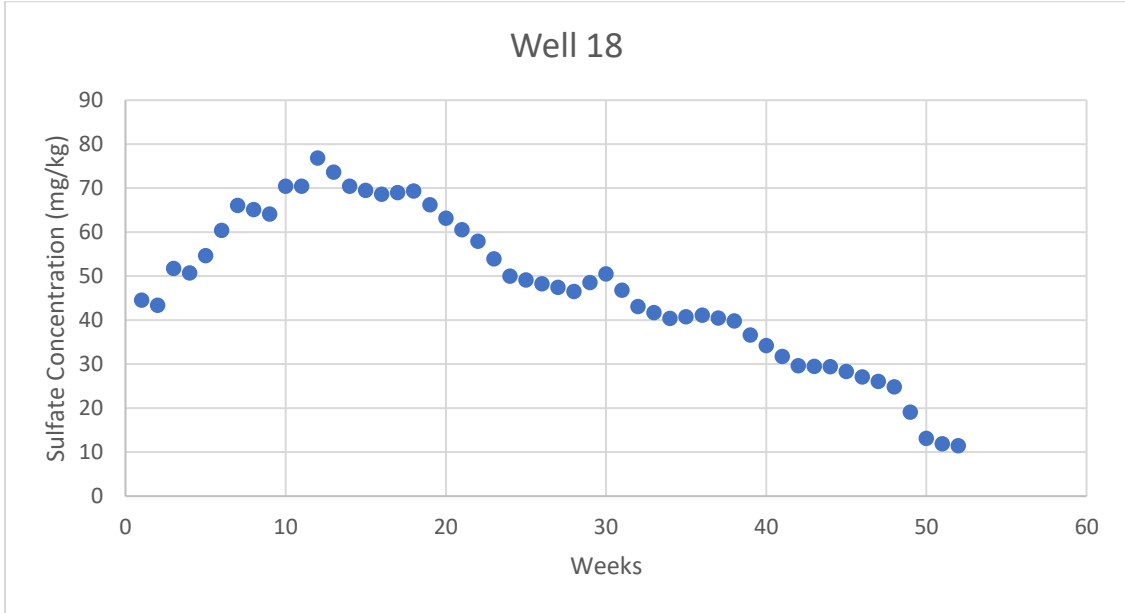


Figure 5a. Sulfate release rate per week for the humidity cell for Well 18.

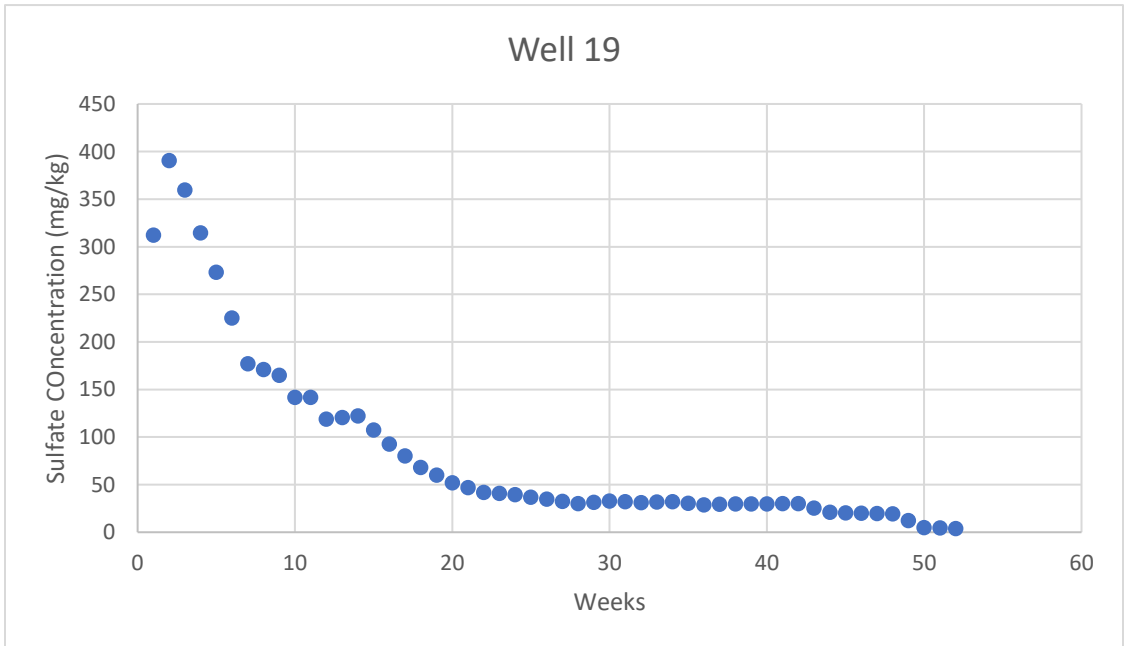


Figure 6a. Sulfate release rate per week for the humidity cell for Well 19.

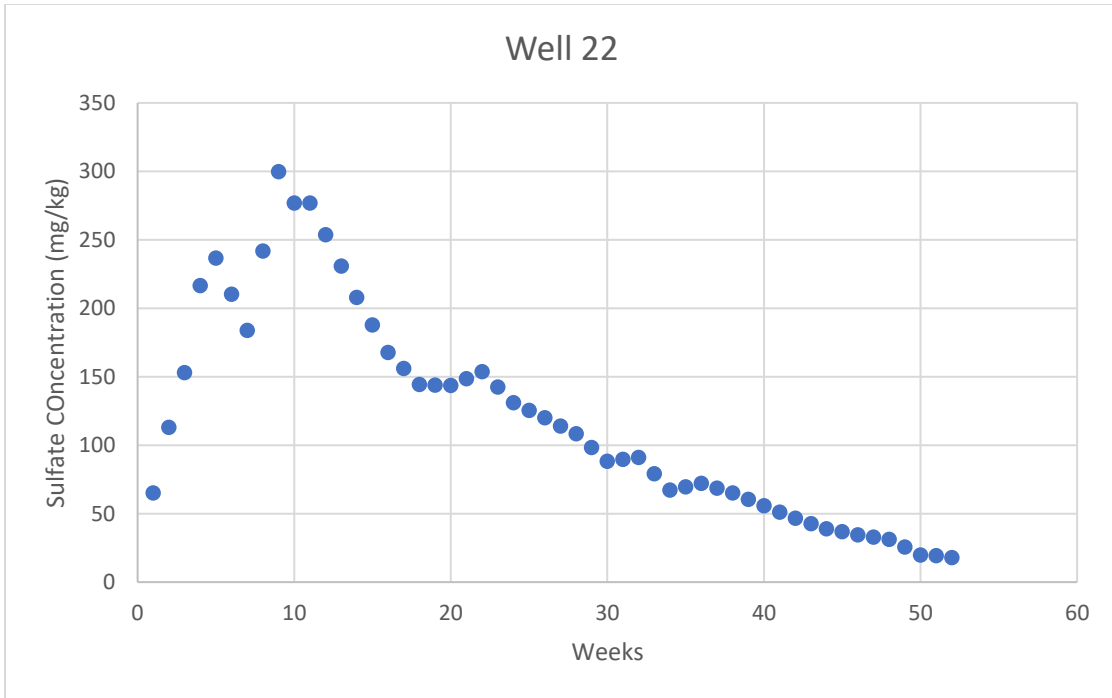


Figure 7a. Sulfate release rate per week for the humidity cell for Well 22.

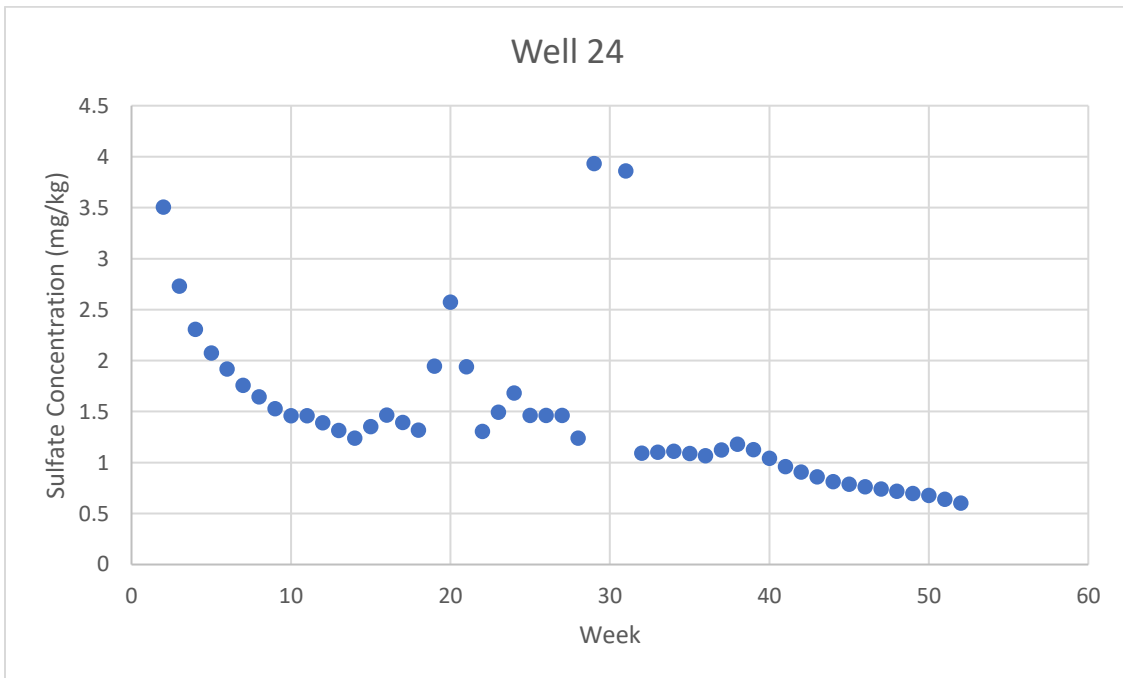


Figure 8a. Sulfate release rate per week for the humidity cell for Well 24.



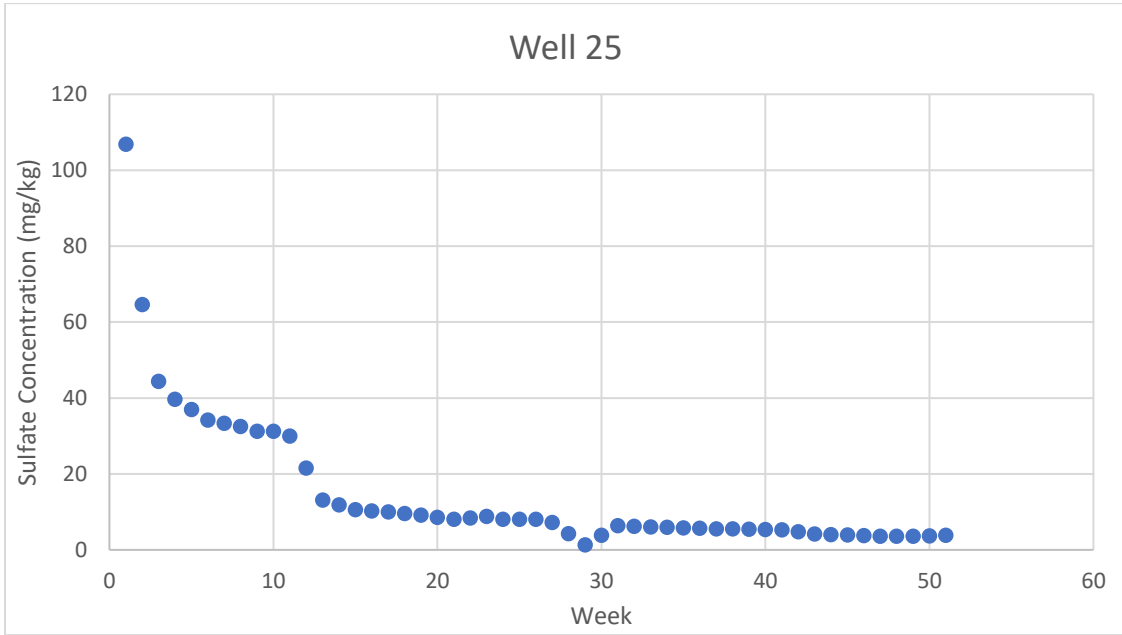


Figure 9a. Sulfate release rate per week for the humidity cell for Well 25.

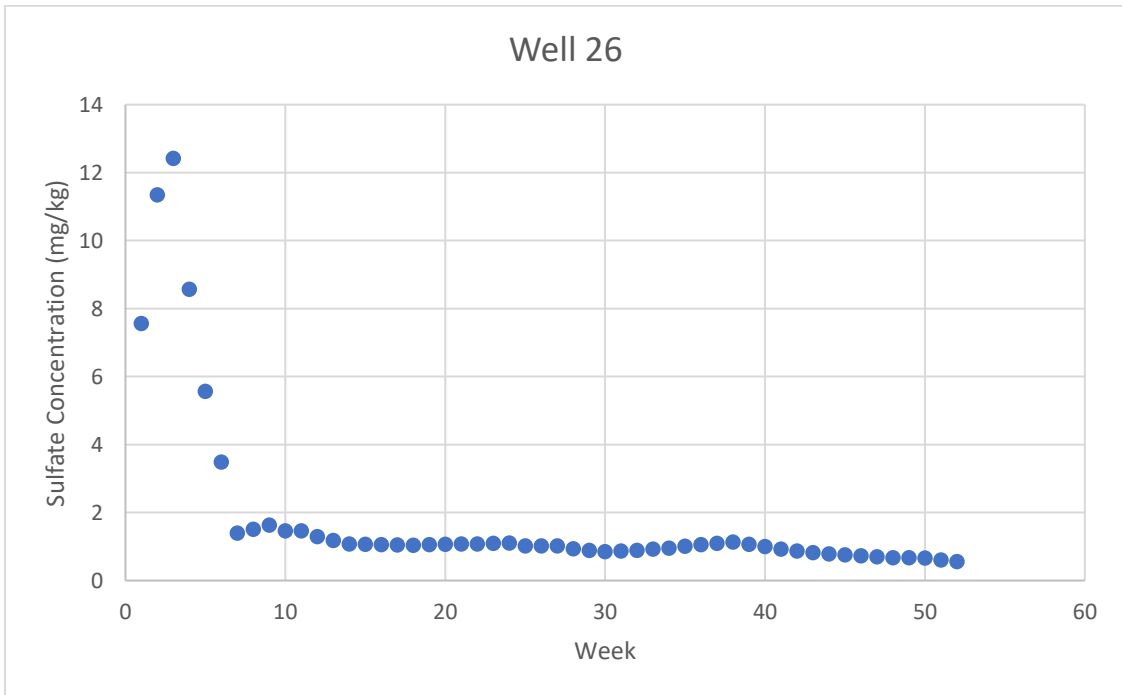


Figure 10a. Sulfate release rate per week for the humidity cell for Well 26.

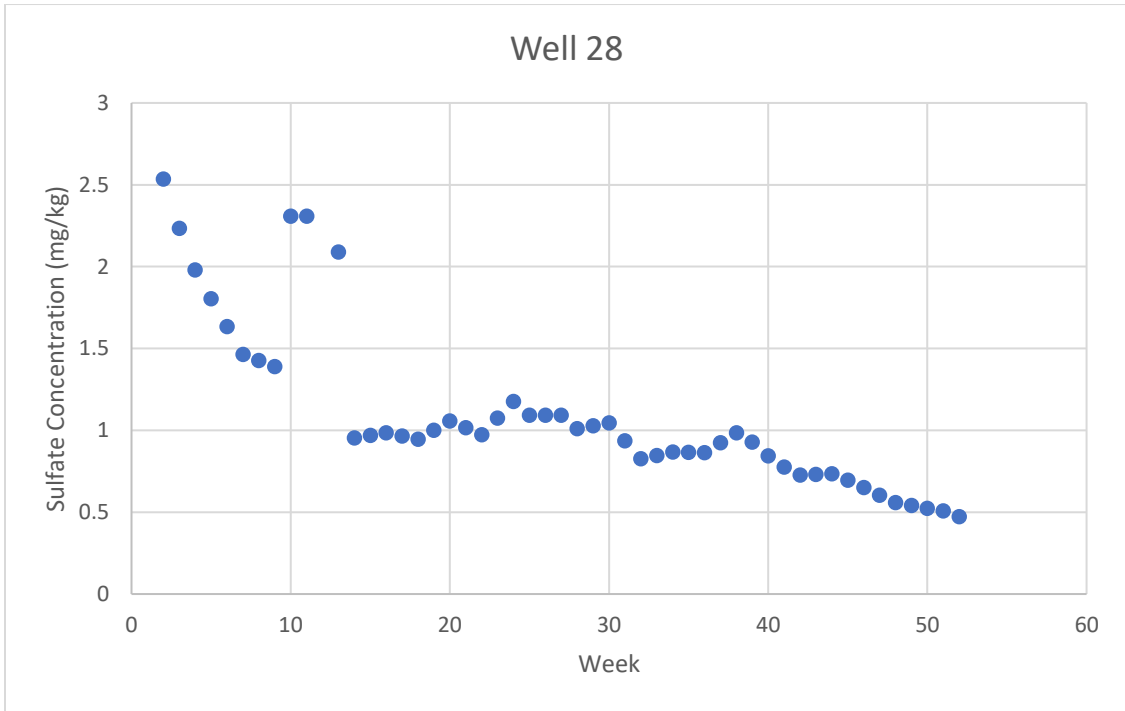


Figure 11a. Sulfate release rate per week for the humidity cell for Well 28.

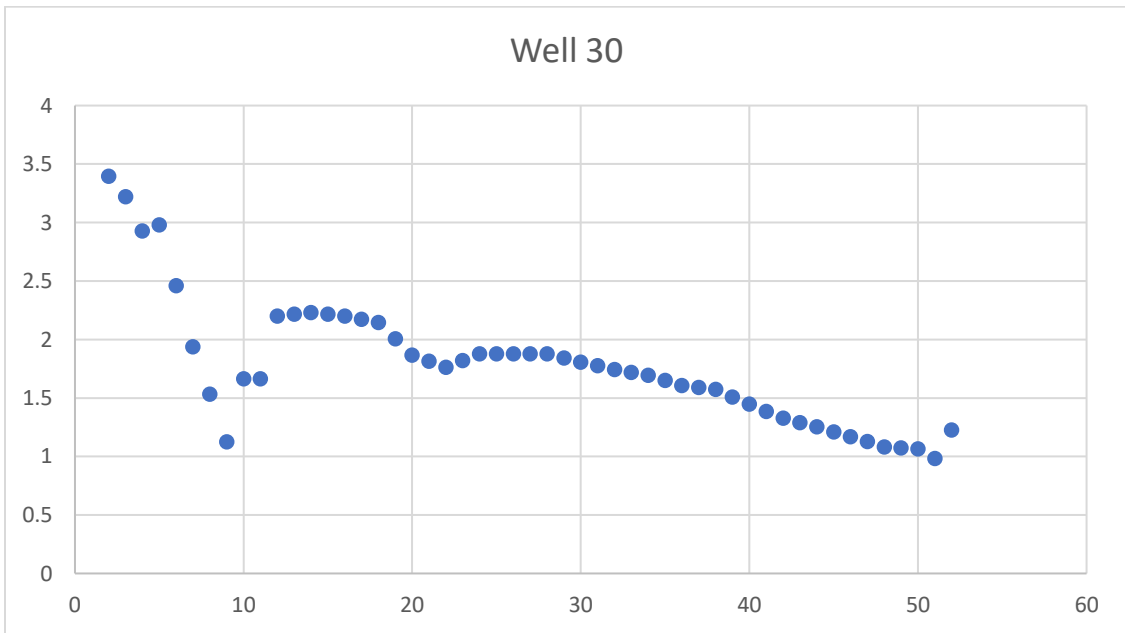


Figure 12a. Sulfate release rate per week for the humidity cell for Well 30.

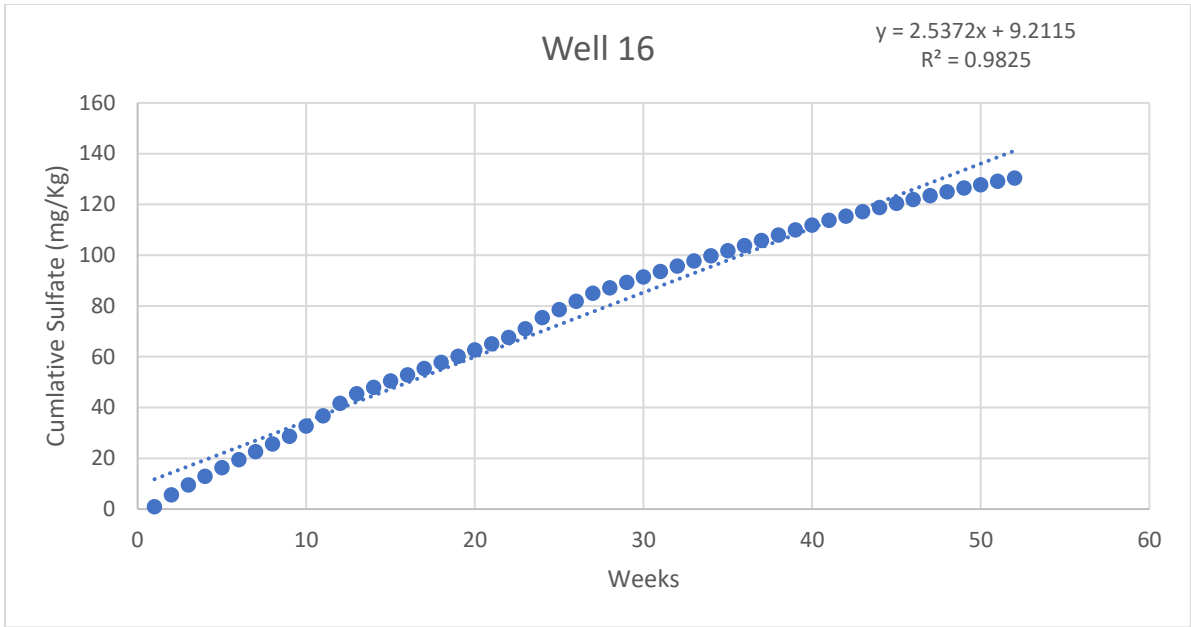


Figure 13a. Cumulative sulfate release and trend line for the humidity cell for Well 16 throughout the duration of the study in mg/kg.

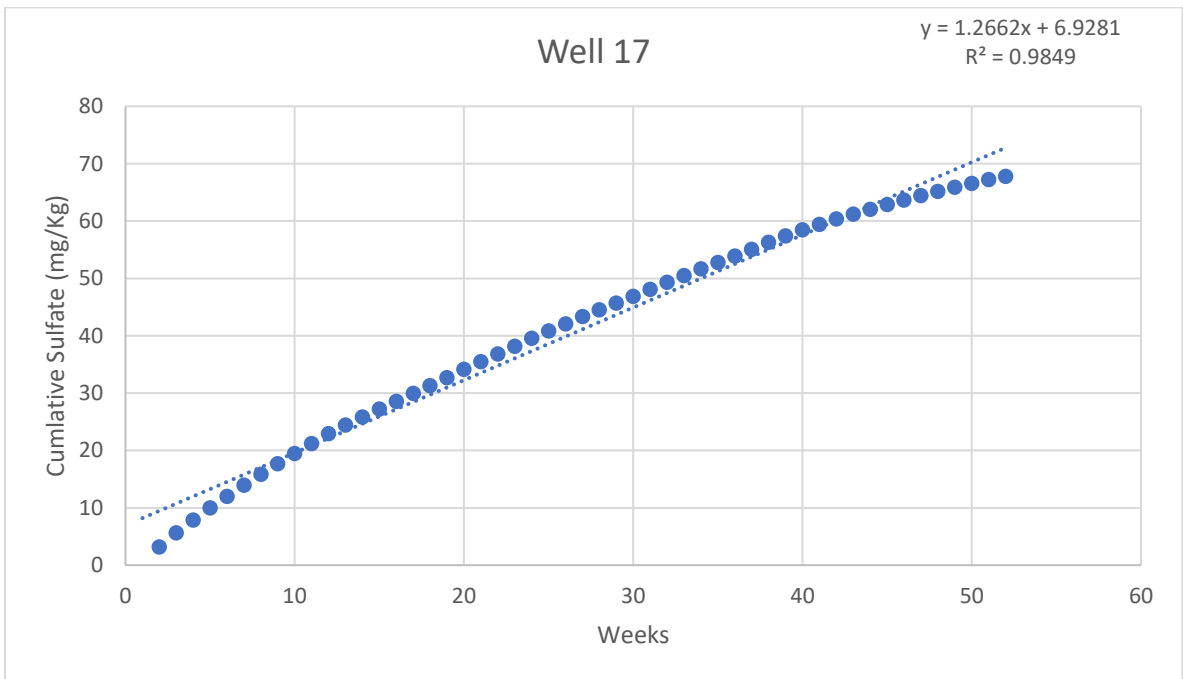


Figure 14a. Cumulative sulfate release and trend line for the humidity cell for Well 17 throughout the duration of the study in mg/kg.

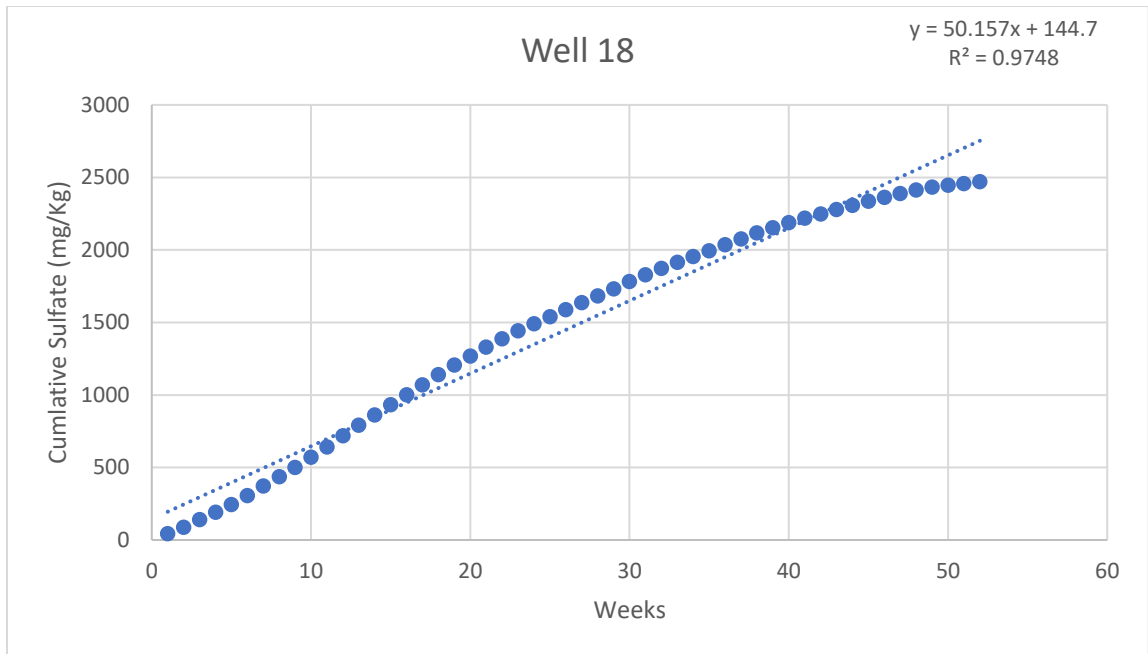


Figure 15a. Cumulative sulfate release and trend line for the humidity cell for Well 18 throughout the duration of the study in mg/kg.

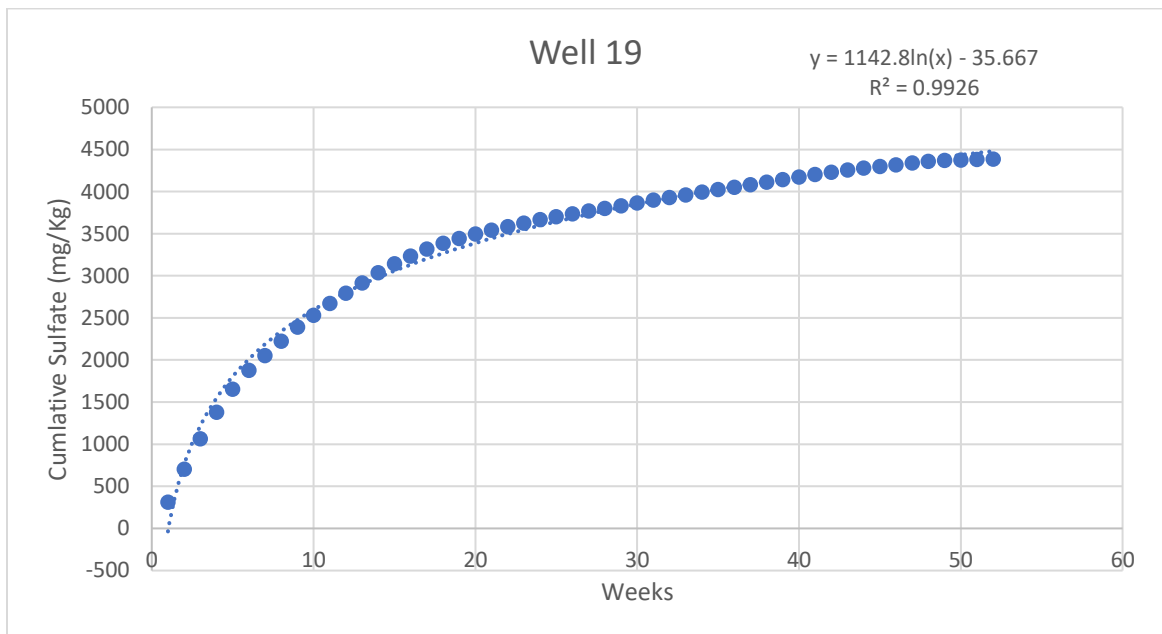


Figure 16a. Cumulative sulfate release and trend line for the humidity cell for Well 19 throughout the duration of the study in mg/kg.

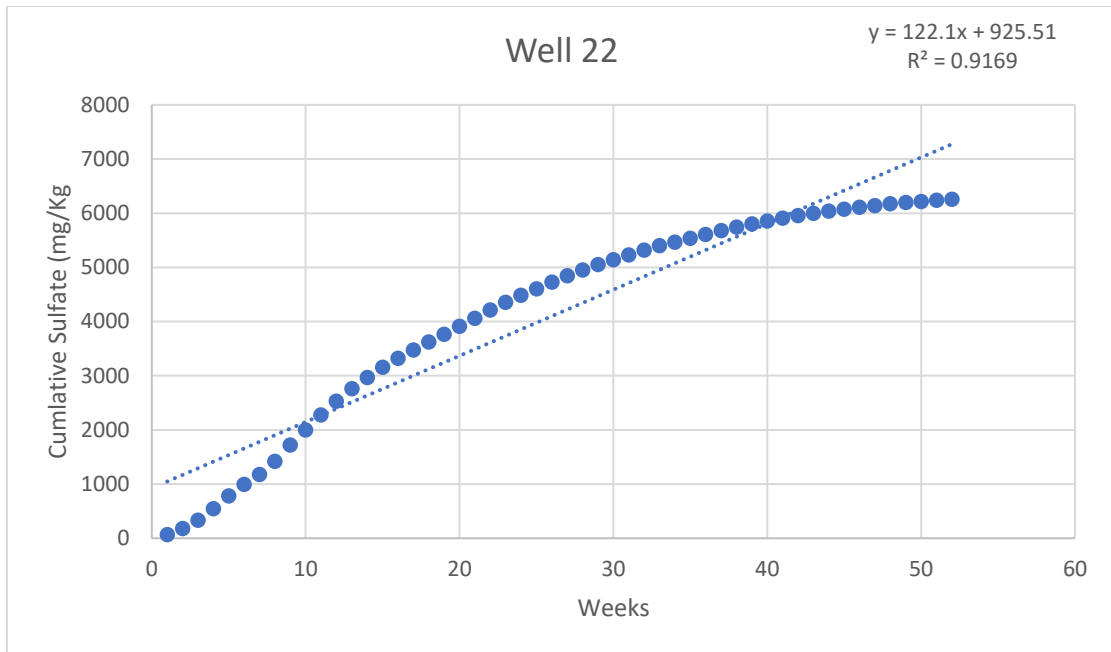


Figure 17a. Cumulative sulfate release and trend line for the humidity cell for Well 22 throughout the duration of the study in mg/kg.

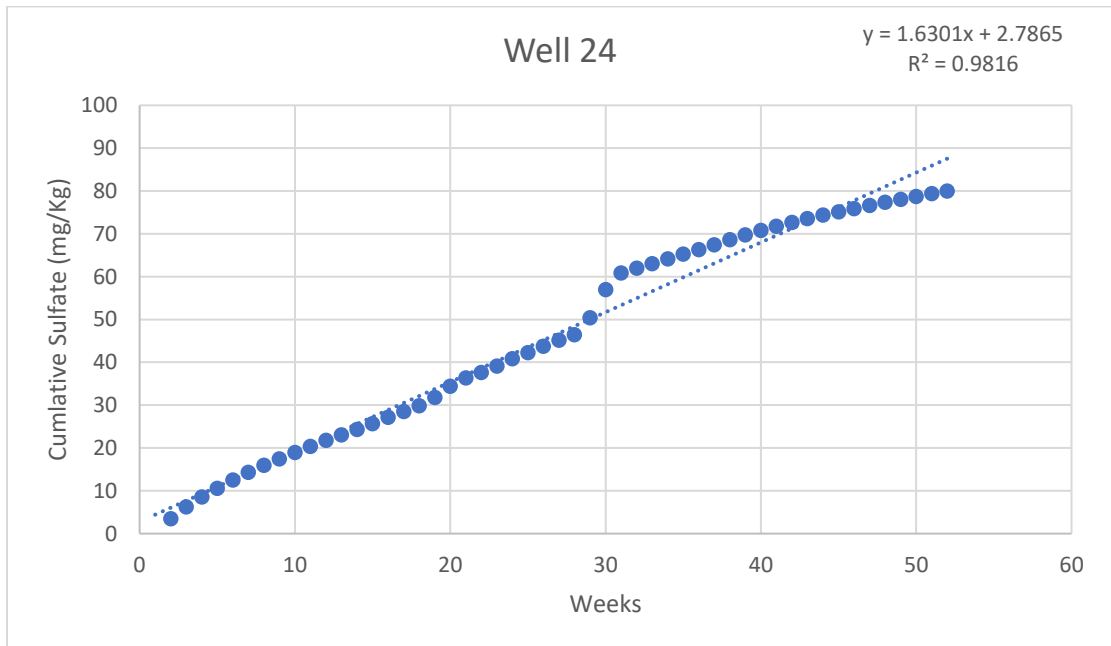


Figure 18a. Cumulative sulfate release and trend line for the humidity cell for Well 24 throughout the duration of the study in mg/kg.

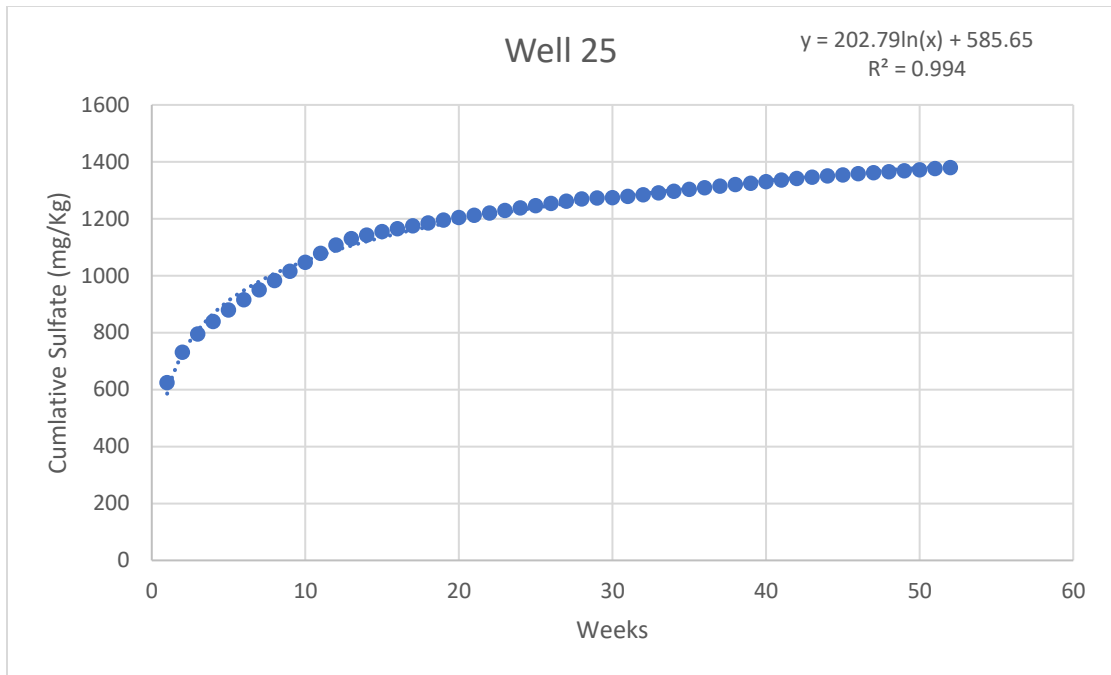


Figure 19a. Cumulative sulfate release and trend line for the humidity cell for Well 25 throughout the duration of the study in mg/kg.

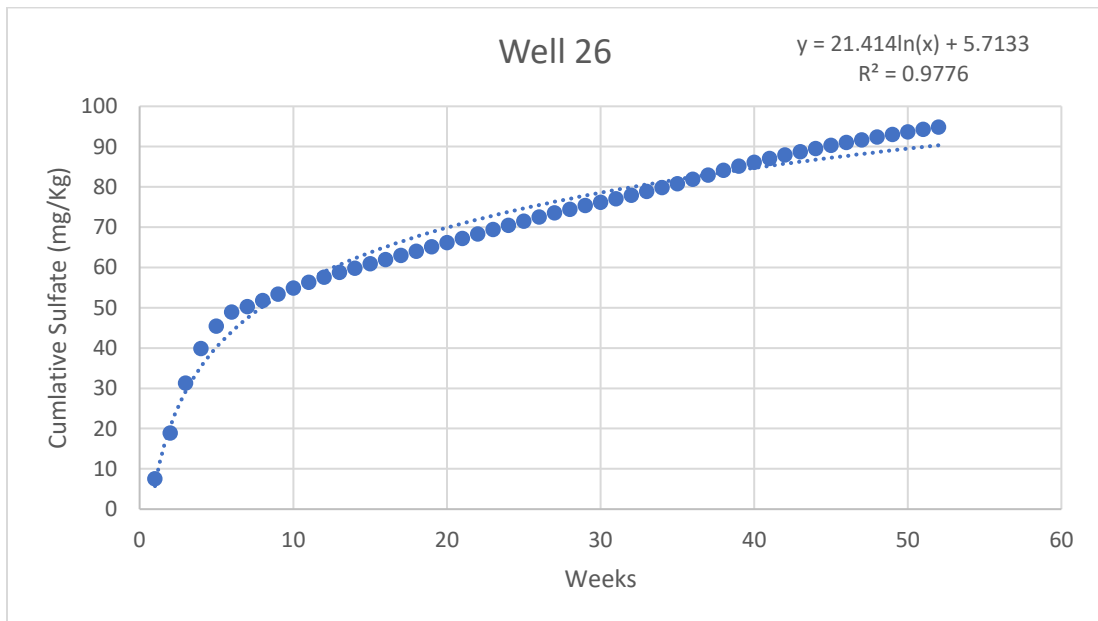


Figure 20a. Cumulative sulfate release and trend line for the humidity cell for Well 26 throughout the duration of the study in mg/kg.

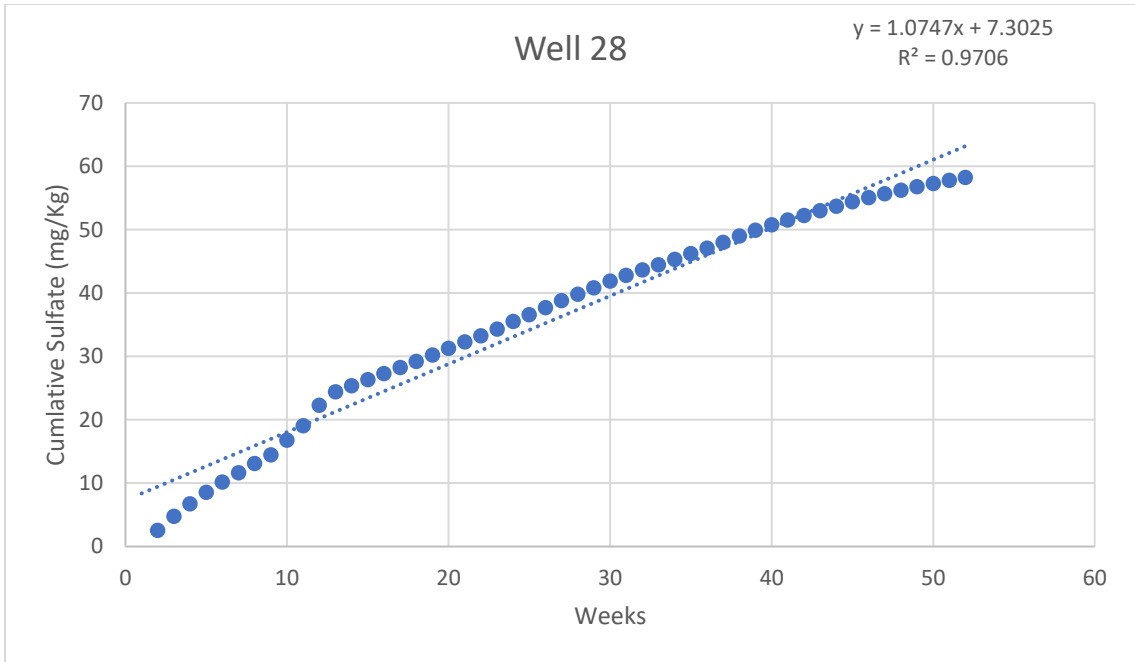


Figure 21a. Cumulative sulfate release and trend line for the humidity cell for Well 28 throughout the duration of the study in mg/kg.

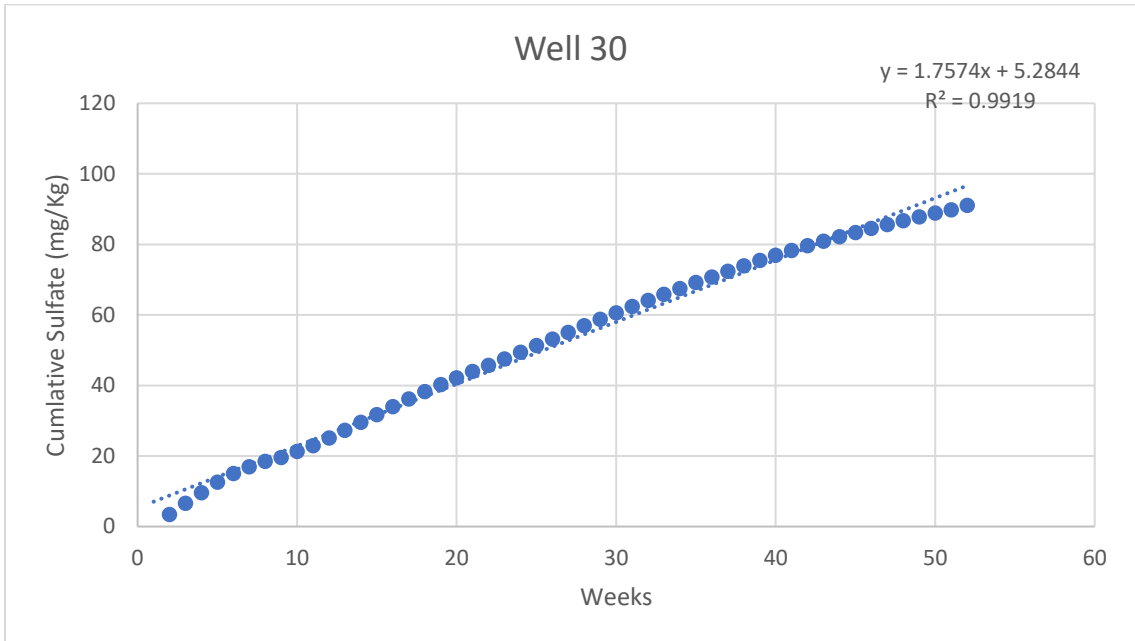


Figure 22a. Cumulative sulfate release and trend line for the humidity cell for Well 30 throughout the duration of the study in mg/kg.

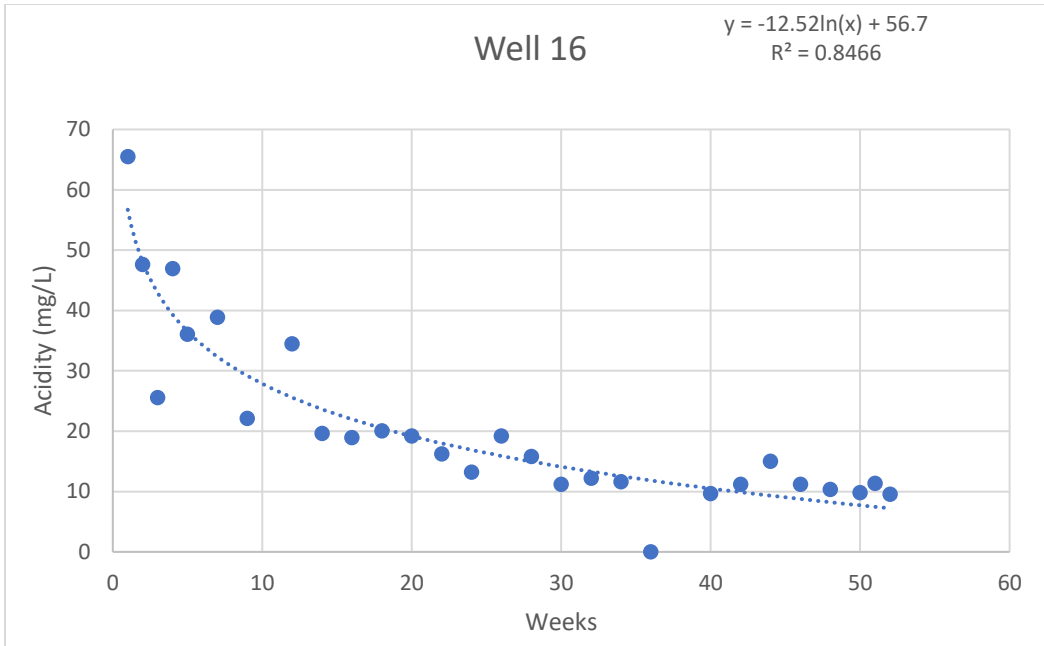


Figure 23a. Acidity release and trend line for the humidity cell for Well 16 throughout the duration of the study in mg/L.

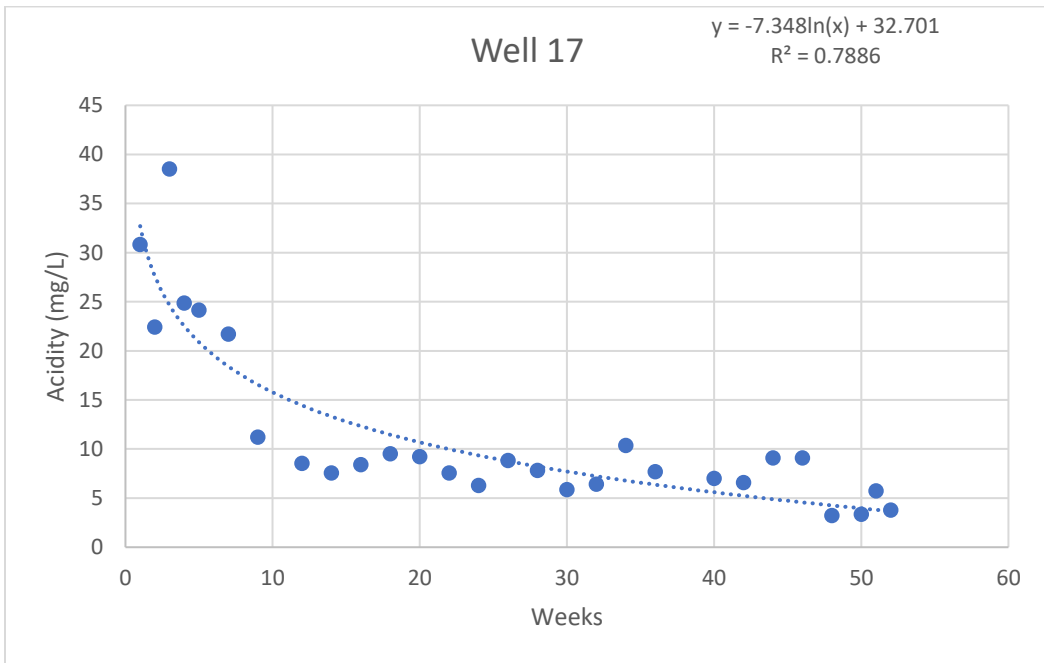


Figure 24a. Acidity release and trend line for the humidity cell for Well 17 throughout the duration of the study in mg/L.



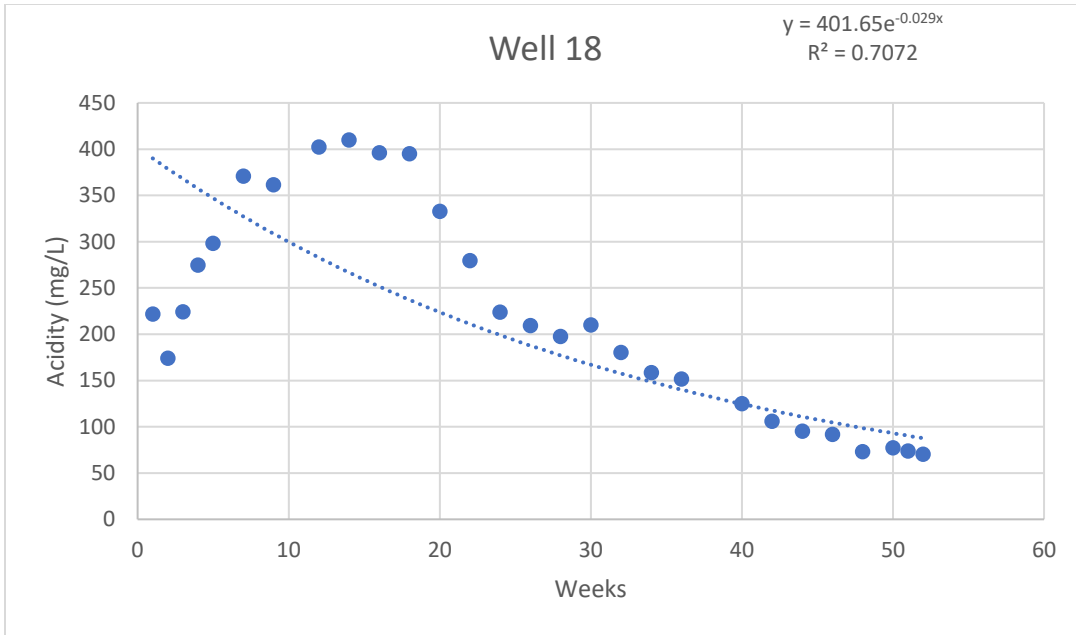


Figure 25a. Acidity release and trend line for the humidity cell for Well 18 throughout the duration of the study in mg/L.

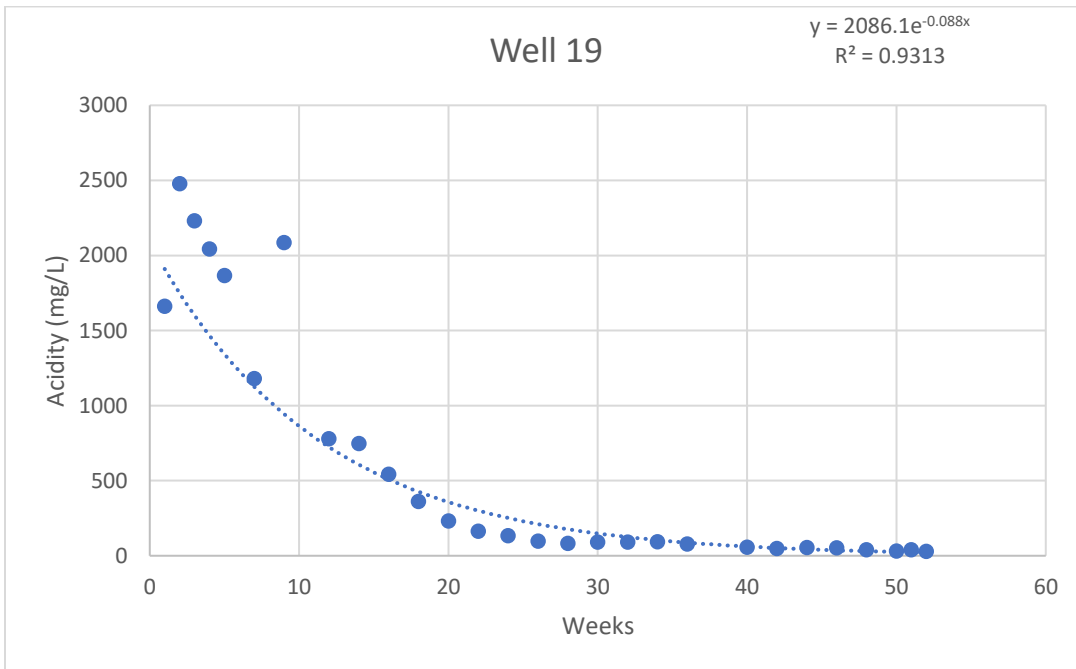


Figure 26a. Acidity release and trend line for the humidity cell for Well 19 throughout the duration of the study in mg/L.

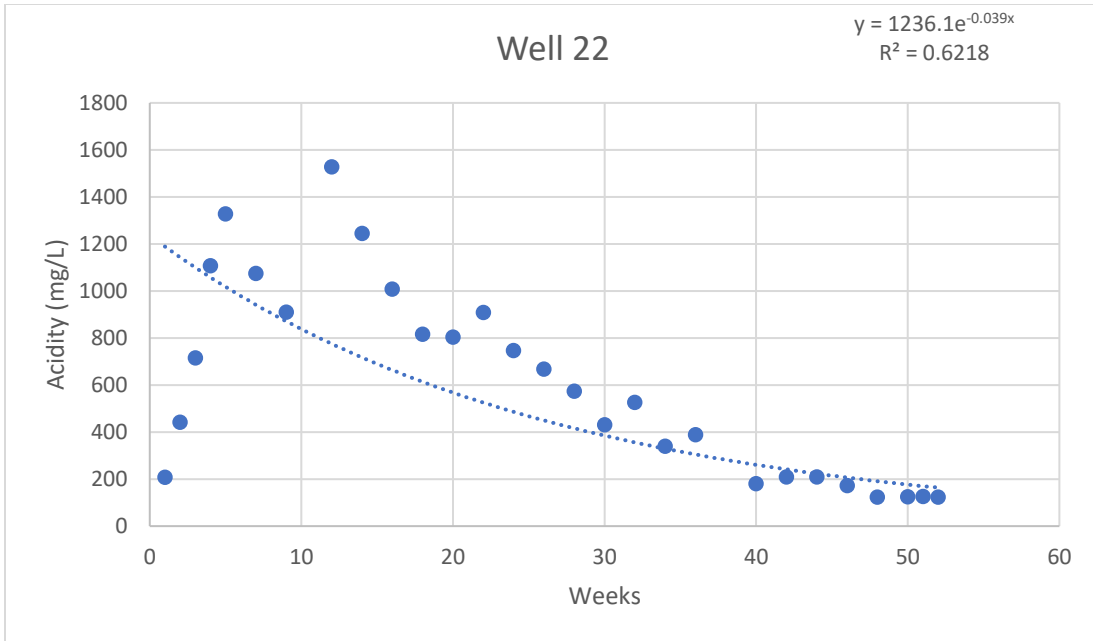


Figure 27a. Acidity release and trend line for the humidity cell for Well 22 throughout the duration of the study in mg/L.

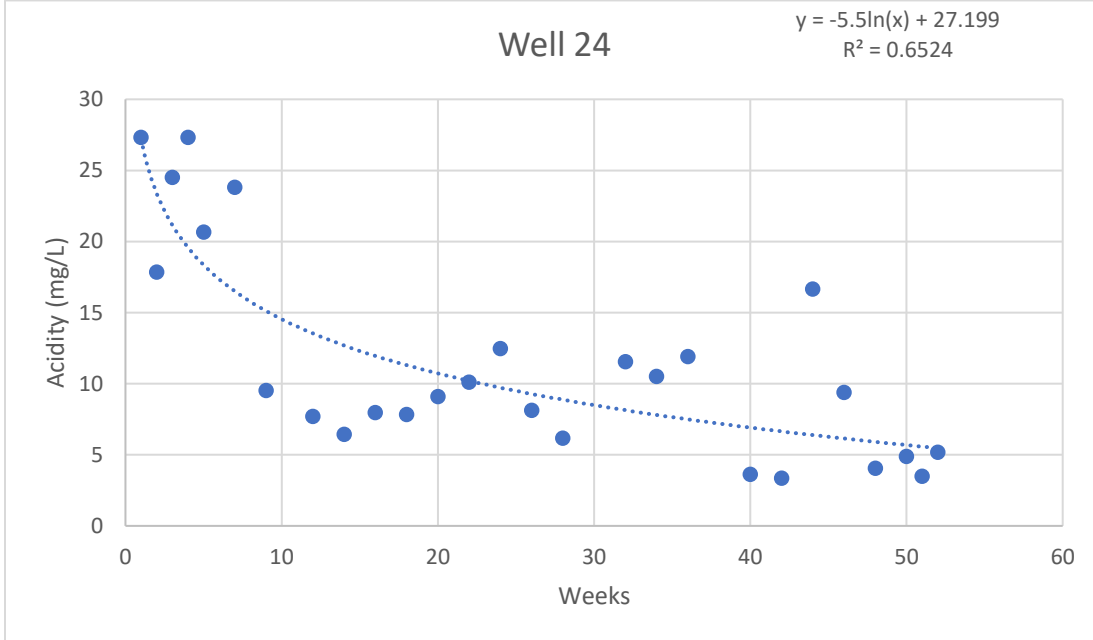


Figure 28a. Acidity release and trend line for the humidity cell for Well 24 throughout the duration of the study in mg/L.

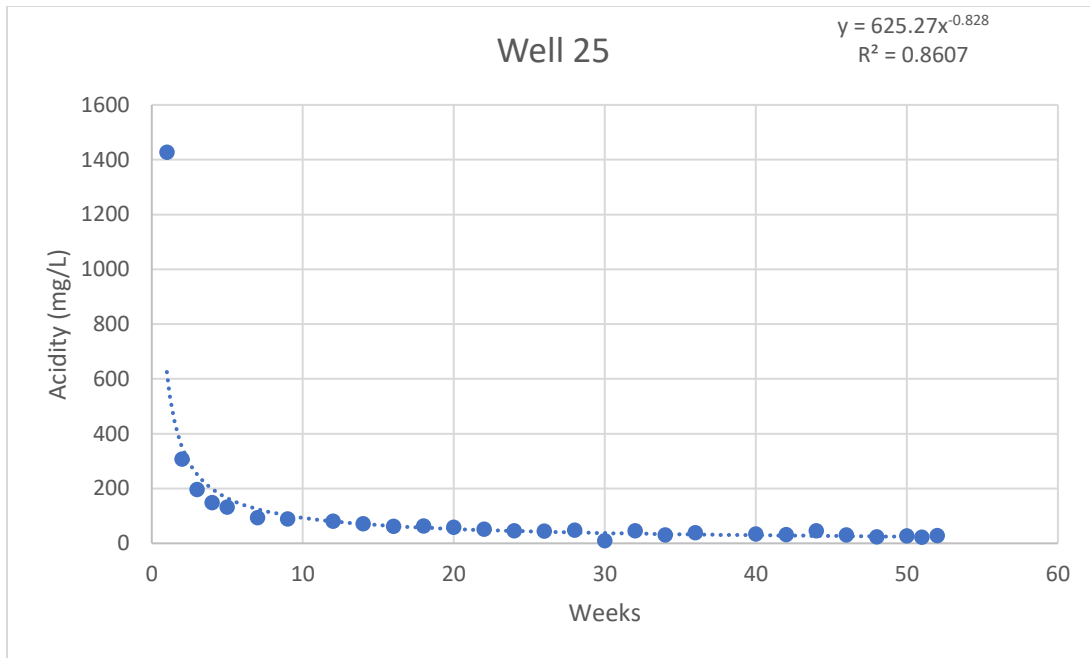


Figure 29a. Acidity release and trend line for the humidity cell for Well 25 throughout the duration of the study in mg/L.

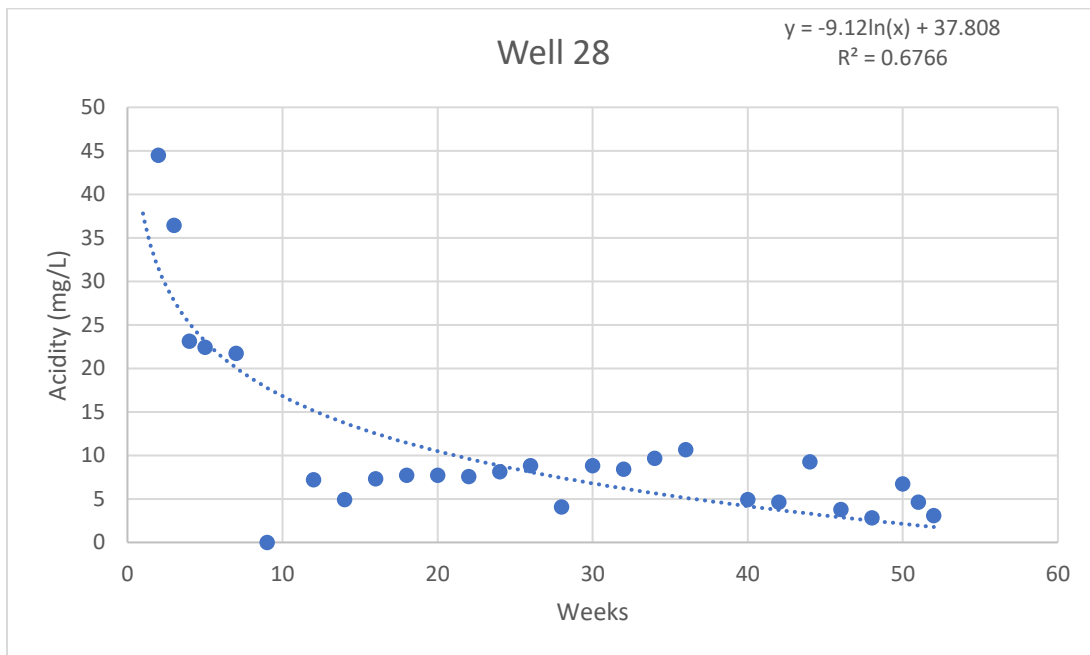


Figure 30. Acidity release and trend line for the humidity cell for Well 28 throughout the duration of the study in mg/L.

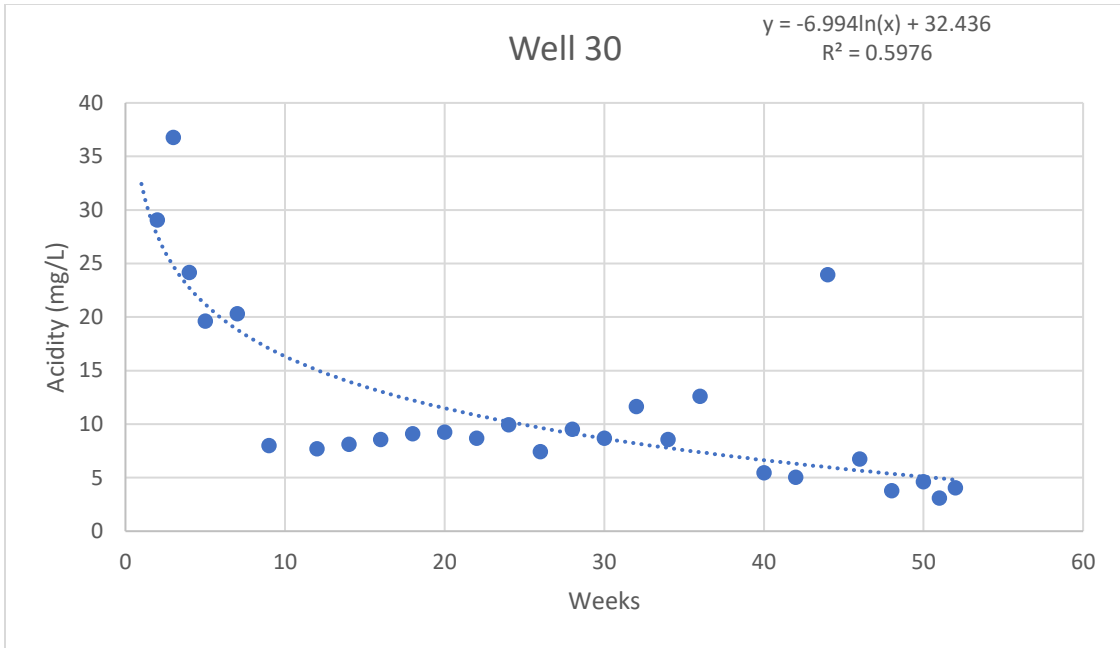


Figure 31a. Acidity release and trend line for the humidity cell for Well 30 throughout the duration of the study in mg/L.

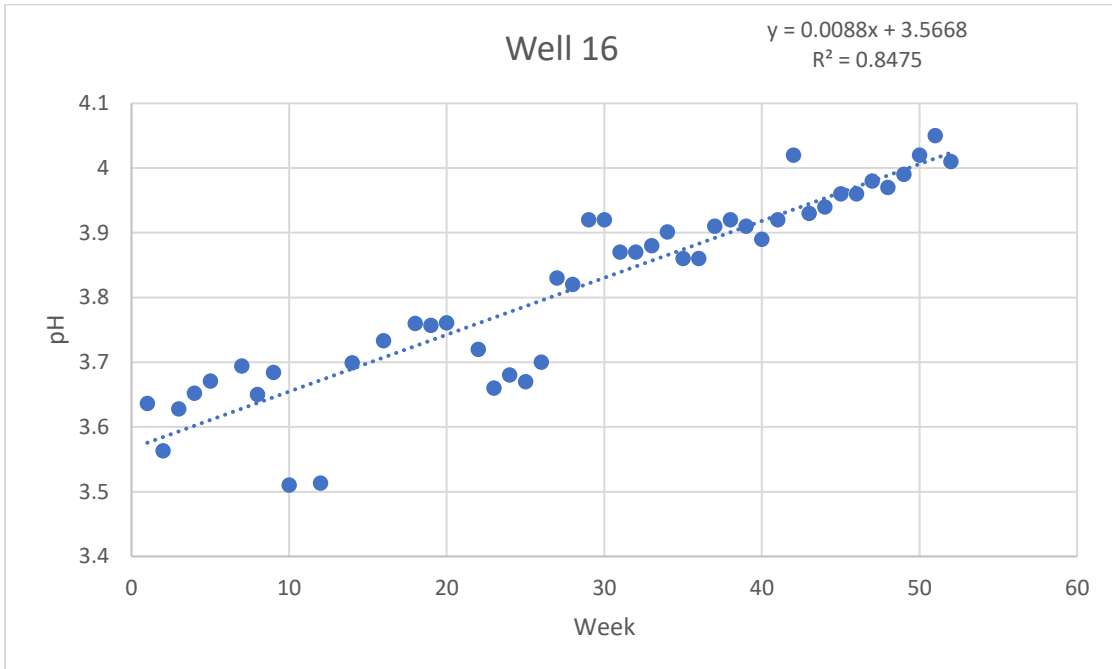


Figure 32a. pH values and trend for the humidity cell for Well 16.

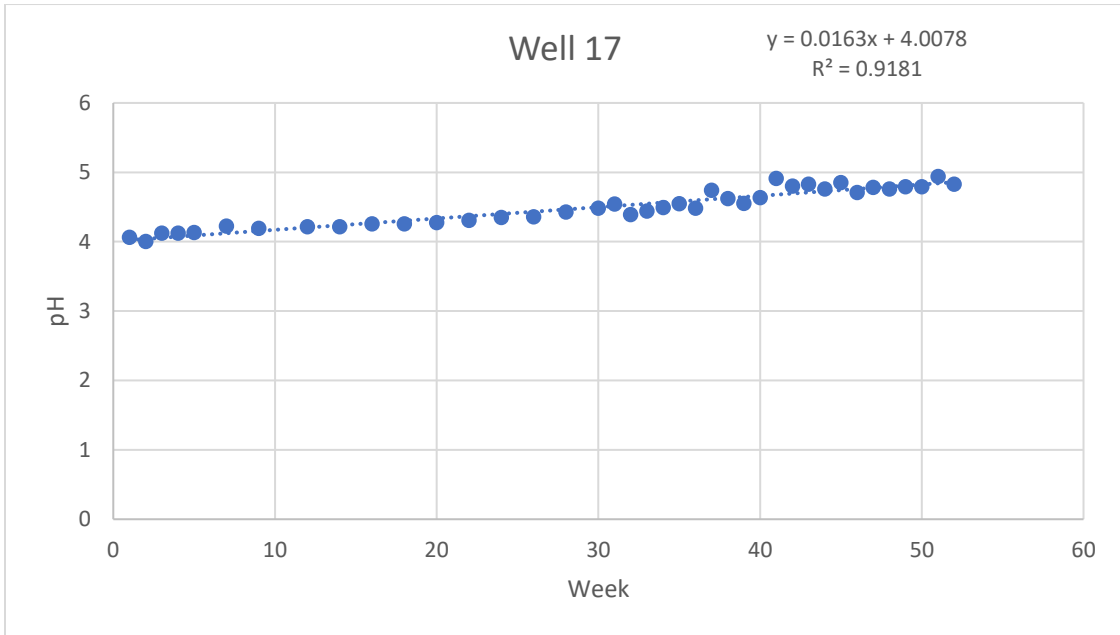


Figure 33. pH values and trend for the humidity cell for Well 17.

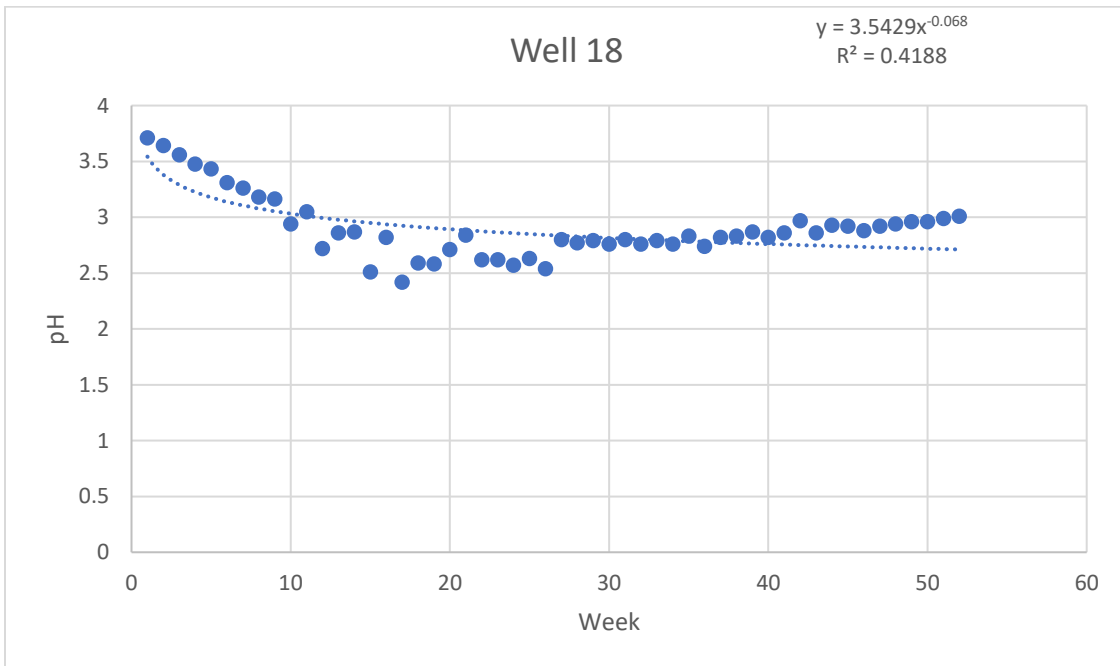


Figure 34a. pH values and trend for the humidity cell for Well 18.

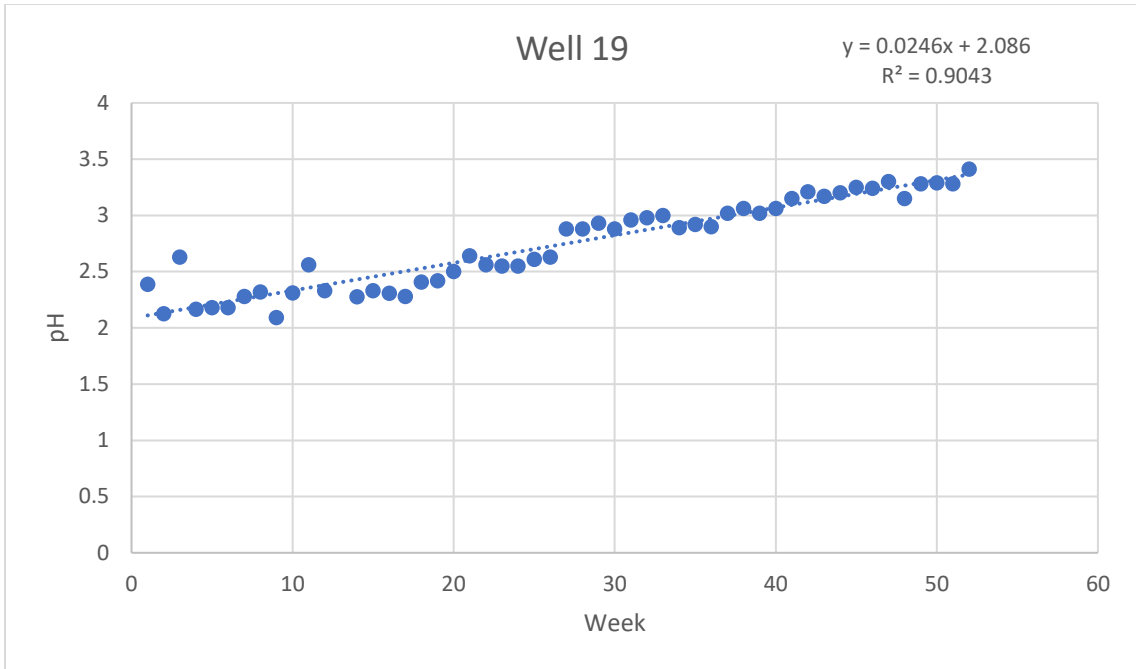


Figure 35a. pH values and trend for the humidity cell for Well 19.

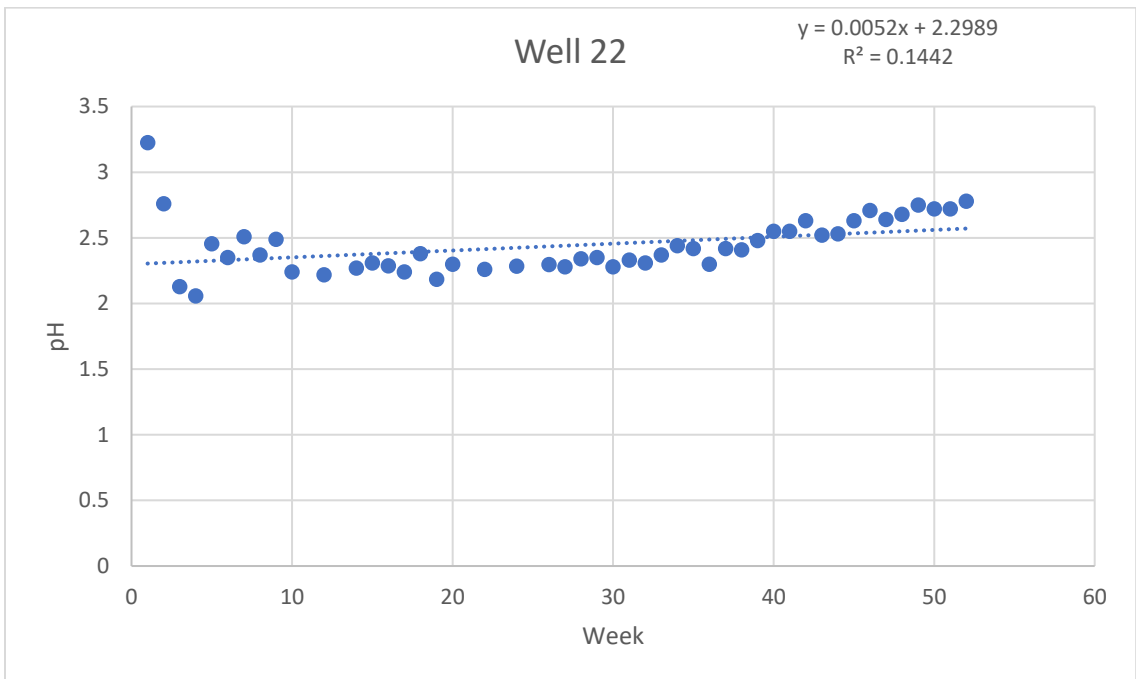


Figure 36a. pH values and trend for the humidity cell for Well 22.

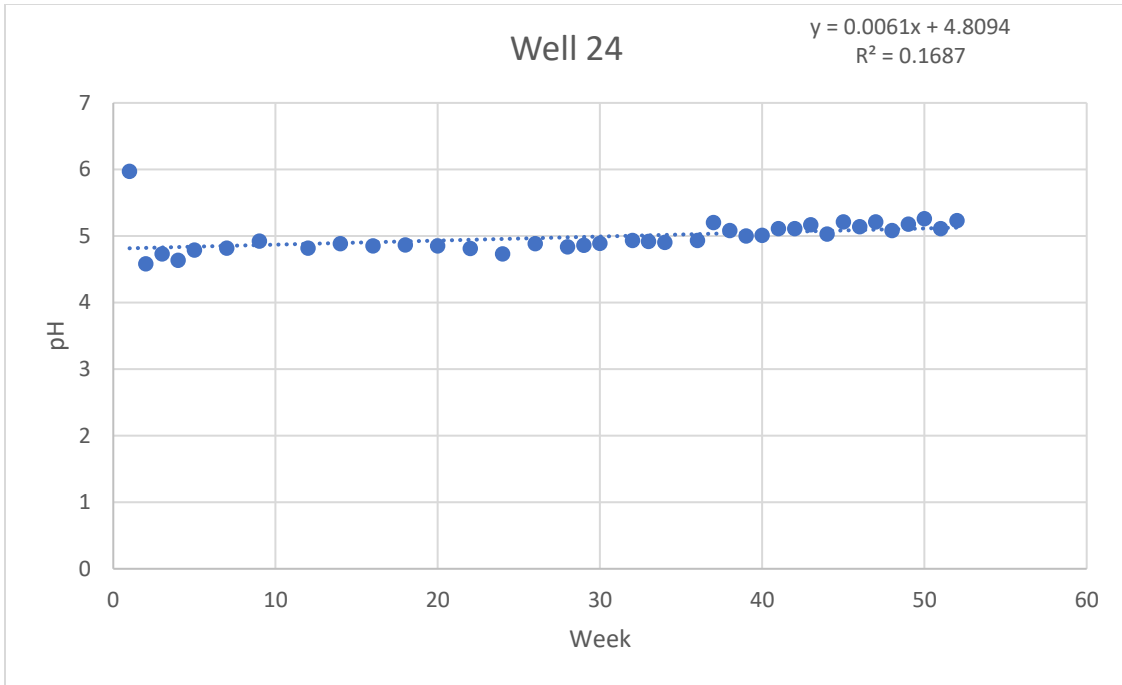


Figure 37a. pH values and trend for the humidity cell for Well 24.

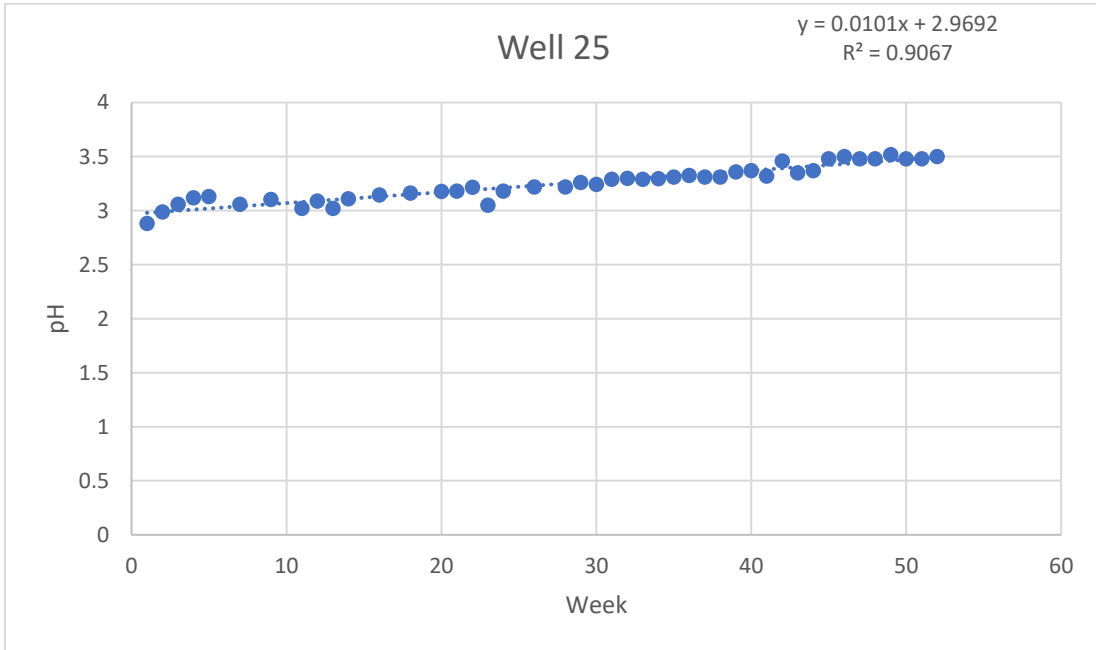


Figure 38a. pH values and trend for the humidity cell for Well 25.

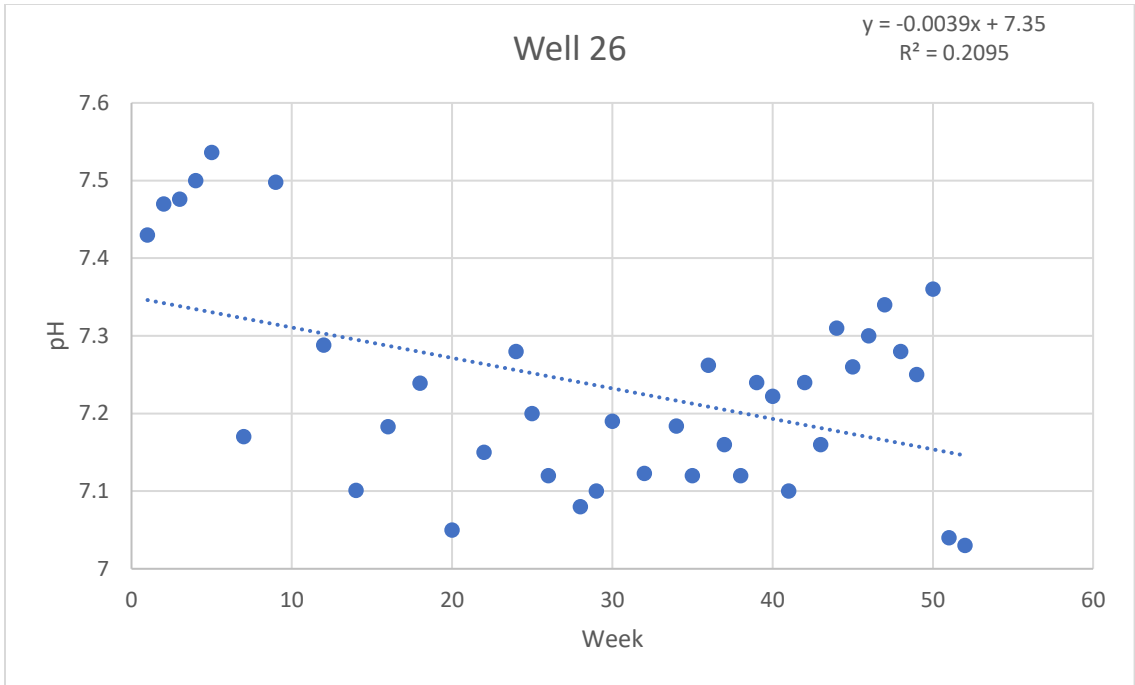


Figure 39a. pH values and trend for the humidity cell for Well 26.

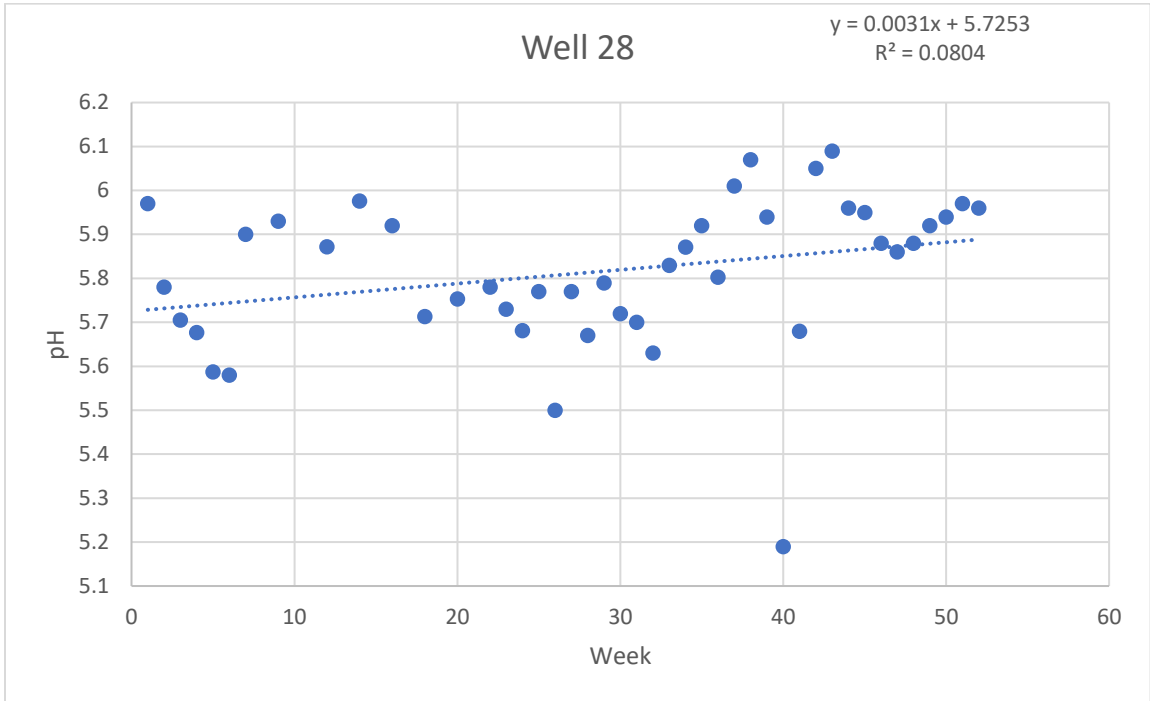


Figure 40a. pH values and trend for the humidity cell for Well 28.



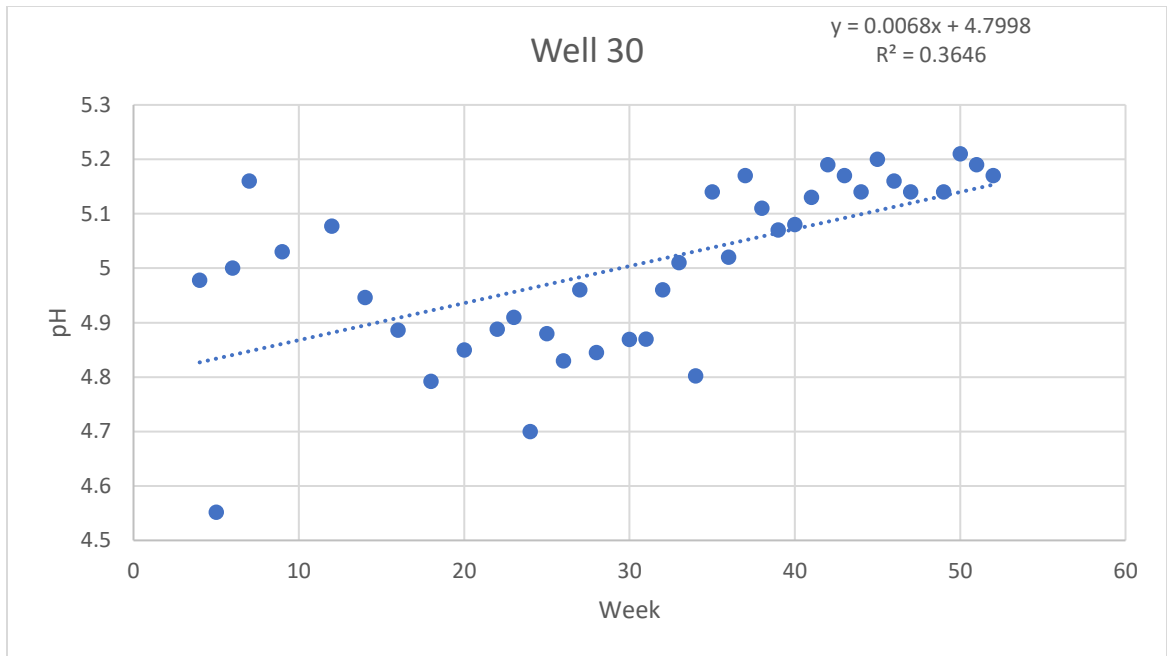




Figure 41a. pH values and trend for the humidity cell for Well 30.

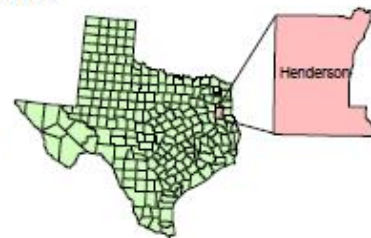
## Groundwater Elevation Points Used to Create Groundwater Contours, Henderson, Texas



0 2 Miles

### Legend

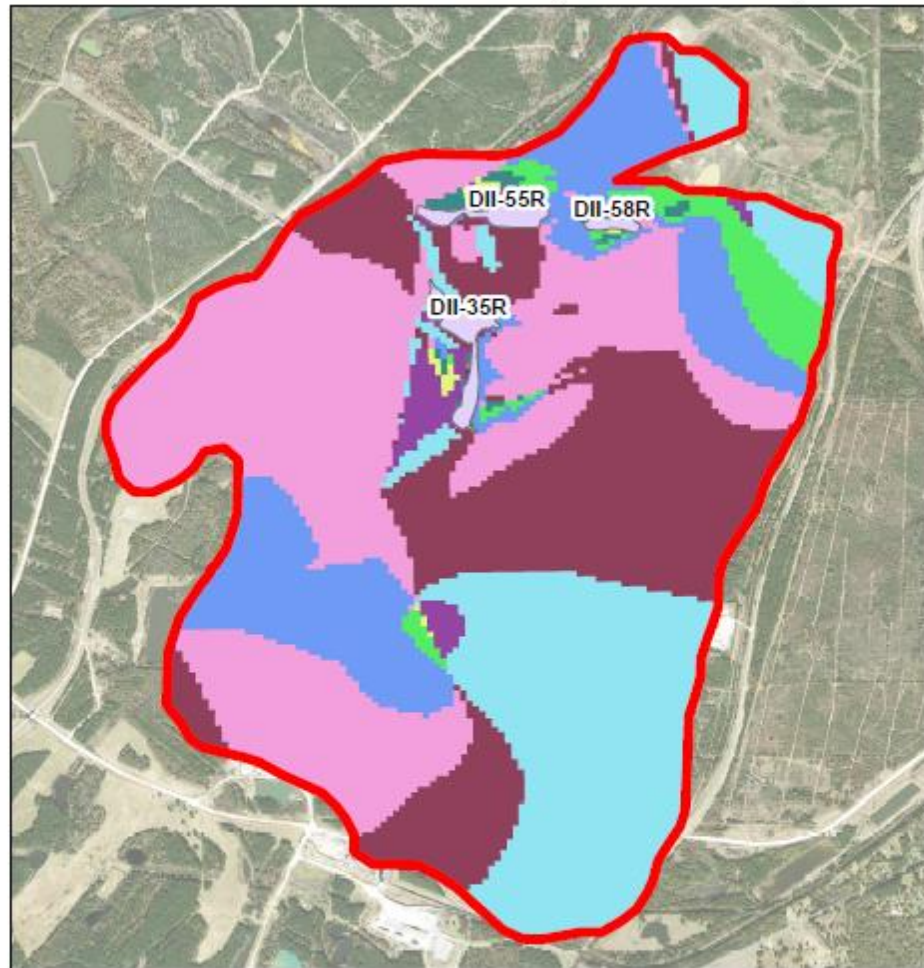
-  Lake of Interest
-  Mined Pit Area
-  Elevation Points



Sarah Zagurski  
September 20, 2020

Figure 42a. Location of water table elevation points used to generate a groundwater contour map.

## Flow Direction Analysis Based on Groundwater Elevation at Oak Hill Mine, Henderson, Texas



0 1 Miles N

### Legend

Lake of interest	17	128	253
Value	28	135	254
1	32	193	
2	48	199	
4	64	207	
7	113	221	
8	120	223	
16	124	252	



### Direction coding

Flow direction is determined based on numerical value from the flow direction coding image, where a value of one means water is flowing east, 4 means south, and so one. Values in between the coding values means flow is moving proportionnaly in that direction.



Sarah Zagurski  
September 20, 2020

Figure 43a. Flow direction map based on groundwater elevation.

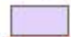




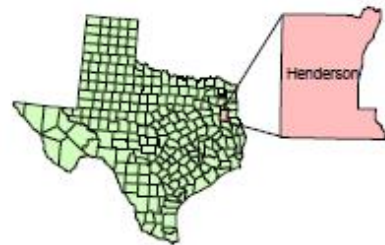
# Zone of Influence for Lake DII-35R at Oak Hill Mine, Henderson, Texas



0 1 Miles

### Legend

-  Lake of Interest
-  Mined Pit Area
-  DII35R Zone of Influence



Sarah Zagurski  
September 20, 2020

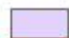

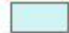
Figure 44a. Zone of Influence for Lake DII-35R.

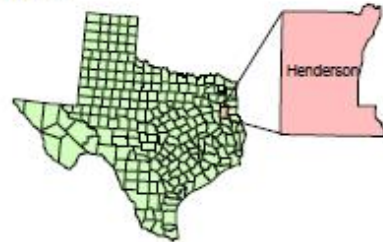
# Zone of Influence for Lake DII-55R at Oak Hill Mine, Henderson, Texas



0 1 Miles

### Legend

-  Lake of Interest
-  Mined Pit Area
-  DII55R Zone of Influence



Sarah Zagurski  
September 20, 2020

Figure 45a. Zone of Influence for Lake DII-35R






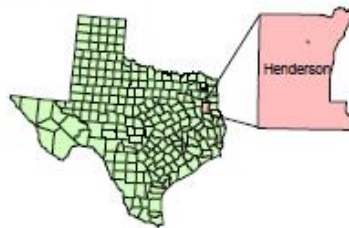
### Zone of Influence for Lake DII-58R at Oak Hill Mine, Henderson, Texas



0 1 Miles

#### Legend

-  Lake of Interest
-  Mined Pit Area
-  DII58R Zone of Influence



Sarah Zagurski  
September 20, 2020

Figure a - 46. Zone of Influence for Lake DII-58R

## APPENDIX A – TABLES

Table 1a. Sulfur content for each depth of soil core used in the study for the

Well	Depth (ft. below surface)	Sulfur
16	6 to 8	496.3
16	8 to 10	356.0
16	10 to 12	ND
16	12 to 14	472.3
17	6 to 8	408.5
17	8 to 10	247.0
17	12 to 14	252.0
18	34 to 36	658.0
18	36 to 38	1291.3
18	38 to 40	227.0
19	6 to 8	869.0
19	8 to 10	548.0
19	10 to 12	ND
19	12 to 14	1443.7
22	10 to 13	1793.7
22	13 to 15	3060.7
22	15 to 17	1296.0
22	17 to 19	ND
24	42 to 44	ND
24	44 to 46	ND
24	46 to 48	344.5
24	56 to 58	ND
25	4 to 6	1688.7
25	6 to 8	1113.7
25	8 to 10	463.0
25	10 to 12	492.0
26	2 to 4	ND
26	4 to 6	ND
26	6 to 8	ND
26	8 to 10	ND
28	6 to 8	ND
28	8 to 10	ND
28	10 to 12	ND
30	4 to 6	ND
30	6 to 8	ND
30	8 to 10	363.0
30	10 to 12	728.3



Table 2a. Weight, volume, and density data from each soil core depth used in the humidity cell.

ID	Weight (g)	Volume (cm <sup>3</sup> )	Density
16-6.3-6.8	17.55	13.4	1.309701
16-10.4-10.9	6.02	2.8	2.15
17-6.5-7.0	10.69	8.36	1.278708
17-12.2-12.7	21.12	11.7	1.805128
18-34.1-34.6	0.71	0.53	1.339623
18-38.6-39.1	2.29	1.48	1.547297
19-6.1-6.6	5.84	3	1.946667
19-10.5-11	18.7	16.75	1.116418
22-10.1-10.6	18.47	12.85	1.437354
22-13.2-13.7	9.03	5.94	1.520202
24-42.0-42.5	3.82	2.8	1.364286
24-48.4-48.9	17.83	11.65	1.530472
25-4.8-5.3	2.26	2.01	1.124378
25-8.4-8.9	9.92	9.18	1.08061
26-4.9-5.4	10.4	8.5	1.223529
26-8.2-8.7	3.24	2.8	1.157143
28-6.5-7.0	2.3	1.8	1.277778
28-10.5-11.0	8.42	5.88	1.431973
30-8.2-8.7	13.29	11.3	1.176106
30-12.5-13.0	5.75	5.68	1.012324
<b>Average</b>			<b>1.391485</b>

Table 3a. Weekly sulfate concentrations in mg/kg with estimated values highlighted in yellow for the determination of cumulative release.

Week	Cell 1	Cell 2	Cell 3	Cell 4	Cell 5	Cell 6	Cell 7	Cell 8	Cell 9	Cell 10
1	0.93	ND	44.60	312.27	65.12	ND	623.84	7.56	ND	ND
2	4.71	3.14	43.40	390.74	112.98	3.51	106.79	11.34	2.53	3.39
3	3.82	2.51	51.77	359.54	153.10	2.73	64.54	12.41	2.23	3.22
4	3.44	2.21	50.75	314.69	216.49	2.31	44.32	8.57	1.98	2.93
5	3.33	2.12	54.70	273.41	236.68	2.08	39.66	5.56	1.80	2.98
6	3.23	2.03	60.42	225.19	210.31	1.92	36.90	3.48	1.63	2.46
7	3.12	1.94	66.13	176.98	183.93	1.76	34.13	1.39	1.46	1.94
8	3.07	1.89	65.13	170.92	241.84	1.64	33.29	1.51	1.43	1.53
9	3.02	1.84	64.14	164.85	299.75	1.53	32.46	1.62	1.39	1.13
10	3.99	1.77	70.49	141.90	276.76	1.46	31.20	1.45	2.31	1.66
11	3.99	1.77	70.49	141.90	276.76	1.46	31.20	1.45	2.31	1.66
12		1.69	76.84	118.94	253.78	1.39	29.94	1.28	3.23	2.20
13	3.75	1.53	73.64	120.61	230.86	1.32	21.51	1.18	2.09	2.21
14	2.53	1.37	70.43	122.27	207.93	1.24	13.08	1.07	0.95	2.23
15	2.50	1.38	69.56	107.52	187.85	1.36	11.80	1.06	0.97	2.21
16	2.47	1.39	68.68	92.76	167.77	1.47	10.53	1.06	0.99	2.20
17	2.45	1.37	69.03	80.43	156.08	1.39	10.24	1.05	0.96	2.17
18	2.42	1.35	69.37	68.10	144.40	1.32	9.96	1.04	0.94	2.15
19	2.44	1.39	66.27	60.02	143.99	1.95	9.56	1.05	1.00	2.01
20	2.46	1.43	63.17	51.94	143.57	2.57	9.16	1.06	1.06	1.87
21	2.46	1.38	60.55	47.02	148.61	1.94	8.58	1.07	1.02	1.81
22	2.45	1.32	57.94	42.10	153.65	1.31	7.99	1.07	0.97	1.76
23	3.43	1.35	53.99	40.87	142.39	1.50	8.40	1.09	1.07	1.82
24	3.10	1.37	50.04	39.63	131.12	1.68	8.81	1.10	1.18	1.88
25	2.85	1.32	49.15	37.00	125.50	1.58	8.40	1.06	1.14	1.88
26	2.51	1.27	48.30	35.00	120.00	1.48	8.00	1.02	1.10	1.88
27	2.25	1.22	47.45	32.50	114.00	1.36	7.60	0.97	1.05	1.88

Table 3a continued.

Week	Cell 1	Cell 2	Cell 3	Cell 4	Cell 5	Cell 6	Cell 7	Cell 8	Cell 9	Cell 10
28	2.04	1.18	46.57	30.26	108.39	1.24	7.20	0.93	1.01	1.88
29	2.14	1.18	48.55	31.57	98.30	3.94	4.23	0.89	1.03	1.84
30	2.24	1.18	50.52	32.88	88.21	6.63	1.26	0.85	1.05	1.81
31	2.15	1.19	46.83	32.04	89.63	3.86	3.81	0.86	0.94	1.77
32	2.06	1.21	43.14	31.21	91.04	1.09	6.36	0.88	0.83	1.74
33	2.05	1.19	41.77	31.70	79.11	1.10	6.17	0.92	0.85	1.72
34	2.04	1.17	40.40	32.19	67.19	1.11	5.98	0.95	0.87	1.69
35	2.02	1.14	40.77	30.55	69.62	1.09	5.89	1.00	0.87	1.65
36	2.00	1.11	41.14	28.90	72.05	1.07	5.79	1.05	0.86	1.61
37	2.05	1.17	40.51	29.39	68.56	1.13	5.66	1.09	0.92	1.59
38	2.09	1.22	39.88	29.88	65.08	1.18	5.53	1.13	0.98	1.57
39	2.00	1.12	36.68	29.93	60.53	1.13	5.47	1.06	0.93	1.51
40	1.92	1.07	34.23	29.98	55.77	1.04	5.41	0.99	0.84	1.45
41	1.82	0.98	31.79	30.02	51.02	0.96	5.35	0.92	0.77	1.39
42	1.75	0.90	29.65	30.07	46.65	0.91	5.29	0.86	0.73	1.33
43	1.70	0.87	29.54	25.55	42.75	0.86	4.74	0.82	0.73	1.29
44	1.66	0.84	29.44	21.02	38.86	0.81	4.18	0.78	0.73	1.25
45	1.61	0.81	28.32	20.60	36.75	0.79	4.01	0.75	0.70	1.21
46	1.57	0.79	27.10	20.14	34.59	0.76	3.86	0.72	0.65	1.17
47	1.53	0.76	26.08	19.69	32.86	0.74	3.70	0.70	0.60	1.13
48	1.49	0.74	24.88	19.30	31.26	0.72	3.53	0.67	0.56	1.08
49	1.43	0.71	19.15	12.29	25.72	0.70	3.56	0.66	0.54	1.07
50	1.37	0.68	13.14	5.12	19.67	0.68	3.59	0.66	0.52	1.06
51	1.35	0.65	11.94	4.80	19.30	0.64	3.65	0.60	0.51	0.98
52	1.29	0.58	11.49	3.84	18.02	0.60	3.84	0.55	0.47	1.23

Table 4a. Weekly acidity concentrations in mg/L.

Week	Well 16	Well 17	Well 18	Well 19	Well 22	Well 24	Well 25	Well 28	Well 30
1	65.50	30.82	221.73	1661.39	207.72	27.32	1426.70	ND	ND
2	47.64	22.42	174.09	2477.90	442.41	17.86	307.20	44.49	29.07
3	25.57	38.53	224.18	2230.60	715.28	24.52	195.81	36.43	36.78
4	46.94	24.87	274.62	2044.60	1106.89	27.32	148.87	23.12	24.17
5	36.08	24.17	298.09	1867.35	1327.57	20.67	132.06	22.42	19.62
7	38.88	21.72	370.95	1180.45	1074.32	23.82	93.88	21.72	20.32
9	22.14	11.21	361.63	2087.12	909.61	9.53	88.55	ND	7.99
12	34.47	8.55	402.26	780.57	1528.49	7.71	80.56	7.20	7.71
14	19.62	7.57	409.83	748.48	1244.20	6.45	71.04	4.90	8.13
16	18.92	8.41	395.96	543.22	1007.83	7.99	61.93	7.29	8.55
18	20.04	9.53	395.12	363.03	816.72	7.85	63.61	7.71	9.11
20	19.20	9.25	332.63	231.61	804.11	9.11	58.01	7.71	9.25
22	16.25	7.57	279.39	163.93	908.77	10.12	51.56	7.57	8.69
24	13.23	6.31	223.76	133.25	746.24	12.47	45.40	8.13	9.95
26	19.20	8.83	209.47	97.66	667.36	8.13	44.28	8.83	7.43
28	15.83	7.85	197.42	83.09	574.32	6.16	47.50	4.06	9.53
30	11.21	5.88	210.03	92.47	430.99		9.39	8.83	8.69
32	12.19	6.45	180.33	92.61	526.40	11.56	45.40	8.41	11.63
34	11.63	10.37	158.61	94.72	339.77	10.51	30.82	9.67	8.55
36	ND	7.71	151.46	79.86	389.37	11.91	38.53	10.65	12.61
40	9.67	7.01	124.84	58.15	180.61	3.64	34.05	4.90	5.46
42	11.21	6.59	106.07	49.18	209.47	3.36	31.53	4.62	5.04
44	14.99	9.11	95.14	55.34	209.47	16.67	45.96	9.25	23.96
46	11.21	9.11	91.63	52.26	172.76	9.39	30.68	3.78	6.73
48	10.37	3.22	73.00	39.51	122.88	4.06	22.98	2.80	3.78
50	9.81	3.36	77.20	32.23	125.40	4.90	26.62	6.73	4.62
51	11.35	5.74	73.84	39.51	126.38	3.50	22.84	4.62	3.08
52	9.53	3.78	70.48	30.54	123.02	5.18	28.16	3.08	4.06

Table 5a. Groundwater data collected from September 2019 to August 2020.

Month	Well 3						Well 5					
	ORP	Temp	SPC	Turbidity	DO	pH	ORP	Temp	SPC	Turbidity	DO	pH
September	181.8	21.6	573	371.278	2.99	4.28	19.4	24.182	1787	1169.12	0.16	4.1
October	138.1	20.9	582	120.85	2.83	4.74	11	21.499	1178	1.62	0.13	4.6
November	21.2	17.7	567	12.97	3.07	4.16	-288.2	17.978	1751	4.32	0.2	4
December	353.3	19.2	571	198.26	3.03	4.07	326.8	19.366	1811	4.43	0.29	3.87
January	38.6	18.6	544	126.77	3.05	4.1	172.2	17.707	1816	14.90	0.17	3.88
February	230.9	19.4	550	92.22	3.00	4.03	237.8	20.377	1697	28.66	0.16	3.85
March	643.4	18.9	532	193.45	3.97	4.12	462.6	21.034	1643	10.71	0.45	3.94
April	625.2	20.5	546	16.08	3.55	4.04	455.9	23.955	1642	56.81	0.23	3.87
May	599.9	18.4	550	51.16	3.66	4.01	443	19.789	1646	47.32	0.19	3.84
June	452.4	21.9	1784	44.62	2.72	3.84	611.9	21.644	547	338.10	0.23	4.11
July	508.6	21.8	572	59.41	2.94	4.08	479.5	22.524	1682	30.64	0.29	4.01
August	586.2	20.9	567	76.97	2.87	4.12	468.5	23.17	1794	60.82	0.19	3.96

Table 5a continued.

Month	Well 9						Well 16					
	ORP	Temp	SPC	Turbidity	DO	pH	ORP	Temp	SPC	Turbidity	DO	pH
September	-211.7	21.2	320.7	208	0.00	5.72	20.5	24.068	2316.5	1506.00	0.1	3.3
October	-205.1	22.5	305.7	126.86	0.08	7.26	-28.5	22.7	154	91.03	0.11	3.91
November	-216.8	20.2	284.3	59.64	0.10	5.81	-8.4	19.7	1620	47.59	0.2	3.29
December	13.5	21.3	383.9	94.99	0.13	6.04	-54.1	19.494	1732	192.20	0.16	3.36
January	-376.3	20.1	374.5	3.03	0.12	6.03	-260.4	19.335	1557	3.04	0.1	3.39
February	193.9	19.3	390.9	33.28	0.23	5.92	144.5	17.205	1477	56.04	0.16	3.33
March	242.5	19.7	424.6	25.29	0.27	6.01	496.8	17.768	1524	123.88	0.18	3.41
April	240.4	21.3	391.4	48.76	0.17	5.94	473.2	19.593	1612	31.42	0.17	3.37
May	228.3	19.6	299.9	81.56	0.17	5.99	468.1	19.544	1647	11.70	0.19	3.38
June	225.5	21.4	297.6	31.9	0.15	5.98	469.9	21.622	1608	69.59	0.18	3.41
July	221.2	22.4	309.8	42.16	0.16	5.93	465.9	22.414	1622	40.51	0.16	3.39
August	229.9	22.6	319.4	29.47	0.13	5.99	471.1	22.871	1756	168.25	0.14	3.4

Table 5a continued.

Month	Well 18						Well 19					
	ORP	Temp	SPC	Turbidity	DO	pH	ORP	Temp	SPC	Turbidity	DO	pH
September	-3.3	23.5	1481.3	963	0.00	3.27	199.7	21.028	2301.6	1497.00	-0.01	2.49
October	27.1	24.3	2463	160.94	0.15	4.78	209.6	22.451	2466	20.52	0.1	3.85
November	31.1	19.6	2609	74.76	0.12	3.48	203.8	19.427	2618	21.86	0.12	2.64
December	-60.5	19.7	2510	72.66	0.22	3.42	40.8	20.256	2948	19.53	0.15	2.45
January	-363.7	18.6	2590	119.07	0.20	3.42	18.8	19.292	3037	33.19	0.12	2.44
February	122.6	18.8	2605	107.77	0.57	3.33	427.6	18.221	3149	0.66	0.12	2.33
March	448.5	20.3	2575	388.44	1.07	3.42	658.7	18.48	3058	24.72	0.18	2.43
April	416.6	21.5	2483	48.24	0.16	3.36	666.6	19.373	3022	10.06	0.15	2.38
May	475.6	21.6	2478	105.4	0.82	3.4	670.1	19.184	3298	75.40	0.17	2.35
June	475.8	25.3	2471	307.1	0.20	3.41	691.7	20.798	3722	41.04	0.19	2.33
July	462.5	24.2	2452	124.61	0.23	3.39	678.5	21.548	3164	15.48	0.18	2.37
August	472.9	23.9	2496	189.63	0.54	3.42	671.4	21.897	3276	26.98	0.15	2.4

Table 5a continued.

Month	Well 20						Well 22					
	ORP	Temp	SPC	Turbidity	DO	pH	ORP	Temp	SPC	Turbidity	DO	pH
September	227.9	22.9	2660.7	1720	0.17	2.4	-63.4	21.597	1490	968.44	0.29	4.21
October	222.4	23.9	2027	111.62	0.23	4.15	-28.3	22.764	1458	10.72	0.1	5.41
November	197.9	20.4	1890	102.11	0.16	2.85	-172	19.171	1372	12.98	0.13	4.61
December	47.1	20.5	1740	81.66	0.23	2.76	-102.8	19.023	1315	10.53	0.19	4.27
January	2.4	21.5	1543	112.33	0.21	2.9	-372	20.555	1212	10.24	0.11	4.47
February	335.8	15.2	1657	98.29	0.38	2.7	102.2	8.197	1185	7.46	0.23	4.42
March	624	20.6	1629	65.12	0.84	2.84	415.3	18.202	1182	20.50	0.32	4.53
April	626.1	21.4	1859	79.67	0.48	2.74	384.8	20.649	1187	30.53	0.2	4.49
May	637.2	21.5	1932	17.06	0.32	2.65	426.1	20.649	1187	19.24	0.15	4.38
June	645	22.7	2011	54.16	0.59	2.73	405.8	25.068	1212	55.31	0.2	4.38
July	635.2	22.8	1957	23.51	0.39	2.7	397.8	24.73	1194	40.23	0.22	4.35
August	631.5	21.9	2005	41.59	0.27	2.68	402.6	23.54	1216	15.84	0.19	4.32



Table 5a continued.

Month	Well 23						Well 24					
	ORP	Temp	SPC	Turbidity	DO	pH	ORP	Temp	SPC	Turbidity	DO	pH
September	-6.8	24.5	5037	3277.821	0.14	3.41	-148.4	26.639	1073	696.79	0.18	5.12
October	-20.1	22.0	4577	150.63	0.24	4.25	-107.8	22.92	1112	29.55	0.17	5.75
November	-207.2	17.7	4882	64.72	0.10	3.57	-215.6	20.193	990	4.11	0.1	5.54
December	-52.8	20.2	4550	114.36	0.72	3.5	20.1	22.064	898	6.59	0.1	5.63
January	183.3	19.1	4267	68.25	0.11	3.51	-353.6	21.933	860	1.30	0.17	5.72
February	238.2	20.9	4340	47.95	0.11	3.44	193.2	19.853	903	17.96	0.59	5.25
March	425.3	21.2	4510	15.94	0.12	3.54	245.7	22.03	851	1.70	0.24	5.77
April	482.3	23.0	4200	289.18	0.14	3.5	232.5	22.926	869	10.89	0.27	5.67
May	434.9	20.8	4144	66.72	0.36	3.47	208.1	21.753	964	10.22	0.14	5.71
June	408.1	22.2	4311	28.07	0.18	3.51	213.4	22.918	1083	25.61	0.17	5.7
July	417.3	22.6	4269	50.13	0.16	3.49	219.4	23.17	1054	30.41	0.19	5.72
August	421.7	22.1	4351	75.97	0.13	3.52	222.4	22.935	1013	15.89	0.22	5.69

Table 5a continued.

Month	Well 25						Well 26					
	ORP	Temp	SPC	Turbidity	DO	pH	ORP	Temp	SPC	Turbidity	DO	pH
September	-202.8	23.5	1722	1119.494	0.16	5.37	-93.1	22.97	927	602.52	0.06	4.49
October	-204.2	23.3	1776	15.39	0.32	6.92	-49	21.33	939	66.30	0.09	5.14
November	-131.6	19.6	1842	50.75	0.48	5.81	-208	20.004	979	25.71	0.09	4.84
December	15.9	20.8	1809	45.77	0.49	5.65	15.9	19.353	991	154.90	0.12	4.51
January	-373.1	20.3	1712	63.75	1.23	5.71	28.8	18.69	929	13.31	0.11	4.51
February	208.4	20.5	1660	9.06	0.58	5.55	201.7	17.661	949	7.41	0.09	4.47
March	243.8	20.6	1512	5.64	0.26	5.71	415.1	17.741	90	45.80	0.17	4.59
April	247.2	22.5	1335	43.16	0.25	5.57	385.9	21.296	1027	24.34	0.17	4.61
May	287.5	20.50	1193	67.59	0.22	5.5	384.8	19.316	1039	13.54	0.11	4.7
June	278.8	23.5	970	32.89	0.24	5.52	345.7	21.731	1076	204.89	0.14	4.82
July	264.7	23.1	1247	47.81	0.20	5.49	358.2	22.745	1024	54.79	0.11	4.75
August	272.5	23.7	1564	53.11	0.19	5.47	362.4	22.652	1039	28.16	0.09	4.7

Table 5a continued.

Month	Well 27						Well 28					
	ORP	Temp	SPC	Turbidity	DO	pH	ORP	Temp	SPC	Turbidity	DO	pH
September	223	24.2	994	645.656	0.21	3.03	-34.2	25.695	85.3	55.39	5.88	5.35
October	236.8	23.2	881	181.94	0.39	4.35	11.8	21.95	81.6	148.09	6.11	6.1
November	249	19.9	878	13.37	0.18	3.212	-21.3	19.499	82.1	183.24	6.48	5.41
December	439.8	21.2	804	8.73	1.16	3.2	376.1	20.811	83.9	209.73	6.5	5.34
January	114	20.1	715	94.73	1.69	3.3	114.8	20.672	86.5	298.61	6.13	5.33
February	254	19.3	765	1.53	1.79	3.24	234.2	21.466	246.1	248.90	5.03	4.86
March	629.1	18.1	636	9.78	0.73	3.29	519.2	21.417	449.9	69.06	5.18	4.71
April	606.6	19.8	845	7.85	0.19	3.26	534.8	22.5	291.1	155.52	6.44	4.86
May	660.2	19.3	434.1	9	0.18	3.23	480.4	20.559	163.9	128.94	7.31	5.19
June	601.3	21.6	1034	21.91	0.24	3.25	479	21.704	131.6	168.62	6.19	5.28
July	610.9	21.9	887	47.51	0.21	3.21	497.2	22.031	107.53	129.65	6.03	5.19
August	620.5	22.0	929	32.69	0.23	3.23	482.3	22.458	96.32	148.72	5.94	5.07

Table 5a continued.

Well 30						
Month	ORP	Temp	SPC	Turbidity	DO	pH
September	-328.1	23.1	640.2	416	0.00	6.10
October	321.2	21.2	643	194.68	0.1	7.50
November	-342.5	21.9	658	124.68	0.1	6.18
December	0.6	20.4	648	405.89	0.09	6.28
January	-373.7	18.8	639	271.3	6.1	6.28
February	161.9	15.3	589	277.05	0.09	6.37
March	137.9	16.6	670	226.11	0.13	6.30
April	121.7	18.6	693	136.82	0.13	6.15
May	133.8	19.4	660	386.74	0.20	6.21
June	123.6	21.7	678	260.13	0.14	6.20
July	127.4	22.0	668	202.39	0.11	6.22
August	124.8	22.3	654	219.65	0.13	6.24

Table 6a. Depth, minerals, and texture for each humidity cell (Paul, 2020).

Humidity Cells	Well depth	Bulk XRD Identified Minerals	Texture
Well 16	16-6-14	Quartz, kaolinite, goethite, muscovite pyrite	Loamy Sand
Well 17	17-6-14	Quartz, kaolinite, pyrite	Loamy sand with silty clay
Well 18	18-34-40	Quartz, kaolinite, montmorillonite, muscovite, albite, goethite, lignite	Silty Clay
Well 19	19-6-14	Quartz, kaolinite-montmorillonite, muscovite, pyrite	Loamy sand to silt loam
Well 22	22-10-18	Quartz, kaolinite, muscovite, microcline, pyrite	Silty clay loam
Well 24	24-42-65, 48-50	Quartz, kaolinite, goethite	Loamy sand to clay loam
Well 25	25-4-12	Quartz, kaolinite, pyrite	Loamy sand to clay loam
Well 26	26-2-10	Quartz, kaolinite, muscovite, microcline, albite, goethite, pyrite	Loamy sand
Well 28	28-6-12	Quartz, kaolinite	Loamy sand
Well 30	30-4-12	Quartz, kaolinite, muscovite, microcline, goethite	Silty clay loam

## APPENDIX B – ACRONYMS

AFM- Acid Forming Material  
AMD- Acid Mine Drainage  
ASTM- American Society for Testing and Materials  
ORP- Oxidation Reduction Potential  
CSF- Cumulative Scaling Factor  
DEM- Digital Elevation Model  
DI- Deionized  
DO- Dissolved Oxygen  
EPA- Environmental Protection Agency  
MASL- Meters Above Sea Level  
MPN- Most Probable Number  
NOAA- National Oceanic and Atmospheric Administration  
NPDES- National Pollution and Discharge Elimination System  
RRC- Railroad Commission  
SC- Specific Conductance  
SEM- Scanning Electron Microscopy  
SF- Scaling Factor  
USGS- United States Geologic Survey  
XRD- X-ray Diffraction  
XRF- X-ray Fractionation

## VITA

Sarah Zagurski graduated from Liberty Highschool, Frisco, Texas in 2014. She graduated as a double major with a Bachelor of Science in Geology and Environmental Science from Stephen F. Austin State University in May, 2018. She was admitted to graduate school at Stephen F. Austin in August 2018 to pursue a Master's degree in Environmental Science. Sarah received her Master of Science degree in December, 2020.

Permanent Address:           2701 Promenade,  
  The Colony, TX 75056

The thesis follows the style guide of the Soil Science Society of America.

This thesis was typed by Sarah Zagurski.